UNIVERSIDADE DE LISBOA
FACULDADE DE CIÊNCIAS

DEPARTAMENTO DE BIOLOGIA ANIMAL

Role of fibronectin in tumor development and progression

Sofia Gouveia Pereira Fernandes

Mestrado em Biologia Humana e Ambiente

2011

UNIVERSIDADE DE LISBOA
FACULDADE DE CIÊNCIAS

DEPARTAMENTO DE BIOLOGIA ANIMAL

Role of fibronectin in tumor development and progression

Sofia Gouveia Pereira Fernandes

Mestrado em Biologia Humana e Ambiente

Dissertação orientada por:

Prof. Doutora Jacinta Serpa (orientação externa)
CIPM-IPO Lisboa Francisco Gentil, EPE; Faculdade de Ciências Médicas da Universidade Nova de Lisboa.

Prof. Doutora Deodália Dias (orientação interna)
CESAM; Faculdade de Ciências da Universidade de Lisboa.

2011

Agradecimentos

Após mais uma etapa na minha vida académica, não posso deixar de expressar os meus sinceros agradecimentos a todos aqueles que, com a sua generosidade, ajuda, paciência e dedicação, contribuíram para a realização deste trabalho, e a quem me dirijo neste texto.

O meu especial agradecimento à Doutora Jacinta Serpa, minha orientadora, por me ter concedido a oportunidade de participar neste projecto, que me possibilitou um contacto mais próximo com o mundo da Ciência, e do qual retiro muito boas experiências. Obrigada por toda a ajuda durante este ano de estágio (e na revisão desta dissertação), pelo incentivo ao pensamento crítico e autonomia, pela confiança, que sempre me confortou, e por todos os conhecimentos transmitidos.

À Doutora Deodália Dias, minha orientadora interna, por ter aceitado co-orientar o meu trabalho, e pela simpatia, generosidade, dedicação e disponibilidade, que tornaram muito mais fácil o meu percurso durante este mestrado.

Ao Doutor Sérigo Dias, pela oportunidade que me concedeu de participar neste projecto e pelo voto de confiança, por toda a ajuda, inclusivamente na revisão desta dissertação, acessibilidade e pelo modo afável com que sempre me recebeu.

Ao grupo da Angiogénese, do qual orgulhosamente fiz parte. Excelentes pessoas e profissionais. Gostaria de dirigir um especial agradecimento à minha colega Germana Domingues, que acompanhou mais de perto o meu trabalho, pela preciosa ajuda que sempre me prestou, simpatia, alegria e boa disposição.

Aos meus colegas de laboratório agradeço também por toda a ajuda e apoio, e pelos bons momentos, e, por extensão, a todos os colegas do CIPM que, directa ou indirectamente, tornaram a conclusão deste trabalho possível.

Ao pessoal técnico do serviço de Anatomia Patológica do IGC e do IPO, particularmente, à Fernanda Silva por toda a ajuda, simpatia e prestabilidade.

À Vanda Póvoa, dirijo também um especial agradecimento, pela ajuda, apoio, incentivo, alegria e boa disposição. Foi muito reconfortante ter tido tão agradável companhia.

Finalmente, agradeço a toda a minha família por nos terem feito sempre sentir especiais e amadas, pelo exemplo e transmissão dos melhores valores. Um obrigada especial aos meus avós, por tudo. Espero que, onde estiverem, estejam orgulhosos de mim.

Aos meus pais, irmã e sobrinha, MUITO OBRIGADA pelo carinho, compreensão, incomensurável ajuda e amor incondicional. São simplesmente os melhores… Os pilares da minha vida…

Resumo

A tumorigénese é um processo complexo cujas várias fases reflectem alterações genéticas que resultam na transformação progressiva de células normais em células malignas (Hanahan & Weinberg, 2000; Renan, 1993). As principais características que ditam colectivamente o cancro são: auto-suficiência em relação aos sinais de crescimento, insensibilidade aos sinais de anti-crescimento, evasão à apoptose, elevado potencial replicativo, angiogénese sustentada, evasão ao controlo imunitário, reprogramação metabólica, invasão tecidular e metastização, representando esta última a principal causa de morbidez e morte associadas à doença (Hanahan & Weinberg, 2011).

Todos estes atributos resultam de uma interacção dinâmica entre as células tumorais e o seu microambiente – microambiente tumoral –, que inclui células normais, factores mediadores e componentes da matriz extracelular (MEC) (Tlsty & Coussens, 2006).

A fibronectina (FN) é uma glicoproteína modular de elevado peso molecular que pode ser classificada, de acordo com a sua solubilidade, em FN plasmática, solúvel, e FN celular, uma forma menos solúvel que representa o maior componente da MEC (Klein *et al*, 2004; Pankov & Yamada, 2002). Estruturalmente, a FN apresenta-se sob a forma de um dímero composto por duas cadeias polipeptídicas aproximadamente idênticas, ligadas covalentemente por um par de pontes dissulfito próximo da extremidade C-terminal. Cada monómero tem um peso molecular de 230-250 kDa e é composto por três tipos de unidades de repetição ou módulos: o tipo I (FI), o tipo II (FII) e o tipo III (FIII) (Hynes & Yamada, 1982; Pankov & Yamada, 2002; Potts & Campbell, 1996).

A FN, que tem como receptores integrinas, está implicada numa grande variedade de funções celulares, sobretudo envolvendo interacções entre as células e a MEC, onde assume grande importância na adesão, morfologia, migração, crescimento e diferenciação celulares, organização do citosqueleto e hemostasia (Hynes & Yamada, 1982; Kornblihtt *et al*, 1996; Labat-Robert, 2002).

As interacções célula-célula e célula-matriz são essenciais para o fornecimento de informações que regulam o normal funcionamento celular, pelo que a degradação ou activação das proteínas de matriz e/ou da superfície celular podem mediar alterações irreversíveis no microambiente celular (Werb, 1997). O crescimento tumoral, angiogénese, invasão e metastização estão fortemente dependentes da natureza permissiva do microambiente. Durante estas fases, a proteólise da MEC representa um passo crucial (Chambers & Matrisian, 1997; Polette *et al*, 2004), sendo reconhecida à FN uma forte susceptibilidade neste âmbito (Kenny *et al*, 2008). As metaloproteases de matriz (MPMs)

constituem a família de proteases mais importante associada à tumorigénese (Kessenbrock *et al*, 2010). As MPM-9 e MPM-2 têm sido apontadas como as MPMs mais importantes na metastização (Coussens *et al*, 2002; Klein *et al*, 2004; Malemud, 2006; Stetler-Stevenson, 1999).

O aumento concomitante de FN e enzimas proteolíticas, bem como de fragmentos de fibronectina tem sido observado em doentes de cancro (Katayama *et al*, 1993; Kenny *et al*, 2008; Kenny & Lengyel, 2009; Labat-Robert, 2002; Labat-Robert *et al*, 1980; Warawdekar *et al*, 2006), sugerindo uma possível intervenção da FN e seus fragmentos no processo tumoral, embora o eventual mecanismo subjacente ao fenómeno não seja ainda claro. Paralelamente, outros estudos têm atribuído propriedades anti-tumorais a alguns fragmentos derivados da FN (Humphries *et al*, 1986; Humphries *et al*, 1988; Kato *et al*, 2002; Saiki, 1997; Yi & Ruoslahti, 2001).

Com base no trabalho científico que vem sendo dedicado a esta temática, foi estabelecido como objectivo deste trabalho o estudo do papel da FN no desenvolvimento e progressão tumorais. Com este intuito, foi desenvolvido um trabalho experimental que partiu do estabelecimento de dois grupos, para diferentes linhas celulares, diferindo entre si nos níveis de FN produzida. Para isso, procedeu-se à construção de um plasmídeo contendo o gene da FN embrionária (*full-length*), pcDNA3-fl*FN*. Este vector foi transfectado em células das linhas celulares tumorais humanas HCT15 (carcinoma colorrectal) e HeLa (adenocarcinoma do colo do útero), e da linha celular não-tumoral CHO, uma linha celular transformada onde o mecanismo de controlo de transcrição se encontra inactivado, tendo sido, por isso, utilizada como controlo positivo, *in vitro*. Para cada linha celular foi mantido um grupo de células controlo, não transfectadas. O trabalho experimental consistiu no desenvolvimento de ensaios *in vitro* e *in vivo,* após a indução da formação de tumores xenógrafos em modelos ortotópicos de ratinhos BALB/c-SCID. Os resultados foram comparados entre grupos.

Após transfecção estável das linhas celulares, a expressão de *FN* foi determinada, para cada grupo, por PCR quantitativo em tempo-real. A detecção de níveis mais elevados de mRNA nos grupos controlo, para todas as linhas celulares – sobretudo em HCT15 e CHO –, validou o sucesso da transfecção, o que permitiu a progressão do trabalho experimental. Análises de *western blotting* – foram utilizadas como amostras a FN imunoprecipitada a partir do meio de cultura das células – e imunofluorescência confirmaram a existência de uma correlação entre níveis de mRNA e proteína, evidenciando valores proteicos de FN aumentados nos grupos transfectados, em comparação com os grupos controlo.

Os resultados obtidos por *western blotting* mostraram, adicionalmente, a presença de fragmentos proteolíticos de FN nas linhas tumorais, não observada no controlo positivo (FN

imunoprecipitada a partir de soro de um individuo saudável), o que está de acordo com as observações de vários estudos realizados em doentes de cancro (Katayama *et al*, 1993; Kenny *et al*, 2008; Kenny & Lengyel, 2009; Labat-Robert, 2002; Labat-Robert *et al*, 1980; Warawdekar *et al*, 2006). Para as linhas celulares CHO e HCT15, foram detectados níveis mais elevados de fragmentos proteolíticos de FN nos grupos transfectados, o que está de acordo com o esperado, dada a maior concentração de FN nestes grupos.

Por imunofluorescência, foi observada, globalmente, uma maior expressão de integrinas nas células transfectadas, resultado esperado sendo essas os receptores da FN.

Por zimografia, foi avaliada a actividade das MPMs. Foi detectada actividade proteolítica das MPM-9 e MPM-2, consideradas as MPMs mais importantes no processo de metastização (Coussens *et al*, 2002; Klein *et al*, 2004; Malemud, 2006; Stetler-Stevenson, 1999). Para a MPM-9 foi observada uma actividade proteolítica aumentada nos grupos transfectados de HCT15 e CHO, assim como para a MPM-2 em HCT15. Estes resultados podem estar relacionados com a maior concentração de FN nos meios de cultura das células transfectadas e revelaram-se também consistentes com o padrão de fragmentos de FN obtido por *western blotting*.

O estudo da migração celular foi abordado por *wound healing assay*, do qual resultaram taxas de migração direccional mais elevadas para as células CHO e HCT15 transfectadas, facto que poderá estar relacionado com os resultados obtidos na zimografia.

Um eventual envolvimento da FN na angiogénese foi avaliado por *tube formation assay* com HUVEC (células endoteliais de cordão umbilical humano) e pela quantificação da expressão, a nível de mRNA, de três isoformas de VEGF (factor de crescimento do endotélio vascular), receptores do VEGF e angiopoietinas. Os resultados mostraram uma relação inversa entre os níveis de FN e a formação de tubos.

Colectivamente, os resultados *in vitro* sugeriram uma correlação entre níveis mais elevados de FN e um comportamento mais agressivo por parte das células, num contexto neoplásico, sugerindo um particular envolvimento da migração das células tumorais.

Após aproximadamente dois meses da indução da formação de tumores nos modelos BALB/c-SCID, os animais foram sacrificados e procedeu-se à colheita dos principais órgão-alvo de metastização. A análise histológica dos tumores e órgãos recolhidos revelou mais invasão e metastização nos grupos inoculados com células controlo. Estas observações foram confirmadas para o grupo inoculado com HCT15, pela detecção de mais mastócitos nos tumores, os quais estão implicados no crescimento tumoral e invasão (Strouch *et al*, 2010), e pela quantificação da expressão de *SCF* (factor de células estaminais) – citocina envolvida na promoção da sobrevivência, proliferação e migração de mastócitos e células progenitoras

(Broudy, 1997) – e *SDF-1* (factor derivado do estroma da medula óssea) – citocina associada ao crescimento tumoral, angiogénese, metastização e recrutamento de células derivadas da medula óssea (Kryczek *et al*, 2007) –, que se revelou menor nas células transfectadas.

Os resultados *in vivo* evidenciam, deste modo, um processo tumorigénico menos avançado nos animais inoculados com células transfectadas, contrariando as observações *in vitro*. Com efeito, uma taxa migratória mais elevada não implica necessariamente uma maior actividade invasiva por parte das céluals tumorais, a principal responsável pela disseminação do cancro. Por outro lado, as condições *in vitro* não incluem muitas variáveis existentes *in vivo*. Recomenda-se, no entanto, a validação dos modelos *in vivo* sob condições técnicas mais apropriadas. Não obstante, parece relevante a sequenciação de um fragmento detectado, para posterior investigação.

Palavras-chave: cancro, metastização, microambiente tumoral, fibronectina (FN), fragmentos de fibronectina.

Abstract

Reciprocal interactions among normal cells, their mediators, components of the extracellular matrix (ECM) and genetically altered cells regulate all aspects of tumorigenicity. Fibronectin (FN), a multidomain glycoprotein, represents the major component of ECM and is implicated in a variety of cell functions, particularly those involving interactions between cells and ECM. ECM proteolysis is a crucial step during cancer stages and FN strong susceptibility to proteolytic degradation is well documented. Indeed, several studies have related FN levels to tumor progression in cancer patients, observing an increase of both FN and FN fragments levels. In parallel, some research has, on the other hand, provided evidence of protective roles of fragments derived from FN.

Based on the literature that has been dedicated to the subject, it was established as objective of this work the study of the role of FN in tumor development and progression. For this purpose, an experimental work was developed arising from the establishment of two groups within each cell line used – tumor cell lines HCT15 and HeLa, and CHO –, differing in the levels of FN produced. *In vitro* and *in vivo* assays were performed and the results compared between groups.

Our findings suggested a correlation between higher FN levels and a more aggressive behavior of cells in a neoplastic context, *in vitro*. *In vivo*, the opposite was observed. It is recommended, however, the validation of the *in vivo* models under improved technical conditions. Nevertheless, the sequence of a fragment detected appeared to be relevant for further investigation.

Keywords: cancer, metastasis, tumor microenvironment, fibronectina (FN), fibronectin fragments.

Table of contents

Index of figures **17-18**

Index of tables **18**

List of abbreviations **19, 20**

1. Introduction **21-34**

1.1 Cancer biology 21-23

1.2 Extracellular matrix and cancer 23-28

1.2.1 Fibronectin 24-26

1.2.2 Extracellular matrix proteolysis: matrix metalloproteinases 26-28

1.3 Other intervenients in the tumorigenic process 28-31

1.3.1 Growth factors and cancer progression 28-30

1.3.2 Tumor microenvironment: bone marrow-derived cells 30, 31

1.4 Metastasis 31, 32

1.5 Fibronectin and the neoplastic process 32-34

2. Aims **35**

3. Material and Methods **36-53**

3.1 Biological materials 36

3.2 Methods 36-53

3.2.1 Construction of pcDNA3 - full-length *fibronectin* (pcDNA3-fl*FN*) expression vector and stable transfection of HCT15, HeLa and CHO cell lines 36-43

3.2.1.1 Amplification of *FN* coding sequence 36-40

3.2.1.1.1 Reverse transcription polymerase chain reaction (RT-PCR) 37

3.2.1.1.2 Expand long template PCR 37-40

3.2.1.1.2.1 DNA sequencing 39, 40

3.2.1.2 Plasmid construction and cloning 40

3.2.1.3 Plasmid isolation 41-42

3.2.1.3.1 Restriction endonucleases digestion 41

3.2.1.3.2 PCR 42

3.2.1.4 Stabel transfection of HCT15, HeLa and CHO cell lines 43

3.2.1.4.1 Cell culture 43

3.2.1.4.2 Transfection 43

3.2.2 *In vitro* assays 44-49

3.2.2.1 Real-time PCR for *FN* 44

3.2.2.2 Immunoprecipitation 45

3.2.2.3 SDS-PAGE (sodium dodecyl sulfate-polyacrilamide gel electrophoresis) and western blotting 45, 46
3.2.2.4 Immunofluorecence 46, 47
3.2.2.5 Zymography 47, 48
3.2.2.6 *In vitro* wound healing assay 48
3.2.2.7 *In vitro* tube formation assay 48
3.2.2.8 Real-time PCR for *VEGF-121*, *VEGF-165* and *VEGF-189* 49
3.2.2.9 Real-time PCR for *KDR*, *FLT-1*, *Angiopoietin-1*, *Angiopoietin*-2, *SCF* and *SDF-1* . 49
3.2.3 *In vivo* assays 50-52
3.2.3.1 Orthotopic xenograft tumors induction 50
3.2.3.2 Flow cytometric analysis of endothelial and hematopoietic progenitor cells 50, 51
3.2.3.3 Animals euthanasia 51
3.2.3.4 Western blotting 51
3.2.3.5 Histological analysis 51, 52
4. Results **54-79**
4.1 *IN VITRO* assays 54-73
4.1.1 Quantification of *FN* expression by real-time PCR 54
4.1.2 Evaluation of FN expression by western blotting 55-58
4.1.3 Expression of FN, integrins and tenascin-C by immunofluorescence 58-66
4.1.4 Evaluation of MMPs activity by zymography 66, 67
4.1.5 Evaluation of cell migration by wound healing assay 67-79
4.1.6 Angiogenesis assays: tube formation assay, real-time PCR for *VEGF-121*, *VEGF-165* and *VEGF-189*, *KDR*, *FLT-1*, *Angiopoietin-1* and *Angiopoietin-2* 69-72
4.1.7 Quantification of *SCF* and *SDF-1* expression by real-time PCR 72, 73
4.2 *IN VIVO* assays 73-79
4.2.1 Flow cytometric analysis of endothelial and hematipoietic progenitor cells 73, 74
4.2.2 Evaluation of FN expression in the serum of the animal models by western blotting 74, 75
4.2.3 Histological analysis 75-79
4.2.3.1 Tumor cells detection 75-77
4.2.3.2 Detection of E-cadherin in xenograft tumors 78
4.2.3.3 Detection of mast cells in xenograft tumors 79
5. Discussion **80-85**
5.1 Future perspectives 85
6. Conclusions **86**
7. References **87-95**
Appendices **97-101**

Index of figures

Figure 1 - Schematic representation of fibronectin and its main binding sites 26

Figure 2 - Real-time-PCR for *FN* expression 54

Figure 3 - Western blotting of FN immunoprecipitated from CHO media supernatants 55

Figure 4 - Western blotting of FN immunoprecipitated from HCT15 media supernatants 56

Figure 5 - Western blotting of FN immunoprecipitated from HeLa media supernatants ... 57, 58

Figure 6 - Immunofluorescence for FN, α3, β1 and β3 integrins, and tenascin-C in CHO ... 59, 60

Figure 7 - Immunofluorescence for FN, α3, β1 and β3 integrins, and tenascin-C in HCT15. 62, 63

Figure 8 - Immunofluorescence for FN, α3, β1 and β3 integrins, and tenascin-C in HeLa .. 64, 65

Figure 9 - Zymography of CHO, HCT15 and HeLa media supernatants 66

Figure 10 - Wound healing assay 67, 68

Figure 11 - Tube formation assay with conditioned medium from CHO cell line 69

Figure 12 - Tube formation assay with conditioned medium from HCT15 cell line 70

Figure 13 - Real-time-PCR for *VEGF* isoforms expression in HCT15..... 70

Figure 14 - Real-time-PCR for *KDR*, *FLT-1*, *Angiopoietin-1 (ANGIOP1)* and *Angiopoetin-2 (ANGIOP2)* in HCT15..... 70

Figure 15 - Tube formation assay with conditioned medium from HeLa cell line 71

Figure 16 - Real-time-PCR for *VEGF* isoforms expression in HeLa 71

Figure 17 - Real-time-PCR for *KDR*, *FLT-1*, *Angiopoietin-1 (ANGIOP1)* and *Angiopoetin-2 (ANGIOP2)* in HeLa 71

Figure 18 - Tube formation assay control experiment with supplemented Alfa-MEM medium and Alfa-MEM medium + FN (1:1000) 72

Figure 19 - Real-time-PCR for *SCF* and *SDF-1* in HCT15 73

Figure 20 - Real-time-PCR for *SCF* and *SDF-1* in HeLa 73

Figure 21 - Flow cytometric analysis of endothelial progenitor cells (Sca+,Flk+ cells) for mice inoculated with HCT15 73

Figure 22 - Flow cytometric analysis of hematopoietic progenitor cells (cKit+) for mice inoculated with HCT15 73

Figure 23 - Flow cytometric analysis of endothelial progenitor cells (Sca+,Flk+ cells) for mice inoculated with HeLa..... 74

Figure 24 - Flow cytometric analysis of hematopoietic progenitor cells (cKit+) for mice inoculated with HeLa 74

Figure 25 - Western blotting of FN immunoprecipitated from the serum of xenograft orthotopic BALB/c-SCID 74

Figure 26 - Macroscopic observation of xenograft orthotopic BALB/c-SCID inoculated with HCT15 75

Figure 27 - Macroscopic observation of xenograft orthotopic BALB/c-SCID inoculated with HeLa..... 75

Figure 28 - Immunoreactivity for cytokeratin-19 (CK-19) in xenograft orthotopic BALB/c-SCID inoculated with control (Ctl) and transfected (FN) HCT15..... 76

Figure 29 - Immunoreactivity for cytokeratin-7 (CK-7) and H&E (Hematoxylin and Eosin) in xenograft orthotopic BALB/c-SCID inoculated with control and transfected HeLa 77

Figure 30 - Immunofluorescence for E-cadherin in the primary tumor of xenograft orthotopic BALB/c-SCID 78

Figure 31 - Toluidine blue staining for mast cells in the primary tumor of xenograft orthotopic BALB/c-SCID 79

Figure 32 - Map of pcDNA3-fl*FN* 101

Index of tables

Table 1 - Program used for the cDNA synthesis 37

Table 2 - Program used for *FN* Expand PCR 38

Table 3 - Program used for sequencing reaction 40

Table 4 - Program used for PCR 42

Table 5 - Program used for real-time PCR 44

Table 6 - Primers and probes used during the experimental work 53

List of abbreviations

ANGIOP1 – Angiopoietin-1

ANGIOP2 – Angiopoietin-2

BM – Bone marrow

BSA – Bovine serum albumine

CDK – Cyclin-dependent kinase

cDNA – Complementary DNA

cFN – Cellular fibronectin

CHO – Chinese hamster ovary (cells)

CK-19 – Cytokeratin-19

CK-7 – Cytokeratin-7

CKI – Cyclin-dependent kinase inhibitor

ddNTPs – Dideoxynucleotides

DNA – Deoxyribonucleic acid

dNTPs – Deoxynucleotides

ECM – Extracellular matrix

EGF – Epidermal growth factor

EGFR – Epidermal growth factor receptor

EMT – Epithelial-mesenchymal transition

EPC – Endothelial progenitor cell

FBS – Fetal bovine serum

FCM – Flow cytometry

FGF – Fibroblast growth factor

FGFR – Fibroblast growth factor receptor

FI – Type I fibronectin module

FII – Type II fibronectin module

FIII – Type III fibronectin module

fIFN – full length fibronectin

FLK-1 – Fetal liver kinase-1

FLT-1 – Fms-like tyrosine kinase-1

FLT-4 – Fms-like tyrosine kinase-4

FN – Fibronectin/*fibronectina*

GRGDS – gly-arg-gly-asp-ser (glycine-arginine-glycine-aspartic acid-serine)

H&E – Hematoxylin and eosin

HER-2 – Human epidermal growth factor receptor 2

HPC – Hematopoietic progenitor cell

HUVEC – Human umbilical vein endothelial cell

IGF – Insulin-like growth factor

KDR – Kinase insert domain receptor

MDSC – Myeloid-derived suppressor cell

MEC – *Matriz extracelular*

MET – Mesenchymal-epithelial transition

MMP – Matrix metalloproteinase

MPM – *Metaloprotease de matriz*

mRNA – Messenger RNA

PBS – Phosphate buffered saline

PCR – Polymerase chain reaction

pFN – Plasma fibronectin

PIGF – Placenta growth factor

RGD – arg-gly-asp (arginine-glycine-aspartic acid)

RNA – Ribonucleic acid

rRNA – Ribosomal RNA

RT – Reverse transcription

SCF – Stem cell factor

SDF-1 – Stromal cell-derived factor-1

SDS-PAGE – Sodium dodecyl sulfate-polyacrylamide gel electrophoresis

sFN – Superfibronectin

TBS – Tris buffered saline

TGF-β – Transforming growth factor-β

UV – Ultra-violet

VCAM-1 – Vascular cell adhesion-1

VEGF – Vascular endothelial growth factor

VEGFR – Vascular endothelial growth factor receptor

1. Introduction

1.1 Cancer biology

Tumorigenesis is a multistep process. Its stages reflect genetic alterations that drive the progressive transformation of normal human cells into highly malignant derivatives (Hanahan & Weinberg, 2000; Renan, 1993). The vast catalog of cancer types is defined as having several properties, also termed "hallmarks", that collectively define cancer: self-sufficiency in growth signals, insensitivity to antigrowth signals, evasion of programmed cells death (apoptosis), limitless replicative potential, sustained angiogenesis, and tissue invasion and metastasis (Hanahan & Weinberg, 2000; Hanahan & Weinberg, 2011).

Evading immune system and reprogramming of metabolism are also two emerging hallmarks of cancer (Hanahan & Weinberg, 2011). In fact, with regard to evading immune system, solid tumors seem to avoid detection or limit the extent of the immune system action, responsible for recognizing and eliminating the majority of incipient cancer cells (Hanahan & Weinberg, 2011). Other evidences have revealed that cancer cells are able to reprogram their glucose metabolism, and thus their energy production, by limiting their energy metabolism largely to glycolysis, even under aerobic conditions (DeBerardinis *et al*, 2008; Hanahan & Weinberg, 2011). Although this metabolic switch represents a disadvantage in metabolic terms, increased glycolysis allows the diversion of glycolytic intermediates into various biosynthetic pathways, including those generating nucleosides and amino acids, facilitating the biosynthesis of the macromolecules and organelles required for assembly of new cells (Hanahan & Weinberg, 2011; Vander Heiden *et al*, 2009).

All these attributes of cancer result from a dynamical interaction between tumor cells and its microenvironment.

In fact, for a long time only the neoplastic cells were the focus of interest in cancer research; the stroma was rather considered a reactive component without major significance (Wernert, 1997). Research on the underlying mechanisms of cancer has, however, changed the level of importance ascribed to the tumor stroma (Kessenbrock *et al*, 2010; Tlsty & Coussens, 2006; Werb, 1997; Wernert, 1997). This is now considered to be an integral part of a neoplasm, perceived then as a complex tissue composed of multiple distinct cell types that participate in heterotypic interactions, creating the concept of tumor microenvironment (reviewed in Hanahan & Weinberg, 2011).

Besides the paracrine mode of action of growth factors that dominates physiological processes, in which cells require exogenous mitogenic growth signals to proliferate, many

tumor cells acquire the ability to generate growth factors to which they are responsive – autocrine stimulation (Sporn & Todaro, 1980; Witsch *et al*, 2010). Along with such autocrine loops, other mechanisms may also lead to constitutive pathway activation in tumors; at the receptor level, overexpression may enable cancer cells to become hyper-responsive to growth factors (for example, epidermal growth factor receptor (EGFR) in head and neck cancer), whereas specific mutations can elicit ligand-independent signaling (for example, brain tumor mutants of EGFR) (Di Fiore *et al*, 1987; Hanahan & Weinberg, 2000; Huang *et al*, 1997; Witsch *et al*, 2010); also the switch of the types of extracellular matrix (ECM) receptors cancer cells express, favoring ones that transmit progrowth signals, contributes to tumor self-sufficiency in growth signals (Lukashev & Werb, 1998).

Loss of sensitivity to anti-growth signals complements the first hallmark of cancer by leading also to unchecked growth (Hanahan & Weinberg, 2000). Cell cycle involves multiple checkpoints that assess extracellular growth signals, cell size and DNA integrity, in which cyclin-dependent kinases (CDKs) and cyclins act by inducing cell cycle progression, and CDKs inhibitors (CKIs) act as negative regulators (Park & Lee, 2003). Deregulation of the cell cycle is one of the most frequent alterations during tumor development (Evan & Vousden, 2001; Park & Lee, 2003).

Cancer cells must also evade antiproliferative signals by turning off expression of integrins and other cell adhesion molecules that send antigrowth signals, favoring instead those that convey progrowth signals, and by avoiding terminal differentiation, for which mutations in the various proliferative control pathways can contribute additionally (Hanahan & Weinberg, 2000).

The ability of tumor cell populations to expand in number is also determined by the resistance to apoptosis. The most common strategy to avoid apoptosis is a mutation involving the *p53* tumor suppressor, resulting in the removal of a key component of the DNA damage sensor that can induce the apoptotic effector cascade (Hanahan & Weinberg, 2000; Harris, 1996; Levine, 1997).

The loss of capacity for senescence leads tumor cells to limitless replicative potential (immortality), an essential feature for malignant growth state, achieved by telemore maintenance, which, in turn, results, in most cases, from the upregulating expression of telomerase, an enzyme that adds hexanucleotide repeats onto the ends of telomeric DNA, maintaining the telomeres at a length above a critical threshold, permitting unlimited multiplication of descendant cells (Bryan *et al*, 1995; Hanahan & Weinberg, 2000; Hayflick, 1997).

Tumor cells initially lack angiogenic ability (Folkman, 1992; Hanahan & Weinberg, 2000). In order to expand in size, inicipient neoplasias must develop angiogenic ability, which seems to be acquired in a discrete step during tumor development, via an "angiogenic switch" (Hanahan & Folkman, 1996). That activation appears to occur by changing the balance of angiogenesis inducers and countervailing inhibitors (Hanahan & Folkman, 1996). This common shifting usually involves altered gene transcription. Many tumors show increased expression of *vascular endothelial growth factor* (*VEGF*) and/or *fibroblast growth factors* (*FGFs*), compared to normal tissues. The downregulation of endogenous inhibitors, such as thrombospondin-1 or β-interferon is also frequent (Hanahan & Weinberg, 2011; Singh *et al*, 1995).

After the ability of tumor to grow beyond the limitations of passive nutrient diffusion, conferred by the acquisition of sustained angiogenesis, primary tumor masses release pioneer cells that invade adjacent tissues, and circulate, through bloodstream, to distant sites, where they may form new tumors, known as metastases (Kawaguchi, 2005; Sporn, 1996).

1.2 Extracellular matrix and cancer

Extracellular matrix (ECM) is a complex mixture of proteins and polysaccharides that are secreted locally and assembled into an organized network in close association with the surface of the cell that produced them (Alberts *et al*, 2002; Mosher *et al*, 1992; Pupa *et al*, 2002). Two main classes of extracellular macromolecules make up the matrix: polysaccharide chains of the class called glycosaminoglycans, which are usually found covalently linked to protein in the form of proteoglycans, and fibrous proteins, including collagen, elastin, fibronectin, and laminin, which have both structural and adhesive functions (Alberts *et al*, 2002).

ECM provides structural and mechanical support to cells and tissues, and is also able to influence and interact with cells in the environment (Mosher *et al*, 1992; Pupa *et al*, 2002). The structural and regulatory molecules of the ECM function cooperatively to regulate a wide variety of cell processes such as growth, death, adhesion, migration, invasion, gene expression and differentiation (Assoian & Marcantonio, 1996; Pupa *et al*, 2002). These cell events, in turn, regulate physiological processes such as embryonic development, tissue morphogenesis and angiogenesis, and also, in certain circumstances, pathological processes (Assoian & Marcantonio, 1996; Mosher *et al*, 1992; Pupa *et al*, 2002).

The tumor stroma contains a variety of macromolecules, most of which constitute the ECM: proteins, metalloproteins, glycoproteins, proteoglycans, proteases and their activators and

inhibitors, plus a variety of cells, including organ host specific cells, endothelial cells, pericytes, immune cells and fibroblasts (Desoize, 2004).

Immune cells include granulocytes, dendritic cells, macrophages, natural killer cells, and mast cells, are components of premalignant and malignant tissues and contribute functionally to cancer development largely due to their release of soluble mediators that regulate cell proliferation, migration, blood vessels formation, tissue remodeling, metabolism, and genomic integrity (Bissell & Radisky, 2001; Tlsty, 2001; Tlsty & Coussens, 2006). Fibroblasts are primarily responsible for the synthesis, deposition, and remodeling of ECM, and for the production of many soluble paracrine growth factors that regulate cell proliferation, morphology, survival, and death (Allinen *et al*, 2004; Tlsty & Coussens, 2006). Blood vessels play a crucial role in maintaining tissue homeostasis and in metastasis (Ronnov-Jessen *et al*, 1996; Tlsty & Coussens, 2006).

Reciprocal interactions among normal cells, their mediators, components of the ECM, and genetically altered neoplastic cells regulate all aspects of tumorigenicity.

1.2.1 Fibronectin

Fibronectin (FN) is a high molecular weight, multidomain glycoprotein (approximately 440 kDa). A single gene codifies the FN protein core, but alternative splicing of its pre-mRNA leads to the expression of several isoforms (Kornblihtt *et al*, 1996; Pankov & Yamada, 2002).

Based on its solubility, FN can be subdivided into two forms: soluble plasma FN (pFN) and less-soluble cellular FN (cFN). Plasma FN is a major protein component of blood plasma (300 µg/ml), being also present in other body fluids, it is synthesized mostly in the liver, by hepatocytes, and shows a relatively simple splicing pattern. Cellular FN is a key component of the extracellular matrix (ECM), secreted by several types of cells, primarily fibroblasts; it consists of a much larger and more heterogeneous group of FN isoforms resulting from cell type-specific and species-specific splicing patterns (Hynes & Yamada, 1982; Klein *et al*, 2004; Pankov & Yamada, 2002; Tamkun & Hynes, 1983).

FN exists, generally, as a dimer, composed of two nearly identical polypeptide chains covalently linked by a pair of C-terminal disulfide bonds. Each monomer has a molecular weight of 230–250 kDa and forms a mosaic protein filled almost entirely with three types of repeating units or modules: type I (FI), type II (FII) and type III (FIII) (figure 1) (Hynes & Yamada, 1982; Pankov & Yamada, 2002; Potts & Campbell, 1996). FN contains 12 FI modules, 2 FII and 15-17 FIII, accounting together for approximately 90% of the FN sequence (Pankov & Yamada, 2002; Potts & Campbell, 1996). The carbohydrates constitute 4-9% of FN molecule, depending

on the cell source of the molecule. Their function on the molecule appears to be the stabilization of the molecule and the protection of specific regions against the proteolytic attack and abnormal turnover rates (Seppa *et al*, 1981).

FI module contains approximately 45 amino acids with four cysteines forming two disulfide bonds. FII module is about 60 residues long and comprises two intrachain disulfide bonds. FIII module is about 90 amino acids in length and does not contain disulfide bonds. The three repeating units are also found in a wide range of vertebrate proteins, suggesting that FN evolved through exon shuffling (Hynes & Yamada, 1982; Kornblihtt *et al*, 1996; Patel *et al*, 1987; Potts & Campbell, 1996).

FN has been implicated in a wide variety of cell functions, particularly those involving interactions between cells and ECM. This glycoprotein plays important roles in cell adhesion, morphology and spreading, cytoskeletal organization, cell migration, growth and differentiation, phagocytosis, hemostasis and embryonic development in vertebrates (Hynes & Yamada, 1982; Kornblihtt *et al*, 1996; Labat-Robert, 2002).

FN receptors are integrins – heterodimeric, transmembrane cell adhesion receptors, composed of two distinct glycoprotein chains, called the α (alpha) and β (beta) subunits, that mediate the attachment between ECM and cytoskeleton, playing also a role in cell signaling (Akiyama, 1996; Akiyama *et al*, 1995). Several integrins recognize FN: α5β1, α8β1, α3β1, αvβ1, αvβ3, αvβ6, αIIbβ3, and α4β1. Only α5β1 recognizes specifically FN, through its RGD (Arg-Gly-Asp) sequence, located in the tenth FIII ($FIII_{10}$) of the molecule; other integrins bind FN via the RGD sequence but bind also other ligands. Other sites recognized by α5β1 are located in $FIII_9$ and in an N-terminal fragment containing repeats FI_{1-9} and FII_{1-2} (figure 1) (Akiyama *et al*, 1995; Akiyama *et al*, 1989; Labat-Robert, 2002; Pankov & Yamada, 2002).

Determination of integrin binding sites as well as of other important domains within the FN was greatly facilitated by the evidence that all FNs are cleaved only in specific regions when subjected to limited proteolytic digestion. FN binding activities are frequently preserved after such proteolysis (Akiyama *et al*, 1995; Hynes & Yamada, 1982; Pankov & Yamada, 2002). In fact, it has long been recognized that the functionality of FN is dissectable, and binding sites for a wide range of molecules have been associated with various fragments (Potts & Campbell, 1996).

Besides binding to cell surface through integrins, FN also interacts with several biologically important molecules, including heparin, collagen/gelatin and fibrin, and also some bacteria, being those interactions mediated by several distinct structural and functional domains (figure 1). N-terminal domain has a central role in a number of important physiological processes: it

contains both covalent and a non-covalent fibrin binding sites, being the major site formed by $FI_{4,5}$, and also binds to some bacteria; FI_{1-5}, located in this domain, plays an important role in matrix assemby; heparin-binding sites are located also in the N-terminal end of the protein and in the C-terminal part (Hynes & Yamada, 1982; Mosher *et al*, 1991; Potts & Campbell, 1996). FIII modules also play a role in matrix assembly and heparin binding (Potts & Campbell, 1996). The collagen-binding domain include repeats FI_{6-9} and $FII_{1,2}$ (Leikina *et al*, 2002; Pankov & Yamada, 2002).

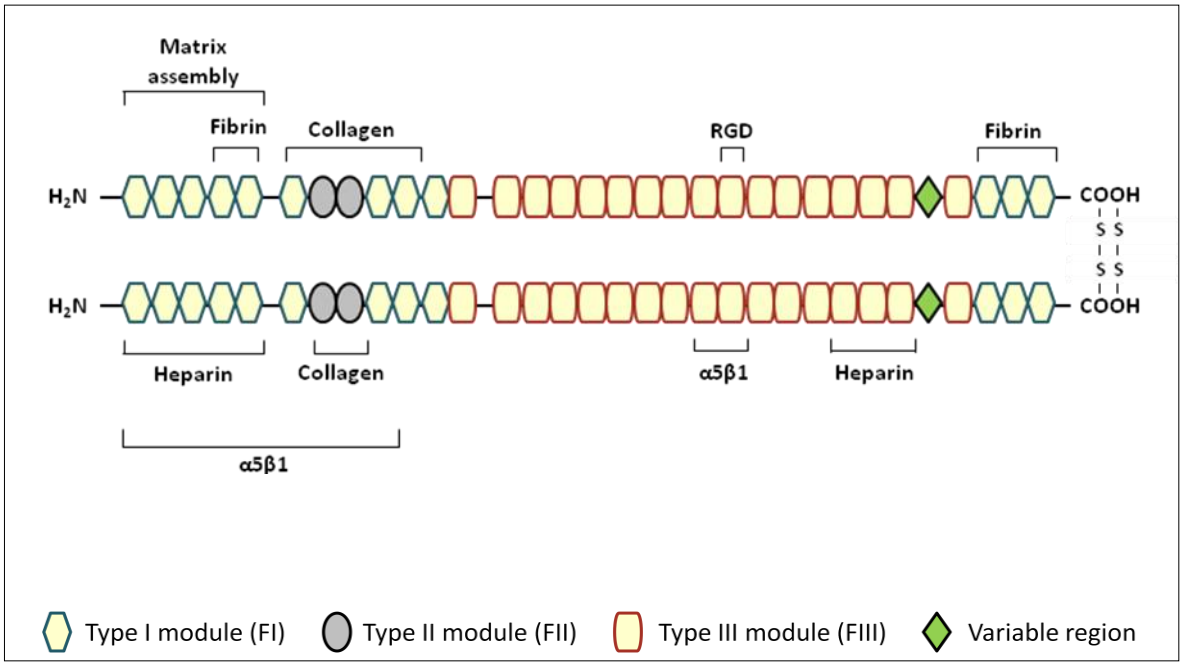

Figure 1 – Schematic representation of fibronectin and its main binding sites.

1.2.2 Extracellular matrix proteolysis: matrix metalloproteinases

Cell-cell and cell-ECM interactions provide cells with information essential for controlling morphogenesis, cell fate specification, gain or loss of tissue-specific functions, cell migration, tissue repair, and cell death. Degradation or activation of cell surface and ECM proteins by proteolysis can mediate rapid and irreversible changes in the cellular microenvironment (Werb, 1997).

Proteolysis plays an important role in regulating ECM formation and its structure remodeling, and in releasing of bioactive fragments and growth factors during growth, morphogenesis, and tissue repair. However, a deficient proteolytic activity, such as the excessive production of proteases, leads to the occurrence of pathological processes (Bugge *et al*, 1996).

Malignant transformation deeply modifies the cell-cell and cell-ECM interactions. These alterations are globally defined as stromal reaction (Desoize, 2004; Labat-Robert, 2002; Wernert, 1997).

Tumor growth, angiogenesis, invasion and metastasis are greatly dependent on the permissive nature of the microenvironment (Chambers & Matrisian, 1997; Polette *et al*, 2004). During these stages, ECM proteolysis represents a crucial step. Cancer cells and other cells belonging to the tumor stroma secrete, activate and/or induce high levels of proteolytic enzymes degrading ECM and cell-associated proteins. The main enzymes that degrade ECM are tissue serine proteinases, including tissue plasminogen activator, urokinase, thrombin and plasmin, and the matrix metalloproteinases (MMPs) (Werb, 1997). Blocking the function of ECM proteases can decrease tumor growth, while their ectopic expression can increase carcinogenic potential, which suggests their contribution to the neoplastic process (Martin *et al*, 1996; Werb, 1997; Wilson *et al*, 1997). Some proteases, however, may inhibit tumorigenesis by inducing apoptosis or by releasing latent angiogenic inhibitors (Kaspar *et al*, 2006; Martin & Matrisian, 2007; Werb, 1997; Wilson *et al*, 1997).

MMPs are a family of zinc-dependent endopeptidases produced by a number of cell types, capable of cleaving several macromolecules of the ECM, including FN (Giavazzi & Taraboletti, 2001; Klein *et al*, 2004). MMPs are required for several normal physiological processes, including the skeletal and cardiovascular development, but also in diverse conditions and diseases, such as skeletal dysplasias, cardiovascular diseases, arthritis (Malemud, 2006). These enzymes represent also the most prominent family of proteases associated with tumorigenesis, where they play crucial functions in the molecular communication between tumor and stroma (Kessenbrock *et al*, 2010). MMP-2 and MMP-9 are thought to be the most important MMPs in metastasis (Coussens *et al*, 2002; Klein *et al*, 2004; Malemud, 2006; Stetler-Stevenson, 1999).

Based on their structure and substrate specificity, MMPs are divided into five groups: collagenases, gelatinases, stomelysins, membrane-type MMPs and the others (MMPs not fully characterized). The substrates of collagenases substrates are mainly collagens; gelatinases mostly hydrolyze components of the basal lamina, gelatin and collagen type IV; and stromelysins mainly hydrolyze elastin and collagens types IV, V, XI and X; membrane-type MMPs are not grouped for their substrate specificity, but because they are all membrane bound (Klein *et al*, 2004; Vihinen & Kahari, 2002).

During the neoplastic process, MMPs are produced mostly by tumor stroma cells and by tumor cells themselves (Page-McCaw *et al*, 2007). Their best known function is the degradation of ECM macromolecules, which permits to uncover or release cryptic sites of ECM

macromolecules that function to modulate a cellular response – matricryptic sites or matrikins – and which facilitates, thereby, the tumor cells migration and invasion (Polette *et al*, 2004). More recently, MMPs functions were, however, extended, being now recognized a more complex role in this context, although their role in the process of cancer is first attributed to their degradative capacity (Klein *et al*, 2004): MMPs also act as key regulators of various neoplastic processes, due to their abilities to mediate differentiation, proliferation and survival of tumor cells (Kenny *et al*, 2008; Lakka *et al*, 2003), to release growth factors from cell surfaces and reservoirs contained in the ECM, and to regulate tumor angiogenesis, mediating, therefore, great alterations in the microenvironment during tumor progression (Chantrain *et al*, 2004; Kenny *et al*, 2008). In tumor angiogenesis, the main role for MMPs is degradation of ECM, which can result in migration of tumor cells as well as of endothelial cells, due to loss of cell-matrix contacts and cell-cell contacts, and release and/or activation of pro-angiogenic growth factors from ECM and/or inactive complexes, resulting in new vessel formation locally, although, almost simultaneously, negative regulators of angiogenesis, including MMP-inhibiting fragments are formed through ECM degradation to control the local process of new vessel formation (Cao, 2001; Colorado *et al*, 2000; Klein *et al*, 2004; Nguyen *et al*, 2001). By regulating angiogenesis, MMPs become, consequently, important players in tumor growth and metastasis, for which these endopeptidases also contribute more directly enabling – again due to their degradative capacity – tumor cells to migrate and colonize host tissues (Klein *et al*, 2004).

1.3 Other intervenients in the tumorigenic process

1.3.1 Growth factors and cancer progression

Growth factors are compact polypeptides which bind to transmembrane receptors harboring kinase activity to stimulate specific combinations of intracellular signaling pathways, mediating the interplay between tumors and the ECM and non-cancer cells (Witsch *et al*, 2010).

In the neoplastic context, growth factors assume a relevant role by representing the major regulators of all subsequent steps of tumor progression, after tumor initiation, instigated by oncogenic mutations, namely clonal expansion, invasion, angiogenesis and metastasis (Perona, 2006; Witsch *et al*, 2010).

The majority of growth factors receptors are single-pass transmembrane proteins harboring an intracellular tyrosine kinase domain (Perona, 2006; Witsch *et al*, 2010). Evidences have shown a critical involvement of tyrosine kinase receptors in the development and progression of human cancers (Zwick *et al*, 2001). Constitutive activation of tyrosine kinase receptors,

which has been shown to be important for malignant transformation and tumor proliferation, can occur by several mechanisms, being, in most cases, gene amplification, overexpression or mutations the main responsible for the acquired oncogenic potential of RTKs (Kolibaba & Druker, 1997; Zwick *et al*, 2001).

Epidermal growth factor (EGF), insulin-like growth factor (IGF), transforming growth factor-β (TGF-β), fibroblast growth factor (FGF) and vascular endothelial growth factor (VEGF) are some of the relevant growth factor families in tumor progression (Perona, 2006; Witsch *et al*, 2010).

Several FGFs have been identified as genes isolated from tumors due to their ability to induce proliferation or transformation of fibroblasts, which indicated a role in tumorigenesis (Kornmann *et al*, 1997; Zwick *et al*, 2001). Studies have demonstrated that alterations in the expression patterns of FGFs may contribute to growth deregulation of human tumor cells: expression of FGF-1 and FGF-2 in fibroblasts leads to transformation and tumor formation in nude mice; interferences with growth factor action have also resulted in impaired tumor growth (Auguste *et al*, 2001; Wang & Becker, 1997; Zwick *et al*, 2001). Changes at the level of FGFs receptors (tyrosine kinase receptors), have also been identified in a variety of human tumors: for instance, FGFR overexpression was observed in breast, prostate, melanoma, thyroid and salivary gland tumors (Giri *et al*, 1999; Shingu *et al*, 1998; Zwick *et al*, 2001); somatic mutations in FGFR-3 have been identified in bladder cancer and multiple myeloma (Cappellen *et al*, 1999; Chesi *et al*, 1997; Zwick *et al*, 2001).

VEGF is one of the main inducers of endothelial cell proliferation and permeability of blood vessels, regulating, therefore, angiogenesis and vasculogenesis (Witsch *et al*, 2010; Zwick *et al*, 2001). This growth factors family consists of five glycoproteins, VEGFA (VEGF), VEGFB, VEGFC, VEGFD and PIGF (placenta growth factor), which bind at least to one of the three VEGF receptors, FLT-1 (VEGR-1), KDR (VEGFR-2, FLK-1) and FLT-4 (VEGFR-3). Several studies have provided evidence for the role of VEGF-VEGFR ligand-receptor system in tumor vascularization and metastasis (Padro *et al*, 2002; Trojan *et al*, 2004; Zwick *et al*, 2001). VEGF has been detected in different types of tumors. Besides the proangiogenic effects, which confer to VEGF a pivotal role in maintaining the tumor growth by facilitating growth of new blood vessels (Perona, 2006), VEGF exerts independent of vascular processes, such as autocrine effects on tumor cell function (survival, migration, invasion), immune suppression and recruitment of bone marrow progenitors, which may dictate organ-specific tumor spread by homing to tumor-specific premetastatic sites and forming clusters that provide a permissive niche for incoming tumor cells (Kaplan *et al*, 2005; Santos & Dias, 2004; Serpa *et al*, 2010; Tammela *et al*, 2005). Expression of FLT-1 (VEGR-1) and KDR (VEGFR-2, FLK-1) has been detected on subsets of solid tumors and the activation of FLT-1 (VEGR-1) in breast cancer cells supports

their growth and survival (Witsch *et al*, 2010; Wu *et al*, 2006). Overexpression of VEGF and KDR (VEGFR-2, FLK-1) was also observed in the bone marrow of patients with acute myeloid leukemia (Padro *et al*, 2002).

1.3.2 Tumor microenvironment: bone-marrow-derived cells

Bone marrow (BM) contributes to the tumor microenvironment and recent studies have suggested that BM-derived microenvironments exert a direct impact in tumor pathophysiology (Gao & Mittal, 2009; Witsch *et al*, 2010). Growing tumors secrete growth factors into the peripheral circulation, causing the marrow microenvironment to acquire a highly pro-angiogenic and protumorigenic environment, which promotes the mobilization of vascular, pericyte and hematopoietic progenitors, further recruited to the tumors, modifying the neoplastic properties of the malignant tumor cells (Gao & Mittal, 2009; Kopp *et al*, 2005).

Of the BM-derived cells, much focus has been directed towards the pro-angiogenic hematopoietic cells, which exert their functions perivascularly through the paracrine release of pro-angiogenic cytokines (Gao & Mittal, 2009; Kopp *et al*, 2006; Lyden *et al*, 2001).

Among the cells of the myeloid lineage, macrophages are prominent cells of the immune system that are recruited to tumors. Increased macrophage infiltration correlates with tumor stage and poor survival (Gao & Mittal, 2009; Torisu *et al*, 2000). BM-derived pericytes, vascular smooth muscle cells and mural cells stabilize nascent blood vessels by intimate perivascular association and contribute to neovascularization (Gao & Mittal, 2009; Song *et al*, 2005). BM-derived mast cells have been implicated in tumor growth and invasion and associated with poor prognosis, being an abundant source of angiogenic factors, including VEGF and TGF-β, and MMP-9 (Theoharides & Conti, 2004).

BM-derived endothelial progenitor cells (EPCs) contribute to neoangiogenesis by providing an alternative source of endothelial cells that contribute to neovessel formation, namely through paracrine secretion of proangiogenic growth factors as well as by direct luminal incorporation into sprouting nascent vessels (Lyden *et al*, 2001; Witsch *et al*, 2010).

BM myeloid-derived suppressor cells (MDSCs) also contribute to tumor pathophysiology by participating in tumor immunity, inflammation and evasion or resistance to therapy. MDSCs, whose levels are often elevated in cancer patients, comprehend a heterogeneous group of cells that contribute to tumor escape, immune tolerance and suppression and also to TGF-β-mediated metastasis (Gao & Mittal, 2009; Yang *et al*, 2008). These BM-derived cells have also been shown to provide resistance to immunotherapeutics by blocking immune responses

through suppression of antibody-producing B cells, CD4+ T cells and CD8+ T cells (Nagaraj *et al*, 2007).

1.4 Metastasis

A major cause of morbidity and death due to cancer is the metastasis of cells from the primary tumor to distant sites where secondary tumors become established (Akiyama *et al*, 1995).

Primary tumors are originally incapable of invading the surrounding tissue. In the course of the disease the tumor mass becomes heterogeneous: primary tumor cells accumulate genetic alterations and interact with the local microenvironment (Scheel *et al*, 2007; Voulgari & Pintzas, 2009). As a result, some cells detach from neighboring ones, migrate and locally invade the surrounding tissue. Further access to the vascular or lymphatic systems leads to their dissemination in the body and finally to the re-establishment at distant sites. The first and determinant step of this process is the local invasion through the epithelial basement membrane, as it requires modifications in cell-cell and cell-matrix interactions, remodeling of the ECM, modifications of the cytoskeleton and enhancement of cell motility (Voulgari & Pintzas, 2009). However, not all types of cancer are capable of fulfilling these activities. This fact hypothesized that specific events induce a loss of epithelial and a gain of dedifferentiated mesenchymal-like phenotype – epithelial-mesenchymal transition (EMT) (Hugo *et al*, 2007; Voulgari & Pintzas, 2009).

EMT, which represents a key step of embryogenesis, consists of the culmination of protein modification and transcriptional events in response to a defined set of extracellular stimuli leading to a cellular change (Hugo *et al*, 2007). Core elements of EMT include reduction of cell-cell adherence via transcriptional repression and delocalization of cadherins (adherens junctions), occluding and claudin (tight junctions) and desmoplakin (desmosomes) (Hugo *et al*, 2007; Klymkowsky, 2005). Circumferential F-actin fibres of the cytoskeleton are replaced by a network of stress fibers, at the tips of which ECM adhesion molecules localize. Matrix metalloproteinases (MMPs) are frequently upregulated, enabling cells to detach from each other (via E-cadherin cleavage) and to penetrate the basement membrane. These genetic alterations, along with changes in cell shape to a more elongated appearance with front-back polarity signify EMT. Consequently, cells following EMT show increased motile potential (Hay, 1995; Hugo *et al*, 2007; Voulgari & Pintzas, 2009).

Progression of solid tumors involves spatial and temporal occurrences of EMT, whereby tumor cells acquire a more invasive phenotype. Subsequently, the disseminated mesenchymal

tumor cells must undergo the reverse transition – mesenchymal-epithelial transition (MET) –, in order to recapitulate the pathology of the corresponding primary tumor (Hugo *et al*, 2007). This cell plasticity is the key for the success of metastasis, and introduces malignant progression as a dynamic process (Hugo *et al*, 2007).

1.5 Fibronectin and the neoplastic process

Oncogenic transformation causes a pleiotropic change in cellular properties including alterations in adhesion and morphology, loss of cytoskeletal organization, as well as loss of FN. The reasons for the loss appear to vary and include reduced synthesis, reduced binding and increased rates of degradation (Hynes & Yamada, 1982; Olden & Yamada, 1977).

FN is the major component of ECM. Its strong susceptibility to proteolytic degradation was known since its discovery and was largely used to identify the different binding sites of ECM components and others on the molecule. The parallel increase of plasma FN and proteolytic enzymes, namely MMPs, as well as the increased levels of FN fragments is observed in tissues and biological fluids of cancer patients. In addition, it has been observed that the level of cell-surface FN is greatly reduced in transformed cells (Akiyama *et al*, 1995; Furcht *et al*, 1984; Hynes, 1976; Kenny *et al*, 2008; Warawdekar *et al*, 2006). Indeed, given the involvement of FN in adhesion to ECM, effects on invasion and metastasis might be expected from alterations in this aspect of cell function (Hynes & Yamada, 1982). On the other hand, FN fragments may show new properties that the native molecule does not exhibit (Kenny *et al*, 2008).

In studies on the activity of FN in cancer (Labat-Robert, 2002) it was observed, in breast cancer patients, lower levels of pFN in comparison with the levels occurring in healthy subjects. In the same study, the presence of FN degradation products in patients where an increased proteolytic activity could be anticipated: all investigated patients had high levels of FN fragments in the blood plasma; on the contrary, healthy subjects showed the absence of such fragments.

Increased fragmentation of urinary FN was also observed in urine of cancer patients. That increase was even more accentuated in patients with distant metastases (Katayama *et al*, 1993).

FN fragmentation appears to be a frequent event in several pathologies: in patients with rheumatoid arthritis and osteoarthritis, proinflammatory properties were detected in joint tissue and chondrocytes, inducing the activity of MMPs, such as stromelysins, gelatinases and collagenases (Homandberg, 2001; Labat-Robert, 2002).

Other observations attributed proteolytic activity to some fragments resulting from FN proteolysis itself, and also the FN overexpression, thus suggesting the occurrence of a positive feedback, which promotes pathological progression, namely in a neoplastic context (Labat-Robert, 2002; Lopez-Armada *et al*, 1997).

Comparing benign breast tumors with adenocarcionomas, it was observed that, besides some cFN loss, the pericellular FN fragmentation was a sign of malignancy (Labat-Robert, 2002; Labat-Robert *et al*, 1980).

Also in breast cancer, cultivation of MCF-7, a human breast adenocarcinoma cell line, in serum free medium in the presence of FN upregulated the activity of MMP-2 and MMP-9. By blocking α5β1 integrin, the FN-induced MMP activation response was inhibited appreciably, which indicates α5β1 mediated signaling events in activation of MMP-2 and MMP-9 (Das *et al*, 2008).

In another study in which the effects of FN on MMP-9 in HEp-2, laryngeal carcinoma cell line, were studied, as well as the molecular mechanisms involved, it was also suggested that FN induced MMP-9 mainly by involving α5β1 integrin receptor, through the activation of multiple signaling pathways (Sen *et al*, 2010).

Recent studies (Kenny *et al*, 2008; Kenny & Lengyel, 2009) have shown the involvement of FN fragmentation and vitronectin by MMP-2 in the early stages of the metastatic process of the ovarian cancer. Genes encoding several members of MMPs family, including MMP-2 were overexpressed in ovarian cancer cells. Based on the importance of these molecules, MMP-2 inhibition was induced, which resulted in decreased cell proliferation and metastasis in experimental mice.

These results, however, only occurred when the treatment was performed immediately after injection of tumor cells; when the inhibitors were administered at a later stage of tumor progression, efficacy turned out to be minimal, which coincides with other studies, focused, manely, in pancreatic (Bramhall *et al*, 2001) and gastric cancer (Bramhall *et al*, 2002; Davies *et al*, 1993).

The function of MMP-2 proposed in this case is its involvement in promoting adhesive ability of ovarian cancer cells through specific cleavage of FN and vitronectin, facilitating and foresting the adhesion and invasion of cells by binding to the FN and vitronectin fragments, through α5β1 and αvβ3 integrins.

Also in kidney cancer it was observed a correlation between the FN1 mRNA expression and the occurrence of kidney cancer in advanced stage (Waalkes *et al*, 2010).

In parallel, other studies attribute anti-tumor properties to some fragments derived from FN. Synthetic peptides derived from FN have been used to inhibit metastasis, by interfering with

interactions tumor-host and functions as adhesion and motility (anti-adhesion therapy) (Humphries *et al*, 1986; Humphries *et al*, 1988; Saiki, 1997). Peptides derived from FN, including the pentapeptide GRGDS (Gly-Arg-Gly-Asp-Ser), appeared to inhibit lung metastasis when administered in mice tumor cells (Humphries *et al*, 1986; Humphries *et al*, 1988). Further studies used the polymeric peptide poli(RGD), showing also inhibition of lung and liver metastasis in mice with different types of human and murine metastatic cells (Saiki, 1997).

A polymeric form of FN, "superfibronectin" (sFN) – constructed *in vitro*, by treating FN with a 76 amino acids peptide, derived from $FIII_1$, $FIII_1C$ (anastellin) – revealed an antimetastatic activity when administered systemically to tumors implanted in mice. Also anastellin itself reduced the tumor growth in mice, this effect being correlated with a low density of blood vessels in mice treated tumors (Yi & Ruoslahti, 2001).

More recently, a new peptide derived from FN, $FNIII_{14}$, showed antimetastatic properties by inhibiting cell adhesion of lymphoma cells to vascular cell adhesion molecule 1 (VCAM-1) and to FN (Kato *et al*, 2002).

ECM represents a critical target of oncogenic transformation. Among its most abundant components, FN stands out. Given its special role in terms of functional properties, FN can be seen as a potential new tumor marker or even as a target for tumor therapy.

Metastases formation, as a result of secondary tumor growth, is the main cause of mortality in cancer patients. This is particularly relevant in the context of solid tumor growth. For the present study, adenocarcinoma of the uterine cervix and colorectal carcinoma are the elected models.

2. Aims

This work aims to clarify the role of FN, and its proteolytic fragments, in tumor growth and metastases formation, and to determine if the levels of FN expression in solid tumors could be used as a prognostic marker of the disease.

With this intent, an experimental work was performed based on the construction of a plasmid containing the *FN* coding sequence, which was used to transfect human cell lines of colorectal adenocarcinoma (HCT15) and uterine cervix adenocarcinoma (HeLa), and in chinese hamster ovary cells (CHO). *In vivo,* we induced orthotopic xenograft tumors in BALB/c-SCID mice by using control and transfected cells.

As specific aims, we sought to evaluate the expression of *FN* in control and transfected cells, the *in vitro* alterations due to FN expression, particularly on MMPs activity, cell migration and angiogenesis, and the role of FN/FN fragments in tumor progression in *in vivo* models.

3. Materials and Methods

3.1 BIOLOGICAL MATERIAL

The FN gene was amplified by using RNA from human colon adenocarcinoma cell line SW480 (ATCC, CCL-228™).

The plasmid amplification was performed in One-shot TOP 10 Chemically Competent *Escherichia coli* (C4040-10, *Invitrogen).*

In vitro assays were developed in human cancer cell lines: colon adenocarcinoma (HCT15) and uterine cervix adenocarcinoma (HeLa). Chinese hamster ovary cells (CHO) were used as a positive control for FN protein expression.

The assays in which endothelial cells were used were performed with human umbilical vein endothelial cells (HUVEC).

The *in vivo* orthotopic models were developed in 6 weeks old BALB/c-SCID mice, males for colon cancer model and females for uterine cervix cancer model.

3.2 METHODS

The experimental work was performed according to the following tasks.

3.2.1 Construction of pcDNA3 - full-length *fibronectin* (pcDNA3-fl*FN*) expression vector and stable transfection of HCT15, HeLa and CHO cell lines.

3.2.1.1 Amplification of *FN* coding sequence

Total RNA was obtained from SW480 cells, using an *RNeasy RNA extraction* kit (74106, *Qiagen*), according to the manufacturer's protocol.

Specificity and enrichment of cDNA from *FN* was ensured by using a panel of 23 reverse primers of 15 mer (table 6) in the Reverse Transcription (RT) Reaction.

Full-length FN (embryonic) was amplified from cDNA using specific primers (table 6) and Polymerase Chain Reaction (PCR) was performed with Expand Long Template PCR System (11681834001, *Roche*).

3.2.1.1.1 Reverse transcription polymerase chain reaction (RT-PCR)

The RNA concentration was determined spectrophotometrically by measuring absorbance at 260 nm in a *Nanodrop 2000* (*Thermo Scientific*).

Reverse transcription polymerase chain reaction (RT-PCR) is a variant of Polymerase Chain Reaction (PCR) – technique used to amplify a specific DNA fragment – which produces DNA copies of an RNA template. In RT-PCR an RNA strand is first reverse transcribed into its complementary DNA (cDNA), using the enzyme reverse transcriptase, and the resulting cDNA is amplified by PCR.

The cDNA was synthesized from 1 µg of total RNA, to which 0.5 µl of primers mix (10µM, 23 reverse primers of 15 mer, specific to *FN* (table 6)) were added, and sterile bidestilled water to complete a total volume of 8 µl. The mixture was incubated at 70^{o}C, for 10 minutes, in order to occur the annealing between RNA and the reverse primers. Then, at 4^{o}C, the following mixture was added, for a final volume of 20 µl: 4 µl of First Strand Buffer 5X (Y00146, *Invitrogen*), 2 µl of 0.1M DTT (dithiothreitol) (Y00147, *Invitrogen*), 2 µl of 200mM dNTPs (deoxynucleotides), 1 µl of 40 U/µl RNAse OUT™ (10777-019, *Invitrogen*), 1 µl of 200 U/µl Superscript II® (18064-022, *Invitrogen*), 0.5 µl of ssDNAp (single strand DNA binding proteins) (M3011, *Promega*), and sterile bidestilled water up to 12 µl.

The cDNA synthesis was performed in a *T3000 thermocycler* (*Biometra*), using the following conditions:

Table 1 - Program used for the cDNA synthesis.

Stage	Temperature (^{o}C)	Time
First strand cDNA synthesis	**42**	4 hrs
Reverse transcriptase inactivation	**75**	15 min
Cooling	**4**	∞

3.2.1.1.2 Expand Long Template PCR

PCR is a highly sensitive technique used to amplify a DNA sequence of interest. The amplification occurs in a thermocycler, where cyclic temperature variations are generated, so that DNA can be replicated through enzymatic action. The sequence to be amplified is delimited by using a pair of primers – short oligonucleotides, each one complementary to one of the strands of the flanking regions -, which initiate DNA synthesis. The remainder elongation is ensured by a thermostable DNA polymerase.

The reaction proceeds in three steps: heat denaturation of the hydrogen bonds in DNA double helix, producing two single strands; annealing of the primers to each strand at the end of the sequence to be amplified; and an elongation step during which DNA polymerase enzyme attaches strand and continues to synthesize the complementary strand. These three steps must be repeated in 30 to 40 cycles to obtain a satisfactory amount of DNA.

FN (full-length) amplification was accomplished using an *Expand Long Template PCR System* (11681834001, *Roche*), an optimized enzyme blend that contains thermostable Taq DNA polymerase and Tgo DNA polymerase, a thermostable DNA polymerase with proofreading activity, and specially developed three-buffer system optimized to generate PCR products from 5 to 20 kb in length (*FN* is approximately 6.4 kb in length).

The Expand PCR mixture was made for a final volume of 50 µl and contained: 4 µl of cDNA, 5 µl of Buffer 1 (buffer system used to amplify DNA fragments up to 9 kb in length), 1.5 µl of forward primer (table 6), 1.5 µl of reverse primer (table 6), 7 µl of 200mM dNTPs, 0.75 µl of Expand mix, and sterile bidestilled water added to complete the final volume. Primers were designed as instructed by *pcDNA3.1 Directional TOPO Expression* kit protocol (K4900-01, *Invitrogen*) (see 3.2.1.2).

The Expand PCR was performed in a *T3000 thermocycler* (*Biometra*), according to the program described in the table 2.

Table 2 - Program used for *FN* Expand PCR.

Stage	Temperature (°C)	Time	Cycles	Δt
Initial denaturation	**94**	2 min	1	
Denaturation	**94**	10 s		
Annealing	**56**	30 s	10	
Elongation	**68**	10 min		
Denaturation	**94**	15 s		
Annealing	**56**	30 s	25	20 s
Elongation	**68**	10 min		
Cooling	**4**	∞		

After PCR, the amplified product was visualized by electrophoresis, in a 1.2% (w/v) agarose (in TBE buffer 1X (diluted from TBE buffer 10X, EC-860, *National diagnostics*)) gel, stained with 0.05% (v/v) ethidium bromide and under UV (*BioDocAnalyse Transilluminator*, *Biometra*).

The DNA fragment with the expected size was extracted, using a *QIAquick Gel Extraction* kit (28706, *Qiagen*), according to the manufacturer's protocol, and then sequenced.

3.2.1.1.2.1 DNA sequencing

DNA sequencing is the determination of the order of the nucleotides in a DNA molecule.

The DNA sequence can be determined by dye-terminator sequencing. In this method, the double stranded DNA fragment to be analyzed is mixed with a single primer binding to a strand complementary to the strand to be sequenced, DNA polymerase and a nucleotide mixture containing ordinary dNTPs and ddNTPs (dideoxynucleotides), nucleotides lacking a 3'-hydroxyl (-OH) group at the polymerization site, and labeled with a fluorescent molecule – a different fluorochrom specific for each nucleotide. In a reaction based on the same principle as PCR, insertion of ddNTP terminates the extension of that particular strand. The insertion of ddNTPs is random, but, after a series of cycles, the sequencing reaction contains a mixture of copies of one strand ended at each base. Strands are separated by size in a capillary electrophoresis. During the electrophoresis, the dyes of strands of equal length are excited passing a laser and the specific light emission is detected, generating, this way, the nucleotide sequence of the DNA fragment.

DNA sequencing was used to confirm the sequence of the band obtained from Expand PCR. For that purpose two sequencing reaction mixtures were made – one contained the forward primer and the other one the reverse primer, so that the two strands of the DNA fragment could be sequenced – for a final volume of 20 µl for each mixture. Each mixture contained: 3 µl of Big dye ™ Terminator v1.1 and 2 µl of Big dye sequencing buffer 5X (*BigDye® Terminator v3.1 Cycle Sequencing* kit, 4337456, *Applied Biosystems*), 1 µl of forward or reverse primer (table 6), 4 µl of DNA template, and sterile bidestilled water up to 20 µl.

Sequencing reaction was carried out in a *T3000 thermocycler* (*Biometra*), according to the program described in the table 3.

Samples were then purified, using an *AutoSeq G-50 dye terminator removal* kit (27-5340-02, *GE Healthcare Life Sciences*), according to the manufacturer's instructions.

The automated sequencing was performed in an *ABI Prism™ 310 Genetic Analyzer* (*Applied Biosystems*).

The results were obtained as electroferograms after analysis with *Sequencing Analysis 3.4.1* software.

Table 3 - Program used for sequencing reaction.

Stage	Temperature (°C)	Time	Cycles
Initial denaturation	96	5 min	1
Denaturation	96	10 s	
Annealing	56	5 s	25
Elongation	60	4 min	
Cooling	4	∞	1

3.2.1.2 Plasmid construction and cloning

The pcDNA3-fl*FN* construction (appendix B) was used performed by using the *pcDNA™3.1 Directional TOPO Expression* kit (K4900-01, *Invitrogen*), which uses linearized, topoisomerase I-activated pcDNA™3.1D/V5-His-TOPO® for directional cloning of a blunt-end PCR product.

pcDNA™3.1D/V5-His-TOPO® is a 5.5 kb expression vector designed to facilitate rapid directional cloning of blunt-end PCR products for expression in mammalian cells. The plasmid contains an ampicillin resistance gene and a geneticin resistance gene, allowing the selection of transformants and transfectants, respectively (appendix B).

Topoisomerase I binds to duplex DNA at specific sites and cleaves the phosphodiester backbone after 5′-CCCTT in one strand. The energy from the broken phosphodiester backbone is conserved by formation of a covalent bond between the 3′ phosphate of the cleaved strand and a tyrosyl residue (Tyr-274) of topoisomerase I. This bond can subsequently be attacked by the 5′ hydroxyl of the original cleaved strand, reversing the reaction and releasing topoisomerase. TOPO® cloning exploits this reaction to efficiently clone PCR products.

Directional joining of double-strand DNA using TOPO®-charged oligonucleotides occurs by adding a 3′ single-stranded end (overhang) to the incoming DNA. This single-stranded overhang is identical to the 5′ end of the TOPO®-charged DNA fragment.

In this system, PCR products are directionally inserted by adding four bases to the forward primer (CACC). The overhang in the cloning vector (GTGG) invades the 5′ end of the PCR product, anneals to the added bases and stabilizes the PCR product in the correct orientation.

Plasmid cloning was performed by transforming One-shot TOP 10 Chemically Competent *Escherichia coli* (C4040-10, *Invitrogen*), according to the manufacturer's protocol.

3.2.1.3 Plasmid isolation

From each plate (as recommended, two different volumes were plated), 10 colonies were picked and cultured in 5 ml of LB medium (appendix A) containing 50 µg/ml ampicillin, at 37°C, with shaking, overnight.

The plasmid isolation from each culture was accomplished by using a *Plasmid DNA MiniPreps* kit (SP-PMN-100, *EasySpin*), according to the protocol provided by the manufacturer.

The isolated plasmids were then visualized in a 1.2% (w/v) agarose (in TBE buffer 1X (diluted from TBE buffer 10X, EC-860, *National diagnostics*)) gel, stained with 0.005% ethidium bromide, after electrophoresis, under UV transillumination (*BioDocAnalyse Transilluminator*, *Biometra*).

The plasmid with the expected size was lastly confirmed as being pcDNA3-fl*FN* through digestion with restriction enzymes, and PCR followed by DNA sequencing.

3.2.1.3.1 Restriction endonucleases digestion

Restriction enzymes (or restriction endonucleases) are enzymes that cleave DNA at specific sequences, restriction sites, generating restriction fragments. These enzymes can be used for excision of a DNA sequence of interest if the DNA region is flanked by specific restriction sites.

By knowing the pcDNA3-fl*FN* restriction sites (*NEBcutter* analysis (tools.neb.com/NEBcutter2/)) and their respective recognizing restriction enzymes, a restriction digestion was performed on the plasmid. For this purpose, the enzymes NotI (ER0591, *Fermentas*) and BamHI (R01362, *New England BioLabs*) were used.

The digestion reaction took place in a *T3000 thermocycler* (*Biometra*), at 37°C, overnight, and it was prepared as follows: 2 µl of 10 U/µl NotI or 20 U/µl BamHI, 1 µl of Buffer O 10X (B05, *Fermentas*) or NEBuffer 3 10X (B70035, *New England BioLabs*), respectively, 4 µl of DNA template, and sterile bidestilled water up to 20 µl.

The products were loaded in a 1.2% (w/v) agarose (in TBE buffer 1X (diluted from TBE buffer 10X, EC-860, *National diagnostics*)) gel, stained with 0.005% ethidium bromide, and visualized under UV (*BioDocAnalyse Transilluminator*, *Biometra*).

3.2.1.3.2 PCR

PCR was a complement technique used for pcDNA3-fl*FN* validation. For that purpose, a forward primer that attached to a pcDNA3.1D/V5-His-TOPO® sequence, and a reverse primer specific to *FN* fragment were used (table 6).

Three reaction mixtures were made, only varying in the reverse primer, each one for a final volume of 25 µl and containing: 2.5 µl of PCR Rxn Buffer 10X (Y02028, *Invitrogen*), 2 µl of 200mM dNTPs, 1 µl of each primer, 1.5 µl of 50 mM $MgCl_2$ (Y02018, *Invitrogen*), 1 µl of template DNA, 0.5 µl of 5U/µl Taq DNA polymerase (18038-026, *Invitrogen*), and sterile bidestilled water up to 25 µl.

PCR was carried out in a *T3000 thermocycler* (*Biometra*), according to the program described in the table 4.

The PCR products were loaded in a 2% (w/v) agarose (in TBE buffer 1X (diluted from TBE buffer 10X, EC-860, *National diagnostics*)) gel, stained with 0.005% ethidium bromide, and visualized under UV (*BioDocAnalyse Transilluminator*, *Biometra*). The fragment of the expected size was extracted using a *QIAquick Gel Extraction* kit (28704, *Qiagen*), following the protocol provided by the manufacturer, and then sequenced.

The sequencing followed the procedures explained in 3.2.1.1.2.1.

Table 4 - Program used for PCR.

Stage	Temperature (°C)	Time	Cycles
Initial denaturation	95	5 min	1
Denaturation	94	50 s	25
Annealing	variable [1)]	30 s	
Elongation	72	50 s	
Final elongation	72	7 min	1
Cooling	15	∞	

1) 46.8 °C and 51.2 °C.

The pcDNA3-fl*FN* concentration was determined spectrophotometrically by measuring absorbance at 260 nm in a *Nanodrop 2000* (*Thermo Scientific*).

3.2.1.4 Stable transfection of HCT15, HeLa and CHO cell lines

3.2.1.4.1 Cell culture

Cell lines were obtained from American Type Culture Collection (ATCC): HCT15 (CCL-225™), HeLa (CCL-2™) and CHO (CCL-61™).

Cell lines were maintained at 37°C in a humidified 5% CO_2 environment in MEM Alpha Medium 1X (22561-021, *Invitrogen*) (HCT15, HeLa and CHO), supplemented with 10% Fetal Bovine Serum (FBS) (16000-044, *Invitrogen*) and 1X Antibiotic-Antimycotic (15240062, Anti-Anti) (*Invitrogen*). Cells were grown to 75 - 100% optical confluence before they were detached by incubation with 0.05% trypsin-EDTA 1X (25300-054, *Invitrogen*) for 5 min, at room temperature.

Whenever necessary, the cell number was determined with the help of a Bürker counting chamber.

3.2.1.4.2 Transfection

HCT15, HeLa and CHO were transfected with pCDNA3-fl*FN*, using the cationic liposome Lipofectamine™ 2000 (11668019, *Invitrogen*). For that, each cell line was previously grown, in a 25 cm^2 cell culture flask, to approximately 80% confluence. For each flask, 1 µg of DNA (pcDNA3-fl*FN*) was diluted into 500 µl of serum free MEM Alpha Medium 1X (22561021, *Invitrogen*), and 20 µl of Lipofectamine™ 2000 were also diluted into 500 µl of serum free MEM Alpha Medium 1X. After incubation for 5 minutes, at room temperature, the two dilutions were mixed and incubated, at room temperature, for 20 minutes to allow DNA-Lipofectamine™ 2000 complexes to form. The complexes were finally added directly to each flask, replacing the ordinary culture medium.

After incubation for 4-6 hours, at 37°C, in a humidified 5% CO_2 environment, it was added new complete culture medium.

For each cell line, a control group, not transfected, was maintained in parallel.

Transfected cells were selected by continuous supplementation of Geneticin (10131027, *Invitrogen*) to the growth medium. Decreasing concentrations were used, with an interval of one week, until the last concentration that was maintained: 1 mg/ml, 500 µg/ml, 100 µg/ml, 50 µg/ml and 10 µg/ml.

3.2.2 *In vitro* assays

3.2.2.1 Real-time PCR for *FN*

Real-time PCR is the technique of collecting data throughout the PCR process as it occurs, combining amplification and detection. This is achieved using a variety of different fluorescent chemistries that correlate PCR product concentration to fluorescence intensity. Real-time PCR can be used to quantify nucleic acids by two methods: absolute quantification and relative quantification. Absolute quantification gives the exact number of target DNA molecules by comparison with a DNA standard of known concentration, serially diluted. In relative quantification, changes in sample gene expression are measured based on internal reference genes to determine fold-differences in expression of the target gene.

RNA was extracted from each cell line (control and transfected), using an *RNeasy RNA extraction* mini kit (74104, *Qiagen*), according to the manufacturer's protocol.

cDNA synthesis was performed as described in 3.2.1.1.1, but, this time, 10 µM random primers (11043922, *Roche*) were used (0.5 µl), and the first strand synthesis occurred during 90 minutes.

For each sample, a reaction mixture was made, in triplicate, for a final volume of 25 µl, per reaction, containing: 12.5 µl of Fast SYBR® Green Master Mix (4385612, *Applied Biosystems*), 0.75 of forward primer (table 6), 0.75 of reverse primer (table 6), and sterile bidestilled water up to 24 µl.

FN expression was determined by relative quantification. The housekeeping gene used to normalize the samples was 18S. Each PCR experiment included one non-template control well.

Real-time PCR was carried out in an *ABI Prism® 7900HT Sequence Detection System* (*Applied Biosystems*), according to the program described in the table 5.

Tabela 5 - Program used for real-time PCR.

Stage	Temperature (^{o}C)	Time	Cycles
Initial denaturation	95	2 min	1
Denaturation	95	15 s	45
Annealing	60	1 min	
Dissociation curve	95 to 60	15 min	

Dissociation curve was performed exclusively for relative quantification.

3.2.2.2 Immunoprecipitation

Immunoprecipitation is used to precipitate a protein out of a solution using an antibody specific to that particular protein. This technique was used to immunoprecipitate FN out of the media supernatants of the cell lines.

In order to confer a neutral pH – suitable for immunoprecipitation – to supernatants, these were subjected to dialysis with pH 7 phosphate buffer, using a dialysis tubing cellulose membrane (cut-off 10 kDa) (D9777-100FT, *Sigma-Aldrich*). The proteins in each sample were then quantified and the concentrations equalized among the samples, based on the Bradford method, using a Bio-Rad Protein Assay Reagent (161-0156, *Bio-Rad*), according to the protocol provided by the manufacturer.

Once comparable, each sample (21 ml) was divided to be immunoprecipitated with three different antibodies specific to FN – polyclonal anti-human FN (F3648, *Sigma-Aldrich*), monoclonal anti-human FN (F0916, *Sigma-Aldrich*) and polyclonal anti- human/mouse/rat FN1−C-Terminal (SAB4500974, *Sigma-Aldrich*) –: the sample was first incubated with 4 µl of the respective antibody, at 4^{o}C, overnight, under rotatory agitation. Then, it was incubated with 50 µl of Protein G Sepharose® (P3296, *Sigma-Aldrich*), also at 4^{o}C, overnight, under rotatory agitation. The Protein G beads with bound antibodies were finally harvested by centrifugation at 2500 rpm, for 10 minutes, at 4^{o}C. The complexes were still rinsed twice with Dulbecco's Phosphate Buffered Saline 1X (04-479Q, *Cambrex*) and centrifuged at 2500 rpm, for 10 minutes, at 4^{o}C. Forty µl of β-mercaptoethanol:loading buffer 5X (appendix A) (1:10) were added to the sample, which was stored at -20^{o}C.

In parallel, a human serum sample was also immunoprecipitated with polyclonal anti-human/mouse/rat FN1−C-Terminal (SAB4500974, *Sigma-Aldrich*), to be used as a positive control.

3.2.2.3 SDS-PAGE (sodium dodecyl sulfate-polyacrylamide gel electrophoresis) and western blotting

Western blotting is a technique used to detect specific proteins in a given sample. This method uses SDS-PAGE to separate, in this case, denatured proteins by the length. The proteins are then transferred to a membrane to make the proteins accessible to antibody detection.

This technique was used to detect the FN immunoprecipitated.

The complexes immunoprecipitated were boiled at 95-100^{o}C for 10 minutes, to denature the protein and separate it from the protein G beads, and centrifuged at 14000 rpm, for 2 minutes, to precipitate the beads and keep the protein in the supernatant.

The samples were then loaded in a 10% polyacrilamide gel (appendix A) and electrophoresis was carried out in *Mini-PROTEAN Tetra Electrophoresis System* (*Bio-Rad*) at 150V, for 1 hour, into TGS buffer 1X (TGS buffer 10X, 161-0772, *Bio-Rad*).

After electrophoresis, proteins were transferred to a nitrocellulose membrane (162-0112, *Bio-Rad*), into transfer buffer (appendix A), with a *Mini Trans-Blot® Electrophoretic Transfer Cell* (*Bio-Rad*), at 35V, overnight, at 4^{o}C.

Blocking of non-specific binding was achieved by placing the membrane in a 5% (w/v) solution of non-fat milk in PBS Tween 20 (appendix A).

For protein detection, the membrane was incubated with the primary antibody specific to FN, diluted 1:1000 in non-fat milk in PBS Tween 20, overnight, at 4^{o}C, with shaking. Primary antibodies used were: polyclonal anti-human FN (F3648, *Sigma-Aldrich*), monoclonal anti-human FN (F0916, *Sigma-Aldrich*) and polyclonal anti- human/mouse/rat FN1−C-Terminal (SAB4500974, *Sigma-Aldrich*). After rinsing the membrane, three times, with PBS Tween 20, to remove unbound primary antibody, the membrane was exposed to the secondary antibody (anti-rabbit (31460, *Thermo Scientific*) and anti-mouse (31430, *Thermo Scientific*)), conjugated with horseradish peroxidase (HRP) and diluted 1:5000 in non-fat milk in PBS Tween 20. The incubation lasted for 2 hours, at room temperature, shaking. After rinsing the membrane, the reactivity of HRP was developed by SuperSignal® West Pico Chemiluminescent Substrate (34080, *Thermo Scientific*). Digital images of the western blotting were obtained in a *ChemiDoc XRS System* (*Bio-Rad*) with *Image Lab* software. Bands were quantified using *Image J* software (rsb.info.nih.gov/ij/).

3.2.2.4 Immunofluorescence

Immunofluorescence uses the specificity of antibodies labeled with fluorochromes to target specific biomolecules within a cell, allowing their visualization in the sample. In this work, immunofluorescence was performed using sequencially two antibodies: a primary antibody, that recognizes and binds to the target molecule, and a secondary antibody, which carries the fluorophore and recognizes and binds to the primary antibody.

From each cell line (control and transfected), cells were grown on lamellae, previously coated in 0.2% (w/v) gelatin, until they reached approximately 80% of confluence. Cells were

fixed in 2% (w/v) paraformaldehyde for 15 minutes at 4ºC, blocked with 0.1% (w/v) BSA in PBS 1X for 45 minutes at room temperature, and incubated with primary antibody overnight (diluted in 0,1% (w/v) BSA in PBS 1X, 1:100). Antibodies used were polyclonal anti-human FN (F3648, *Sigma-Aldrich*), monoclonal anti-human FN (F0916, *Sigma-Aldrich*) and polyclonal anti-human/mouse/rat FN1−C-Terminal (SAB4500974, *Sigma-Aldrich*), monoclonal anti-human α3 (MAB1952Z, *Millipore*), monoclonal anti-human/mouse/rat β1−C-terminal (EP1041Y, *Abcam*), polyclonal anti-human/mouse β3 (ab47584, *Abcam*) and monoclonal anti-human/mouse tenascin-C (MAB2138, *R&D Systems*). After rinsing three times, 5 minutes, with PBS 1X, cells were incubated with the secondary antibodies for 2 hours, at room temperature. Secondary antibodies used (diluted in 0,1% (w/v) BSA in PBS 1X, 1:1000) were: Alexa Fluor® 488 anti-mouse (A-11001, *Invitrogen*), Alexa Fluor® 488 anti-rabbit (A-11034, *Invitrogen*), Alexa Fluor® 488 anti-rat (A-11006, *Invitrogen*).The slides were rinsed, once again, three times with PBS 1X, prior to be mounted in VECTASHIELD media with DAPI (4'-6-diamidino-2-phenylindole) (H-1200, *Vector Labs*). Cells were examined by standard fluorescence microscopy using an *Axio Imager.Z1* microscope (*Zeiss*).

The same procedures described above were performed for negative controls, with the expception of the incubation with the primary antibody.

Images (x200 field) were acquired with *AxioVision* software and processed with *ImageJ* software.

3.2.2.5 Zymography

Zymography is an electrophoretic technique, performed with native PAGE, for examining MMPs activity in cell extracts and media samples. In this method, proteins are separated, according to their hydrodynamic size, in a gel that includes a substrate co-polymerized with the gel, for the detection of enzyme activity.

Media supernatants of each control and transfected cell line were concentrated by using Amicon® Ultra-4 Centrifugal Filter Units (UFC800308, *Millipore*). Loading buffer 5X (appendix A) was added to each sample and the mixtures were loaded in a 12% polyacrilamide gel (appendix A) with 0.1% (w/v) gelatin. Electrophoresis was performed with a *Mini-PROTEAN Tetra Electrophoresis System* (*Bio-Rad*), at 150V, for 90 minutes, into TGS buffer 1X (TGS buffer 10X, 161-0772, *Bio-Rad*). Gel was incubated in renaturating buffer (25% TritonX-100 (v/v)) for 1 hour, with agitation, after which the gel was incubated, overnight, at 37ºC in collagenase

buffer (appendix A). Staining was performed with 0.5% (w/v) Coomassie Blue R-250 for 30 minutes and destaining with destilled water, with agitation.

The gel was scanned and the bands were quantified using *ImageJ* software.

3.2.2.6 *In vitro* wound healing assay

The *in vitro* wound healing assay is a method to study directional cell migration *in vitro* that mimics cell migration during wound healing *in vivo*.

The cells from each line were grown in a 3.8 cm^2 tissue culture wells to a confluent monolayer. In each well, a scratch was made with a P20 pipette tip to the length of the well. After the scratch, the culture medium was replaced to remove detached cells. A timelapse experiment was performed and followed under an *Olympus CK2* inverted optical microscope (*Olympus*). Phase images (x200 field) were acquired at the following time points: 0, 8, 24 and 36 hours.

3.2.2.7 *In vitro* tube formation assay

Endothelial cells tube formation assay measures the ability of endothelial cells, at subconfluent densities, to form capillary-like structures.

For this experiment, HUVEC – obtained from ATCC (CRL-1730™) –, passages 2 to 5, were previously cultured and maintained according to the standard procedures (see 3.2.1.4.1), in Endothelial Basal Medium-2 (EBM-2) (00190860, *Lonza*) supplemented with 10% FBS (16000-044, *Invitrogen*) and Anti-Anti 1X (15240062, *Invitrogen*) in 0.2% gelatin coated flasks.

HUVEC were seeded on 3.8 cm^2 Matrigel™ Basement Membrane Matrix (356234, *BD Biosciences*) coated wells, at a density of $1x10^4$ cells per well in supplemented EBM-2. After cells adhesion, this culture medium was replaced by: conditioned media from each cell line (control and tranfected), 10% FBS (16000-044, *Invitrogen*) and 1% Anti-Anti (15240062, *Invitrogen*) supplemented MEM Alpha Medium 1X (22561-021, *Invitrogen*), and 10% FBS (16000-044, *Invitrogen*), 1% Anti-Anti 100X (15240062, *Invitrogen*) and 0.1% Fibronectin from bovine plasma (F1141, *Sigma-Aldrich-Aldrich*) supplemented MEM Alpha Medium 1X (*Invitrogen*).

Phase images (x40 field) were acquired in an *Olympus CK2* inverted optical microscope (*Olympus*), 24 hours after the medium replacement.

3.2.2.8 Real-time PCR for *VEGF-121*, *VEGF-165* and *VEGF-189*

VEGF isoforms expression was determined by absolute quantification for each control and transfected group within cell line. The expression of each sample was calculated with respect to a standard calibration curve that represents a serial dilution of cDNA from HUVEC.

cDNA synthesis was performed as described in 3.2.2.1. For each sample, a reaction mixture was made, in triplicate, for a final volume of 25 µl, per reaction, containing: 12.5 µl of TaqMan® Universal PCR Master Mix (2X) (4304437, *Applied Biosystems*), 15.75 µl of forward primer (table 6), 15.75 µl of reverse primer (table 6), 0.83 µl of probe (table 6) and sterile bidestilled water up to 25 µl.

The housekeeping gene used to normalize the samples was 18S (Eukariotic 18S rRNA Endogenous Control - 20x, 4319413E, *Applied Biosystems*). For that, a different reaction mixture was made, containing: 12.5 µl of TaqMan® Universal PCR Master Mix (2X) (4304437, *Applied Biosystems*), 1.25 µl of Eukariotic 18S rRNA Endogenous Control (4319413E, *Applied Biosystems*) and sterile bidestilled water up to 25 µl.

Each PCR experiment included one non-template control well.

Real-time PCR was carried out in an *ABI Prism® 7900HT Sequence Detection System* (*Applied Biosystems*), according to the program described in the table 5.

3.2.2.9 Real-time PCR for *KDR*, *FLT1*, *Angiopoietin-1*, *Angiopoietin-2*, *SCF* and *SDF1*

KDR, *FLT1*, *Angiopoietin-1*, *Angiopoietin-2*, *SCF* and *SDF1* expression was determined by relative quantification for each control and transfected group within cell line.

cDNA synthesis and reaction mixtures for each target were performed as described in 3.2.2.1. The housekeeping gene used to normalize the samples was 18S. Each PCR experiment included one non-template control well.

Real-time PCR was carried out in an *ABI Prism® 7900HT Sequence Detection System* (*Applied Biosystems*), according to the program described in the table 5.

3.2.3 *In vivo* assays [2)]

3.2.3.1 Orthotopic xenograft tumors induction

Tumorigenic capability of control and transfected human cancer cell lines was addressed by inducing the formation of orthotopic xenograft tumors in 6 weeks old BLAB/c-SCID mice.

For establishment of tumor xenografts, cells were rinsed in Dulbecco's phosphate buffered saline (PBS) 1X (04-479Q, *Cambrex*), harvested by scraping, and ressuspended in PBS at a concentration of 2 x 10^7 cells/ml. Each BALB/c-SCID mice was anestheziated by intraperitoneal injection of 100 µl of ketamine/medetonidin anesthesia.

For HCT15, the induction of the formation of xenograft tumors was performed by injection of 1 x 10^6 cells, per mouse (n=3 (male) for control HCT15; n=3 (male) for transfected HCT15), in the visceral wall of cecum. For HeLa, the formation of xenograft tumors was also induced by orthotopic injection of 1 x 10^6 cells, per mouse (n=3 for control HCT15; n=3 for transfected HCT15), in the uterus, by transvaginal inoculation.

After surgery, animals were awakened by receiving 100 µl of atipamezole reversor. Animals also received 100 µl of enrofloxacine antibiotic and enrofloxacine/meloxicam antibiotic/anti-inflammatory during 3 days.

[2)] All procedures involving live animals were performed by a professional authorized by *Direcção Geral de Veterinária*.

3.2.3.2 Flow cytometric analysis of endothelial and hematopoietic progenitor cells

Flow cytometry (FCM) is a technique for the analysis of multiple parameters of individual cells within heterogeneous populations. These analyses are performed by passing the cells through a laser beam and capturing the light that emerges from each cell as it passes through. One of the most common ways to study cell characteristics involves the use of fluorescent molecules, such as fluorophore-labeled antibodies.

For the analysis of endothelial and hematopoietic progenitor cells, blood samples were, periodically, collected (70 µl) from every animal for FCM acquisition. To each 70 µl of blood, 70 µl of 0.1% (w/v) BSA in PBS 1X were added. The mixture was incubated for 20 minutes, at 4^{o}C, with 1 µl of the following antibodies: APC anti-mouse CD117 (c-Kit) (105812, *Biolegend*), PE anti-mouse Flk-1 (555308, *BD Pharmingen*) and FITC anti-mouse Ly-6A/E (553335, *BD Pharmingen*). After an incubation of 15 minutes, at room temperature with 1 ml of Red blood

cells lysis buffer 1X (diluted from RBC lysis buffer 10X, 420301, *Biolegend*), the samples were centrifuged at 1200 rpm, for 5 minutes. The supernatant was discarded and the pellets were rinsed twice with 0.1% (w/v) BSA in PBS 1X. Cells were ressuspended in 200 µl of 0.1% (w/v) BSA in PBS 1X. Acquisitions were performed using a *FACSCalibur* flow cytometer *(BD Biosciences)* with a minimum of 10000 events for each sample, and further analysed using *CellQuest Pro* software.

3.2.3.3 Animals euthanasia

The animals were maintained for approximately 2 months. After this time, they were sacrificed in a carbon dioxide chamber.

From each mouse, tumors and the main target organs for metastases were collected for further histological analysis, as well as the blood for western blotting.

3.2.3.4 Western blotting

FN in the peripheral blood of animals was detected by western blotting. For that, the serum was extracted, after coagulation, and FN immunoprecipitated with polyclonal anti-human FN (F3648, *Sigma-Aldrich*), also used as the primary antibody for western blotting. The secondary antibody was anti-rabbit (31460, *Thermo Scientific*). The procedures involved are described in 3.2.2.2.

3.2.3.5 Histological analysis

The collected organs were fixed in 10% formalin and embedded in paraffin (bones were decalcified into an EDTA solution (appendix A), for one week, at 4^{o}C, before embedding in paraffin). Tissues were serially sectioned (3 µm). After retrieving the antigens in a *PT-Link* device (*Dako*) – module for tissue specimens for pre-treatment process of deparafinization, rehydration and epitope retrieval –, tissues were permanently deparaffinized by incubation, for 1 minute, with decreasing concentrations of ethanol (85%, 70% and 50%) and bidestilled water. Specimens were then stained with hematoxylin and eosin (H&E).

After deparafinization, sections were also stained for mast cells detection. For that, tissues were stained in toluidine blue solution (appendix A) for 3 minutes; after rinsed in bidestilled water, tissues were dehydrated, by incubation, for 1 minute, with increasing concentrations of ethanol (50%, 75%, 80%, 90% and 100%) and xylene. The slides were then mounted with Entellan® (1079610500, *Merck*) and examined with a *Primo Star* optical microscope (*Zeiss*).

Tissues were also used in immunohistochemistry for cytokeratin-19 (CK-19) and cytokeratin-7 (CK-7), and in immunofluorecence for E-cadherin.

Immunohistochemistry staining commonly uses a secondary antibody conjugated to a peroxidase, an enzyme that catalyses a color-producing reaction. Peroxidase is an enzyme found in several tissues, which makes it necessary to block the endogenous peroxidase for a specific staining.

For immunohistochemistry, after antigen retrieval and tissue dehydration (incubation for one minute with decreasing concentrations of ethanol: 50%, 70% and 85%), endogenous peroxidase was blocked by incubating the tissues in 3% (v/v) hydrogen peroxide in methanol, for 30 minutes.

The specimens were then deparaffinized, rinsed three times, for 5 minutes, with tris buffered saline (TBS) 1X (appendix A), and, finally, incubated with BSA 1% (w/v) in TBS, for 20 minutes. The tissues were then incubated with the primary antibody, diluted in 0.1 (w/v) BSA in TBS 1X, overnight, at 4^{o}C. The primary antibodies used were: monoclonal anti-human cytokeratin 19 (1:100) (M0888, *Dako*) and monoclonal anti-human cytokeratin 7 (1:100) (M7018, *Dako*).

The further procedures were performed using a *Dako EnVision+System-HRP (DAB)* (*Dako*) kit for use with mouse (K4006) and rabbit (K4010) antibodies, according to the manufacturer's instructions.

The same procedures described above were performed for negative controls, with the exception of the incubation with the primary antibody.

For immunofluorescence, after deparaffinization, procedures followed the steps described in 3.2.2.3. The primary antibodies used were: monoclonal anti-E-cadherin (1:100) (18-0223, *Sigma-Aldrich*).

The slides were mounted with Entellan® (1079610500, *Merck*) and examined with a *Primo Star* optical microscope (*Zeiss*).

Table 6 – Primers and probes used during the experimental work.

Reference	Primer (5'→3')	Tm (°C)	Technique
FN	Rev1: AACCGGGCTTGCTT	37.0	RT-PCR
	Rev2: CACACACTCTAACA	33.0	RT-PCR; PCR; Sequencing
	Rev3: GGGCCAGATCCGCT	41.0	RT-PCR
	Rev4: CCCTTCTGTGGTGC	39.0	RT-PCR; PCR; Sequencing
	Rev5: CTCATCATGTGACC	35.0	RT-PCR
	Rev6: GTAGCACTGGTATC	35.0	RT-PCR
	Rev7: GGTGTGCTGGTGCT	39.0	RT-PCR
	Rev8: CTCCCCATCCTCAG	39.0	RT-PCR; PCR; Sequencing
	Rev9: AACTGCTGGTCCCT	37.0	RT-PCR
	Rev10: CCACGGTCAGTCGG	41.0	RT-PCR
	Rev11: TTCTACTCCTGGAG	35.0	RT-PCR
	Rev12: GGGATGATGGTATC	35.0	RT-PCR
	Rev13: GGGGAGGTGCCCAG	43.0	RT-PCR
	Rev14: GAGGCTCGAGGAGC	41.0	RT-PCR
	Rev15: ACTTGCTCCCAGGC	39.0	RT-PCR
	Rev16: TGGATTCTGAGCAT	33.0	RT-PCR
	Rev17: GCAGGAGACCCAGG	41.0	RT-PCR
	Rev18: CTGGAACGGCATGA	37.0	RT-PCR
	Rev19: GTCACCTGAGTGAA	35.0	RT-PCR
	Rev20: TGGTCCGCCTAAAA	35.0	RT-PCR
	Rev21: GTCTTTCAGTGCCT	35.0	RT-PCR
	Rev22: GTTGCCTCATGAGC	37.0	RT-PCR
	Rev23: TTACTCTCGGGAAT	33.0	RT-PCR
	Fw: CACCCCGTCTCAACATGCTTAGG	70.5	Expand PCR; Sequencing
	Rev: TTACTCTCGGGAATCTTCTC	57.5	Expand PCR; Sequencing
	Fw: AAGGTTCGGGAAGAGGTTGT	63.7	Real-time PCR (RQ)
	Rev: TGGCACCGAGATATTCCTTC	63.8	Real-time PCR (RQ)
T7	Fw: TAATACGACTCACTATAGGG	50.9	PCR; Sequencing
18S	Fw: GCCCTATCAACTTTCGATGGT	65.1	Real-time PCR (RQ)
	Rev: CCGGAATCGAACCCTGATT	66.0	Real-time PCR (RQ)
KD	Fw: GTGACCAACATGGAGTCGTG	64.2	Real-time PCR (RQ)
	Rev: CCAGAGATTCCATGCCACTT	64.0	Real-time PCR (RQ)
FLT1	Fw: CACCAAGAGCGACGTGTG	64.5	Real-time PCR (RQ)
	Rev: TTTTGGGTCTCTGTGCCAG	63.9	Real-time PCR (RQ)
SDF1	Fw: CAGATGCCCATGCCGATT	67.2	Real-time PCR (RQ)
	Rev: AGTTTGGAGTGTTGAGAATTT	64.9	Real-time PCR (RQ)
Angiopoietin-1	Fw: AGGAAATGCTGCAGATGTTGATAA	65.4	Real-time PCR (RQ)
	Rev: GCAGCTCTTCACAGACTGACCA	67.0	Real-time PCR (RQ)
Angiopoietin-2	Fw: GGAACACTCCCTCTCGACAA	64.2	Real-time PCR (RQ)
	Rev: ATTCACCGTGGCAGTCACTA	63.2	Real-time PCR (RQ)
SCF	Fw: GTAGCAGTAATAGGAAGGCCA	64.1	Real-time PCR (RQ)
	Rev: AGAAAACAATGCTGGCAATGC	66.0	Real-time PCR (RQ)

Reference	Primer (5'→3')	Probe (6-FAM-5'→3' TAMRA)	Tm (°C)	Technique
VEGF-121	Fw: CCAGCACATAGGAGAGATGAGCTT	ACAGCACAACAAATGTGAATGC AGACCAAA	66.6	Real-time PCR (AQ)
	Rev: CGGCTTGTCACATTTTTCTTGTC		66.5	Real-time PCR (AQ)
VEGF-165	Fw: CCAGCACATAGGAGAGATGAGCTT	ACAGCACAACAAATGTGAATGC AGACCAAA	66.6	Real-time PCR (AQ)
	Rev: AGGCCCACAGGGATTTTCTT		65.7	Real-time PCR (AQ)
VEGF-189	Fw: AATGTGAATGCAGACCAAAGAAAG	AGAGCAAGACAAGAAAAAAAAT CAGTTCGAGGAA	65.0	Real-time PCR (AQ)
	Rev: AGGGAACGCTCCAGGACTTATA		64.7	Real-time PCR (AQ)

Tm: melting temperature;

RQ : relative quantification;

AQ: absolute quantification.

4. Results

With the intent to study the role of FN in tumor development and progression, an experimental work was designed arising from the establishment of two groups within each cell line used, differing in the levels of FN produced. That difference was achieved by transfecting a group of cells of each cell line with a plasmid containing the human *embryonic FN* gene (*full length FN*), pcDNA3-fl*FN*. As mentioned above, the cell lines used were HCT15, HeLa and CHO. For each cell line, it was also maintained a control group of cells composed of cells not transfected. CHO was used as a positive control, due to their lack of a control mechanism of transcription.

During the experimental work, several experiments were developed and the results compared between the groups.

4.1 *IN VITRO* ASSAYS

4.1.1 Quantification of *FN* expression by real-time PCR

To quantify the difference between groups within each cell line in relative expression levels of *FN* after stable transfection with pcDNA3-fl*FN*, a Real-time PCR assay was carried out (figure 2).

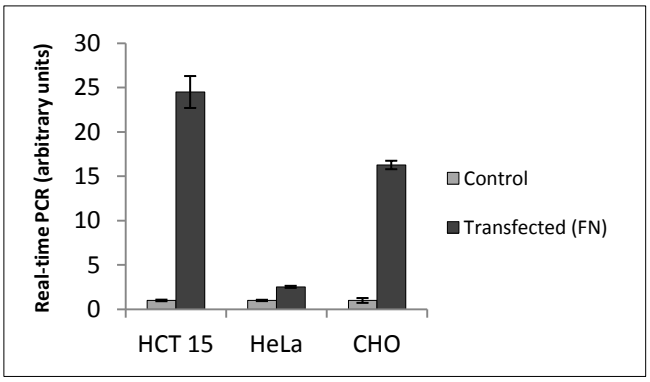

Figure 2 – Real-time-PCR for *FN* expression. Relative quantification of *FN* mRNA levels in control and transfected HCT15, HeLa and CHO. Error bars represent standard deviation.

Indeed, it was observed an increase of *FN* mRNA levels in all transfected groups. That increase was higher in HCT15 (24.3 fold) and CHO (16.3 fold) cell lines, than in HeLa (2.5 fold).

4.1.2 Evaluation of FN expression by western blotting

Western blotting was performed to verify if the difference in *FN* mRNA levels observed between control and transfected groups was reflected in FN protein levels, and also if there were alterations between groups in regard to FN fragmentation. Once FN is an extracellular molecule, the supernatants from the two groups within each cell line were collected and, after immunoprecipitation of FN, the protein was detected and quantified by western blotting (figures 3, 4 and 5).

CHO:

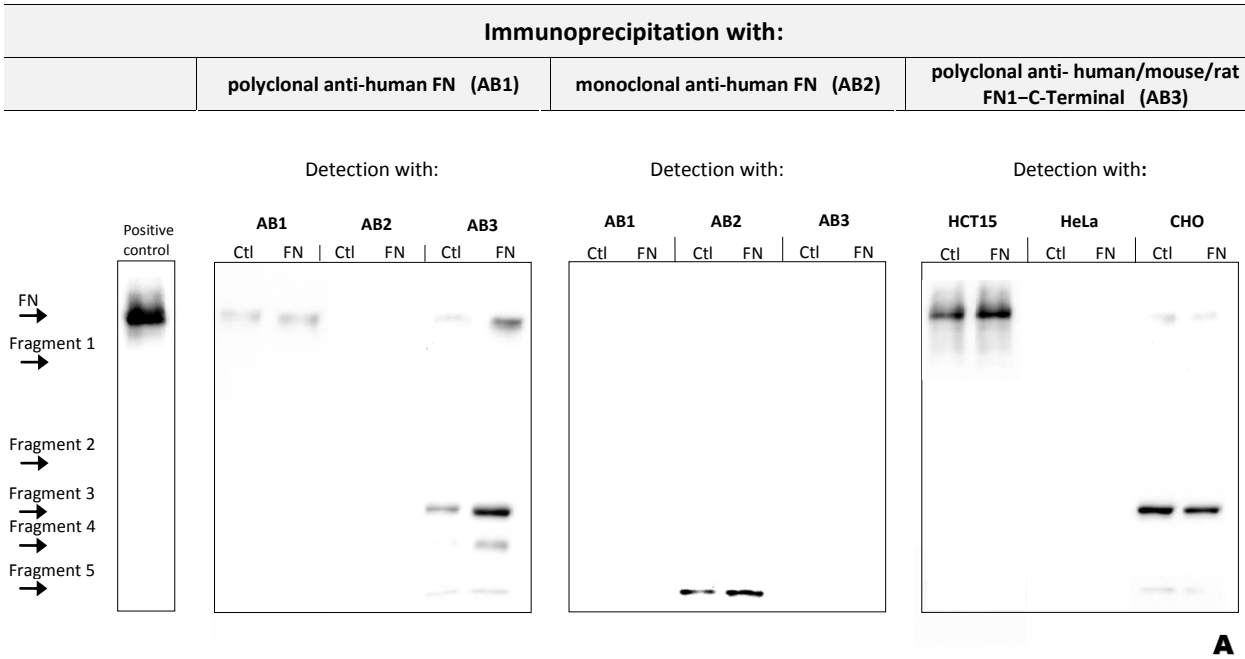

IMMUNOPRECIPITATION	polyclonal anti-human FN (AB1)						monoclonal anti-human FN (AB2)						polyclonal anti- human/mouse/rat FN1–C-Terminal (AB3)					
DETECTION	**AB1**		**AB2**		**AB3**		**AB1**		**AB2**		**AB3**		**AB1**		**AB2**		**AB3**	
	C	FN	C	FN	C	FN	C	FN	C	FN	C	FN	C	FN	C	FN	C	FN
FN	1	1.46	—		1	6.27	—		—		—		1	1.32	—		1	0.62
Fragment 3	—		—		1	3.87	—		—		—		—		—		1	0.77
Fragment 4	—		—		1	10.18	—		—		—		—		—		—	
Fragment 5	—		—		1	2.02	—		1	1.70	—		—		—		1	0.41

B

Figure 3 – Western blotting of FN immunoprecipitated from CHO media supernatants. (A) Western blotting analysis of FN from the supernatants of control (Ctl) and transfected (FN) cells. For each group, FN was immunoprecipitated with three different antibodies specific for FN: polyclonal anti-human FN, monoclonal anti-human FN and polyclonal anti-FN1–C-Terminal. Membranes were detected also with the three antibodies specific for FN. The positive control used is FN from human serum of a healthy individual, immunoprecipitated with polyclonal anti-FN1–C-Terminal and detected with the same antibody. Fragments denomination was arbitrary. (B) Western blotting quantification for each band detected. Bands are compared between control (C) and transfected (FN) groups.

The results from western blotting for CHO (figure 3) revealed, globally, higher FN levels in transfected group than in control, with a greater significance in the immunoprecipitation with polyclonal anti-human FN - detection with polyclonal anti-FN1−C-Terminal condition. An exception was observed in the immunoprecipitation with polyclonal anti-FN1−C-Terminal - detection with polyclonal anti-FN1−C-Terminal condition, where FN levels were slightly higher in control group than in transfected cells.

In relation to FN fragments detected, for fragment 3 and 5, results differed among conditions. However, largest differences were observed in all situations in which fragments levels, including fragment 4, were higher in transfected cells than in control.

HCT15:

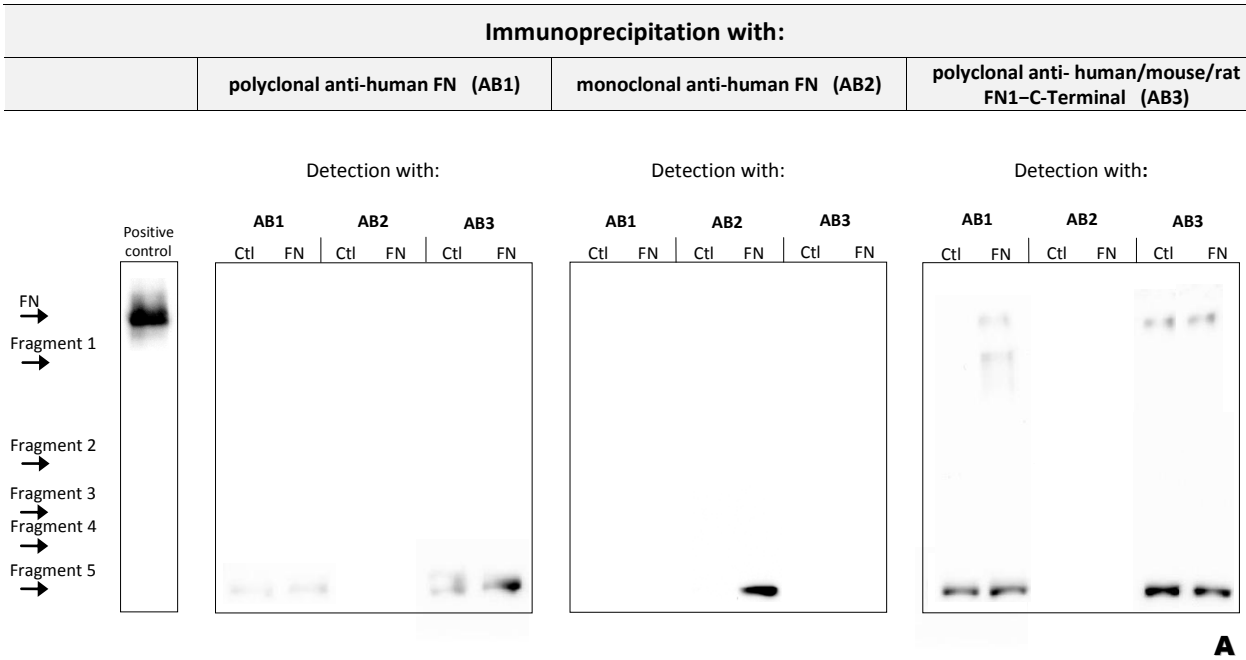

A

IMMUNOPRECIPITATION	polyclonal anti-human FN (AB1)						monoclonal anti-human FN (AB2)						polyclonal anti- human/mouse/rat FN1−C-Terminal (AB3)					
DETECTION	AB1		AB2		AB3		AB1		AB2		AB3		AB1		AB2		AB3	
	C	FN	C	FN	C	FN	C	FN	C	FN	C	FN	C	FN	C	FN	C	FN
FN		—		—		—		—		—		—	1	173.64		—	1	1.06
Fragment 1		—		—		—		—		—		—	1	165.48		—		—
Fragment 5	1	1.24		—	1	3.09		—	1	272.86		—	1	1.18		—	1	0.76

B

Figure 4 – Western blotting of FN immunoprecipitated from HCT15 media supernatants. (A) Western blotting analysis of FN from the supernatants of control (Ctl) and transfected (FN) cells. For each group, FN was immunoprecipitated with three different antibodies specific for FN: polyclonal anti-human FN, monoclonal anti-human FN and polyclonal anti-FN1−C-Terminal. Membranes were detected also with the three antibodies specific for FN. The positive control used is FN from human serum of a healthy individual, immunoprecipitated with polyclonal anti-FN1−C-Terminal and detected with the same antibody. Fragments denomination was arbitrary. (B) Western blotting quantification for each band detected. Bands are compared between control (C) and transfected (FN) groups.

Western blotting for HCT15 (figure 4) revealed higher FN levels in transfected cells than in control, in both conditions that resulted in its detection, although the difference detected in immunoprecipitation with polyclonal anti-FN1−C-Terminal - detection with polyclonal anti-FN1−C-Terminal condition was almost insignificant; the difference observed in immunoprecipitation with polyclonal anti-FN1−C-Terminal - detection with polyclonal anti-human FN condition was, on the contrary, very significant. Te latter condition also detected fragment 1, for each a similar difference was observed.

Fragment 5 levels were, globally, higher in transfected cells, with a major significance in the immunoprecipitation with monoclonal anti-human FN - detection with monoclonal anti-human FN condition. The contrary was observed in the immunoprecipitation with polyclonal anti-FN1−C-Terminal - detection with polyclonal anti-FN1−C-Terminal, but with a small difference.

HeLa:

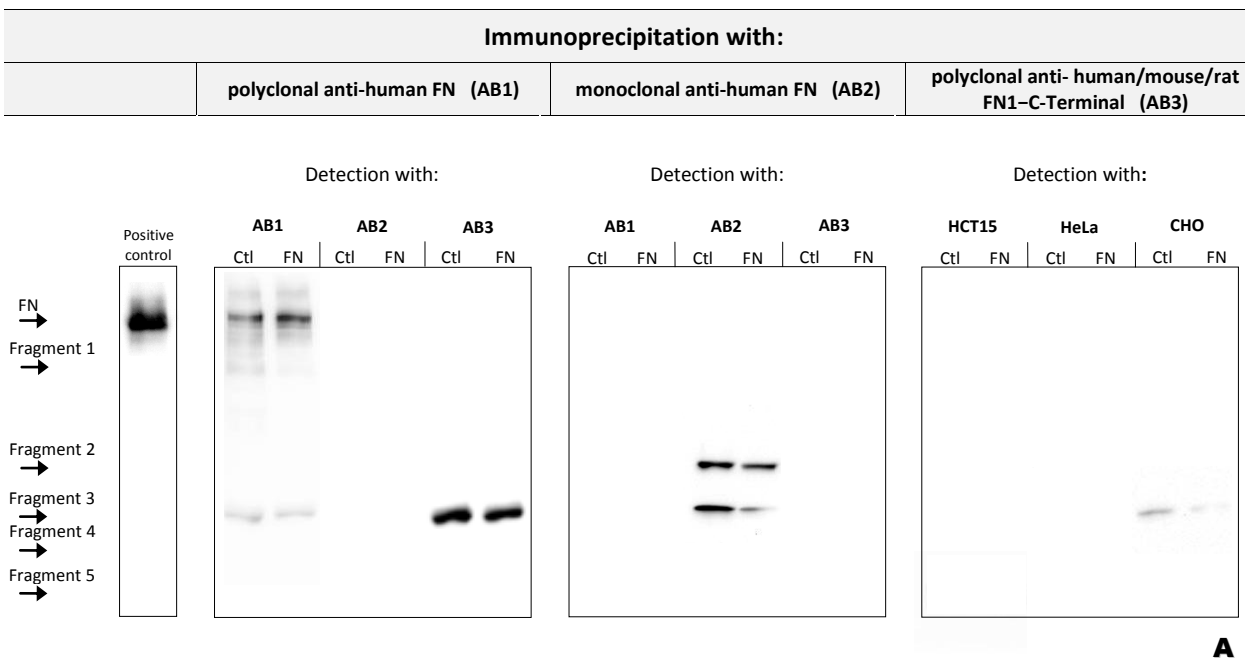

IMMUNOPRECIPITATION	polyclonal anti-human FN (AB1)						monoclonal anti-human FN (AB2)						polyclonal anti- human/mouse/rat FN1–C-Terminal (AB3)					
DETECTION	**AB1**		**AB2**		**AB3**		**AB1**		**AB2**		**AB3**		**AB1**		**AB2**		**AB3**	
	C	FN	C	FN	C	FN	C	FN	C	FN	C	FN	C	FN	C	FN	C	FN
FN	1	1.34	—		—		—				—		—		—		—	
Fragment 2		—		—		—		—	1	0.72		—		—		—		—
Fragment 3	1	0.69		—	1	0.88		—	1	0.19		—		—		—	1	0.27

B

Figure 5 – Western blotting of FN immunoprecipitated from HeLa media supernatants. (A) Western blotting analysis of FN from the supernatants of control (Ctl) and transfected (FN) cells. For each group, FN was immunoprecipitated with three different antibodies specific for FN: polyclonal anti-human FN, monoclonal anti-human FN and polyclonal anti-FN1−C-Terminal. Membranes were detected also with the three antibodies specific for FN. The positive control used is FN from human serum of a healthy individual, immunoprecipitated with polyclonal anti-FN1−C-Terminal and detected with the same antibody. Fragments denomination was arbitrary. (B) Western blotting quantification for each band detected. Bands are compared between control (C) and transfected (FN) groups.

The results from western blotting for HeLa (figure 5) showed a modest difference between the two groups of cells, with higher FN levels in transfected cells in comparison to control group. For the fragments detected, fragments 2 and 3, lower levels were observed in the transfected group, also with small differences.

For every cell line, FN fragments were detected that were not observed in the positive control.

4.1.3 Expression of FN, integrins and tenascin-C by immunofluorescence

FN, α3, β1 and β3 integrins, and tenascin-C were detected by immunofluorescence for CHO, HCT15 and HeLa cells. Protein expression was compared between control and transfected cells.

CHO:

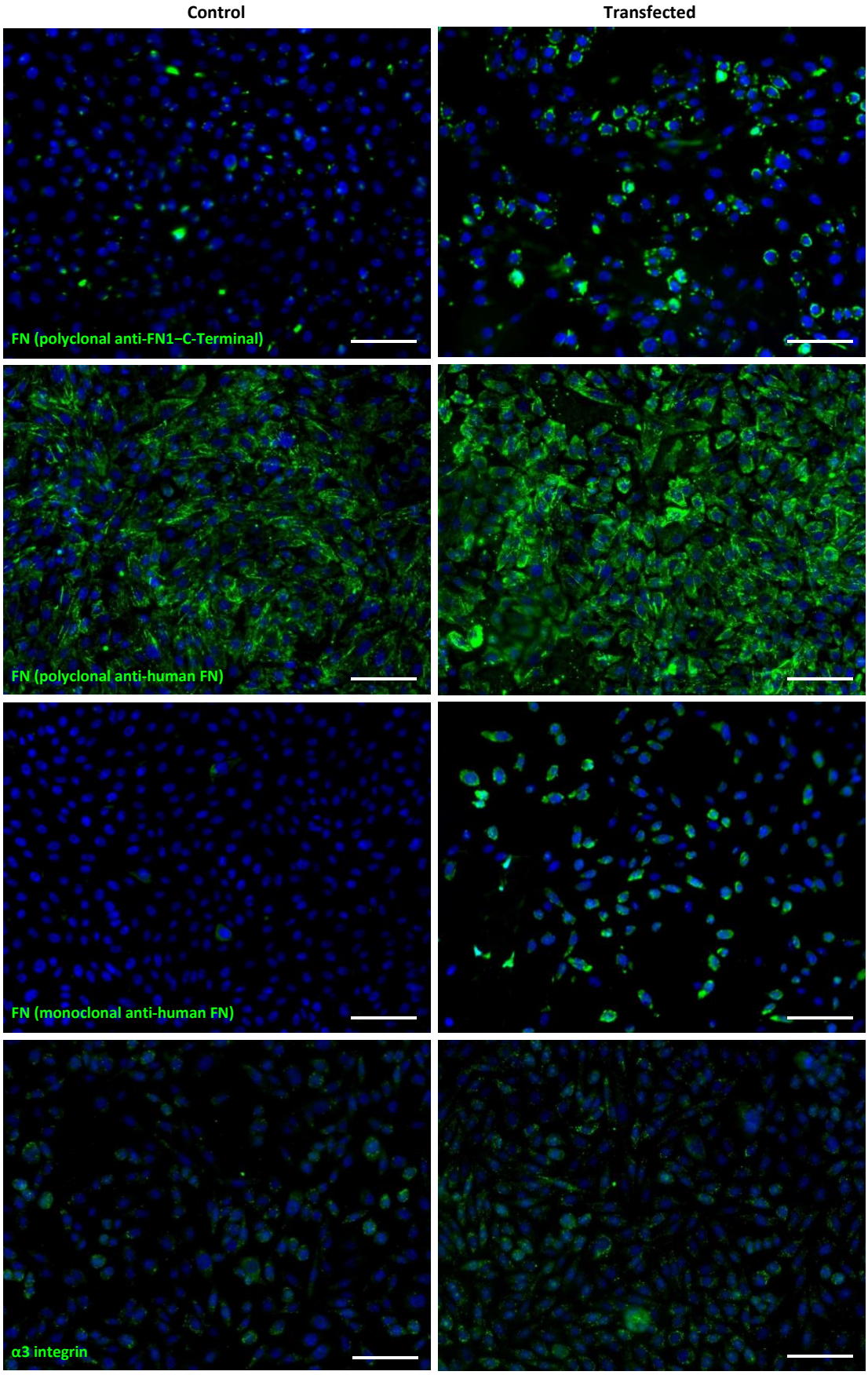
Control
Transfected
FN (polyclonal anti-FN1–C-Terminal)
FN (polyclonal anti-human FN)
FN (monoclonal anti-human FN)
α3 integrin

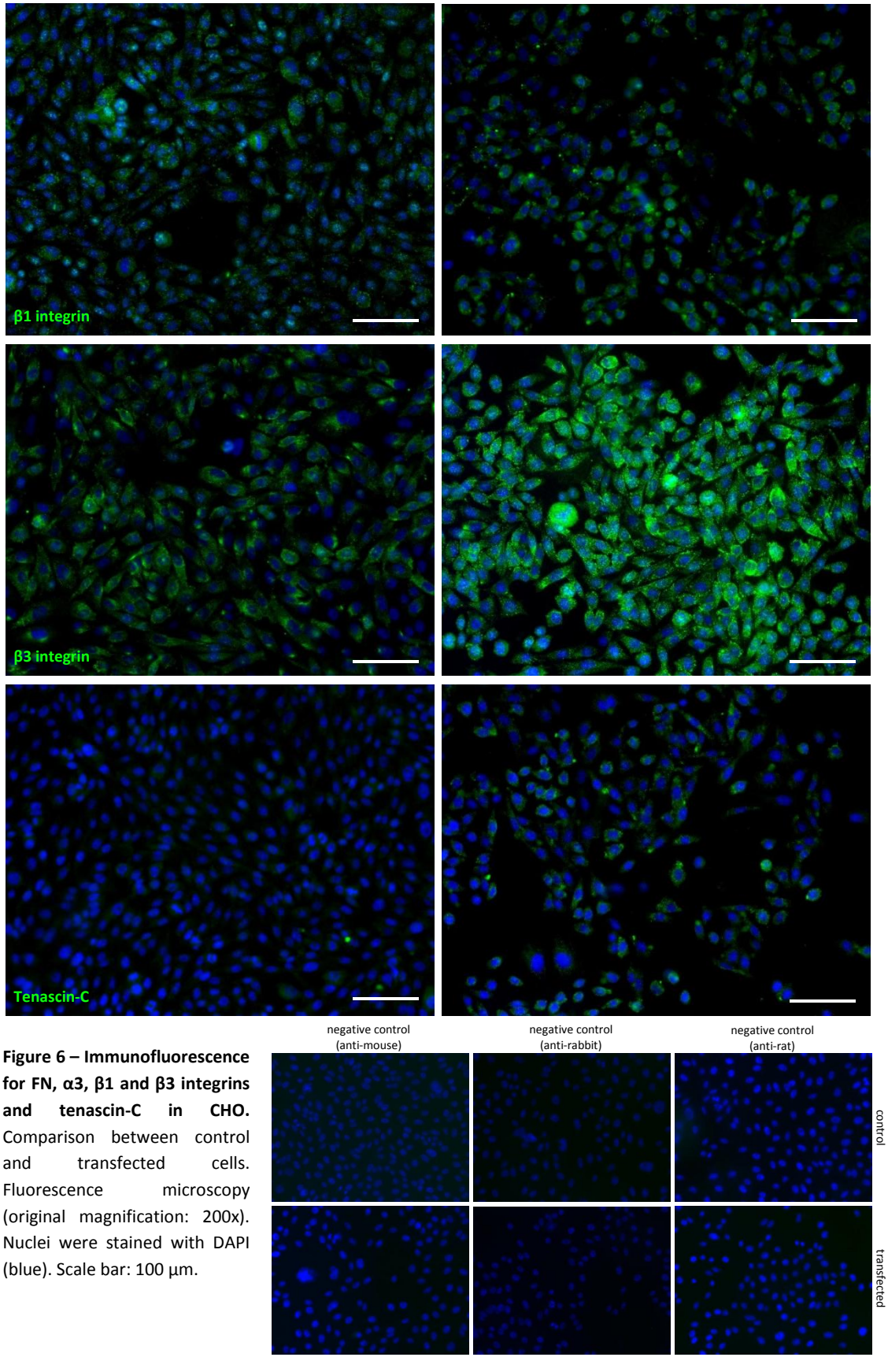

Figure 6 – Immunofluorescence for FN, α3, β1 and β3 integrins and tenascin-C in CHO. Comparison between control and transfected cells. Fluorescence microscopy (original magnification: 200x). Nuclei were stained with DAPI (blue). Scale bar: 100 µm.

For CHO (figure 6), a clear difference was observed between control and transfected cells, showing higher protein levels in transfected cells than in control. FN detection with monoclonal and polyclonal anti-human FN revealed a very tenuous protein expression in control cells, mainly with monoclonal antibody.

For β3 integrin, expressive higher levels were also found in transfected cells. Tenascin-C detection revealed increased levels in transfected cells, but in a less expressive manner.

No evident differences were verified for the other targets.

HCT15:

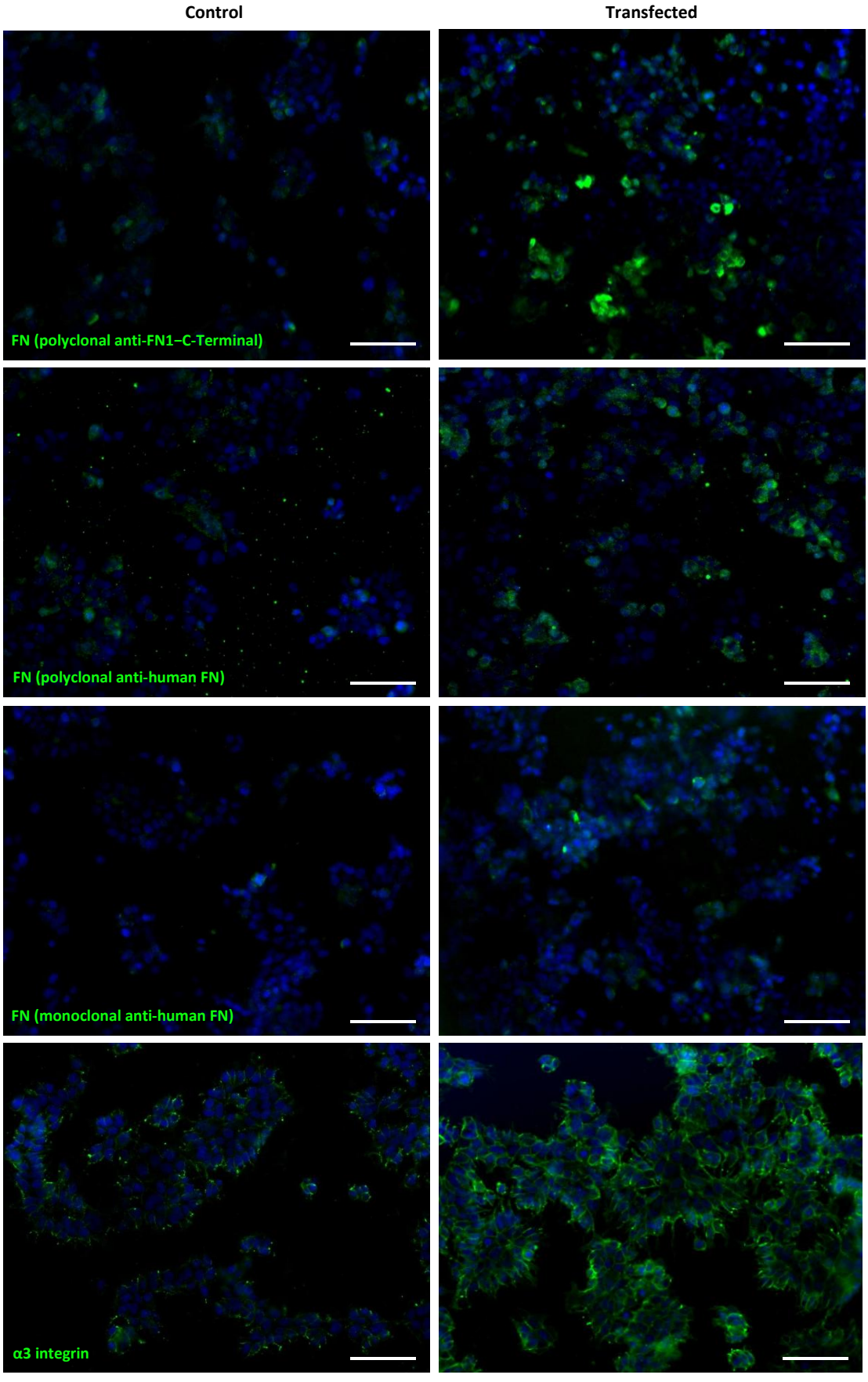
Control
Transfected
FN (polyclonal anti-FN1–C-Terminal)
FN (polyclonal anti-human FN)
FN (monoclonal anti-human FN)
α3 integrin

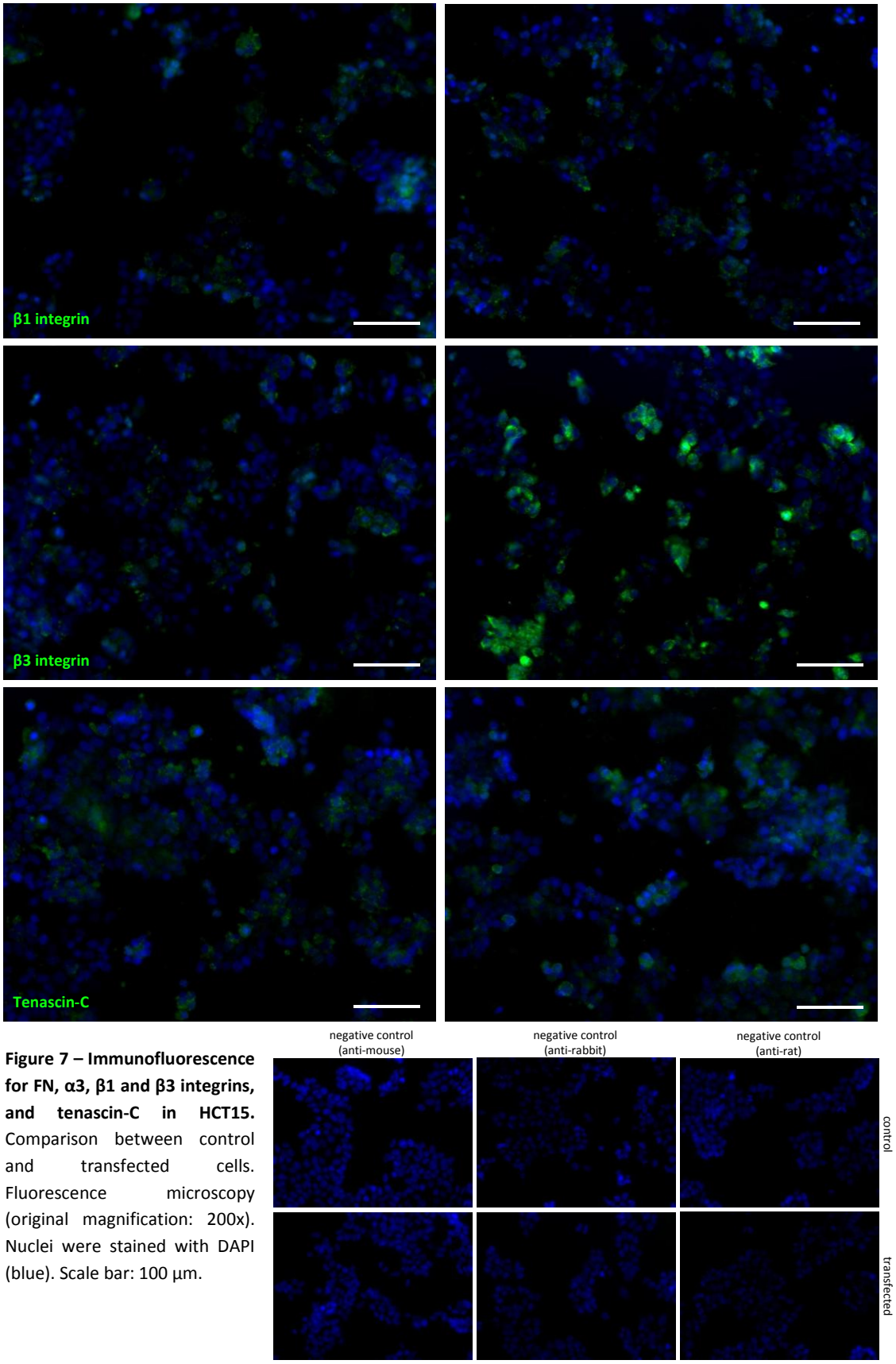

Figure 7 – Immunofluorescence for FN, α3, β1 and β3 integrins, and tenascin-C in HCT15. Comparison between control and transfected cells. Fluorescence microscopy (original magnification: 200x). Nuclei were stained with DAPI (blue). Scale bar: 100 µm.

In HCT15 (figure7), for transfected cells, higher FN levels were observed, as well as for α3 and β3 integrins. No significant differences were detected for the remaining targets.

HeLa:

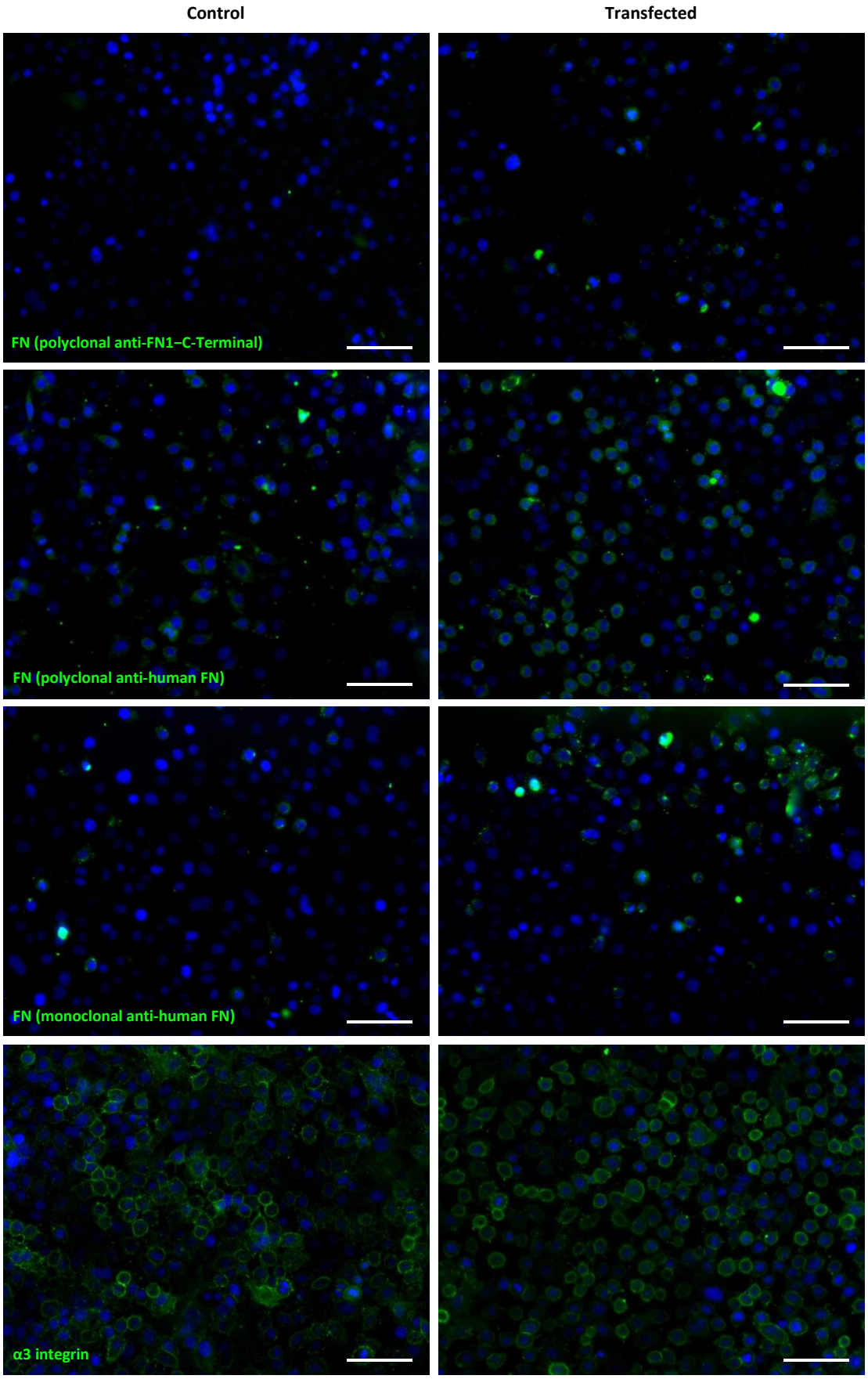
Control
Transfected
FN (polyclonal anti-FN1–C-Terminal)
FN (polyclonal anti-human FN)
FN (monoclonal anti-human FN)
α3 integrin

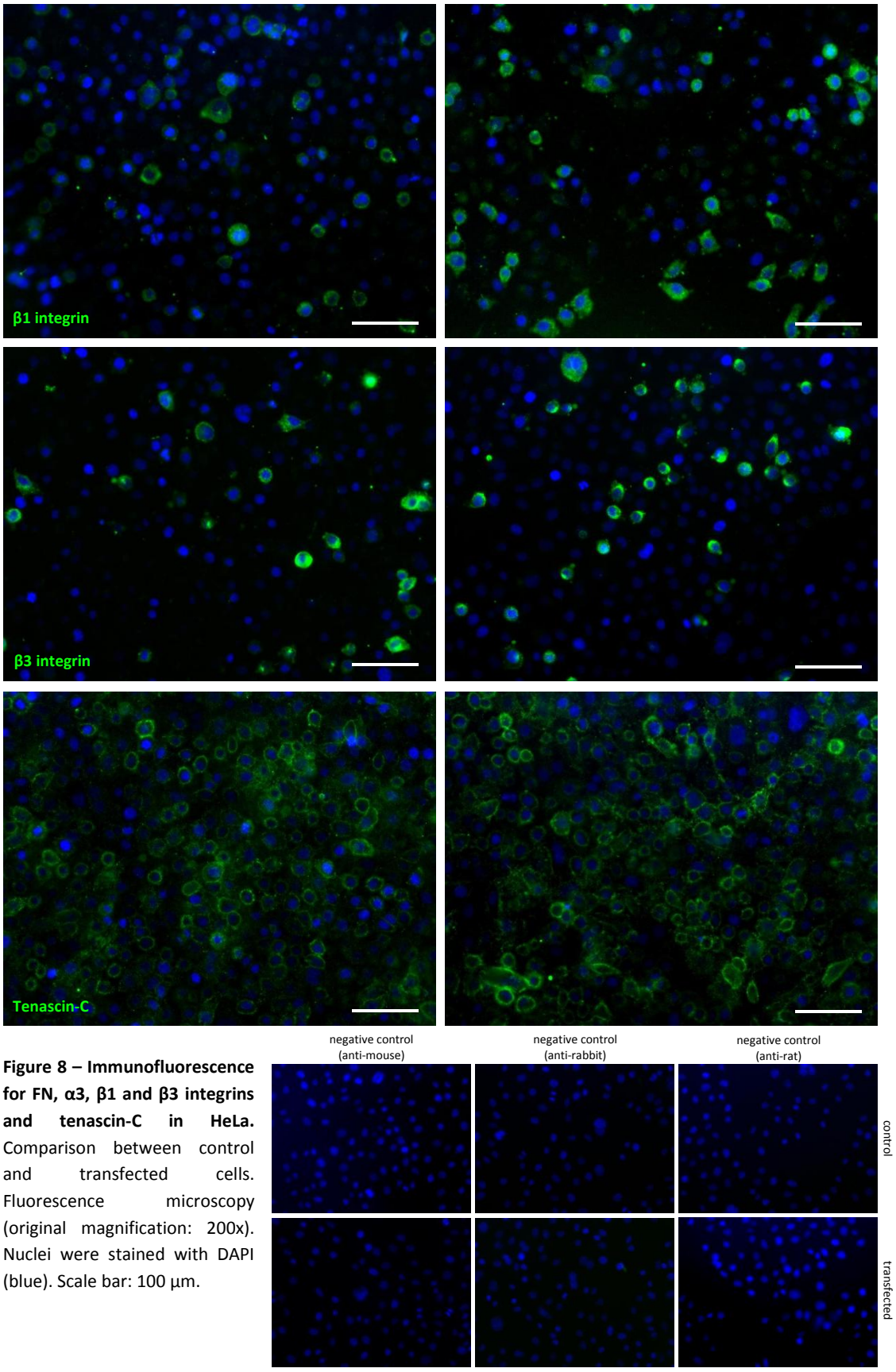

Figure 8 – Immunofluorescence for FN, α3, β1 and β3 integrins and tenascin-C in HeLa. Comparison between control and transfected cells. Fluorescence microscopy (original magnification: 200x). Nuclei were stained with DAPI (blue). Scale bar: 100 µm.

Immunofluorescence for HeLa (figure 8) showed increased FN levels in transfected cells in comparison to control cells, although with a slight significance. For β1 integrin, the same difference was observed, also with a moderate expression.

For the remaining targets, no differences were detected between groups.

4.1.4 Evaluation of MMPs activity by zymography

Zymography was used to verify if FN is able to interfere in MMPs production/secretion or activity in the cell lines used. For that purpose MMPs activity was compared between groups within each cell line, by zymography (figure 9).

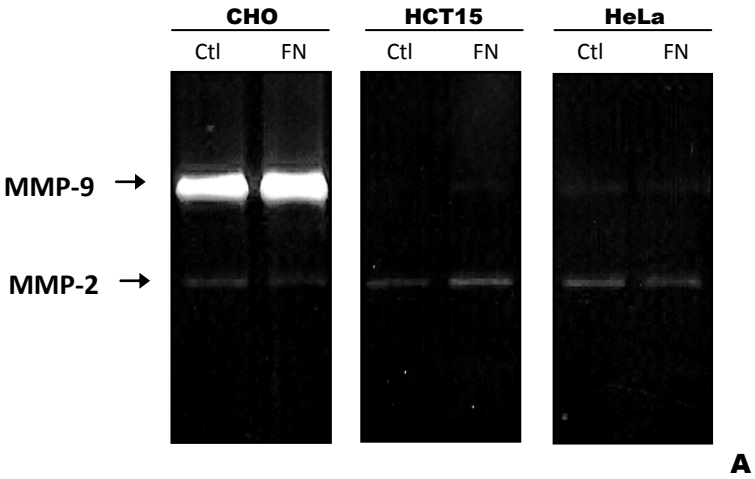

A

	CHO		HCT15		HeLa	
	Ctl	FN	Ctl	FN	Ctl	FN
MMP-9	1	1.15	1	1.63	1	0.83
MMP-2	1	0.67	1	2.23	1	0.72

B

Figure 9 – Zymography of CHO, HCT15 and HeLa media supernatants. (A) Zymogram for control and transfected groups of each cell line. (B) Quantification of each band detected. Bands are compared between control and transfected groups.

The zymogram obtained (figure 9) revealed enzymatic activity of MMP-9 and MMP-2.

In CHO cell line, MMP-9 activity was much higher than MMP-2, in both control and transfected cells.

For MMP-9, it was observed a higher activity in control group. The contrary was detected for MMP-2.

In HCT15, a higher enzymatic activity was verified for MMP-2, in both groups.

For both MMPs, a higher activity was found in transfected cell group.

In HeLa cells, a higher activity was also detected for MMP-2, in both control and transfected cells.

In this cell line, for MMP-9 and MMP-2, a small difference showed a higher enzymatic activity observed in control cell group.

4.1.5 Evaluation of cell migration by wound healing assay

In vitro wound healing assay was performed to investigate a possible role of FN on the migration rate of cells, by comparing control and transfected cell groups (figure 10). The evolution of the experiment was monitorized at the following time points: 0, 8, 24 and 30 hours.

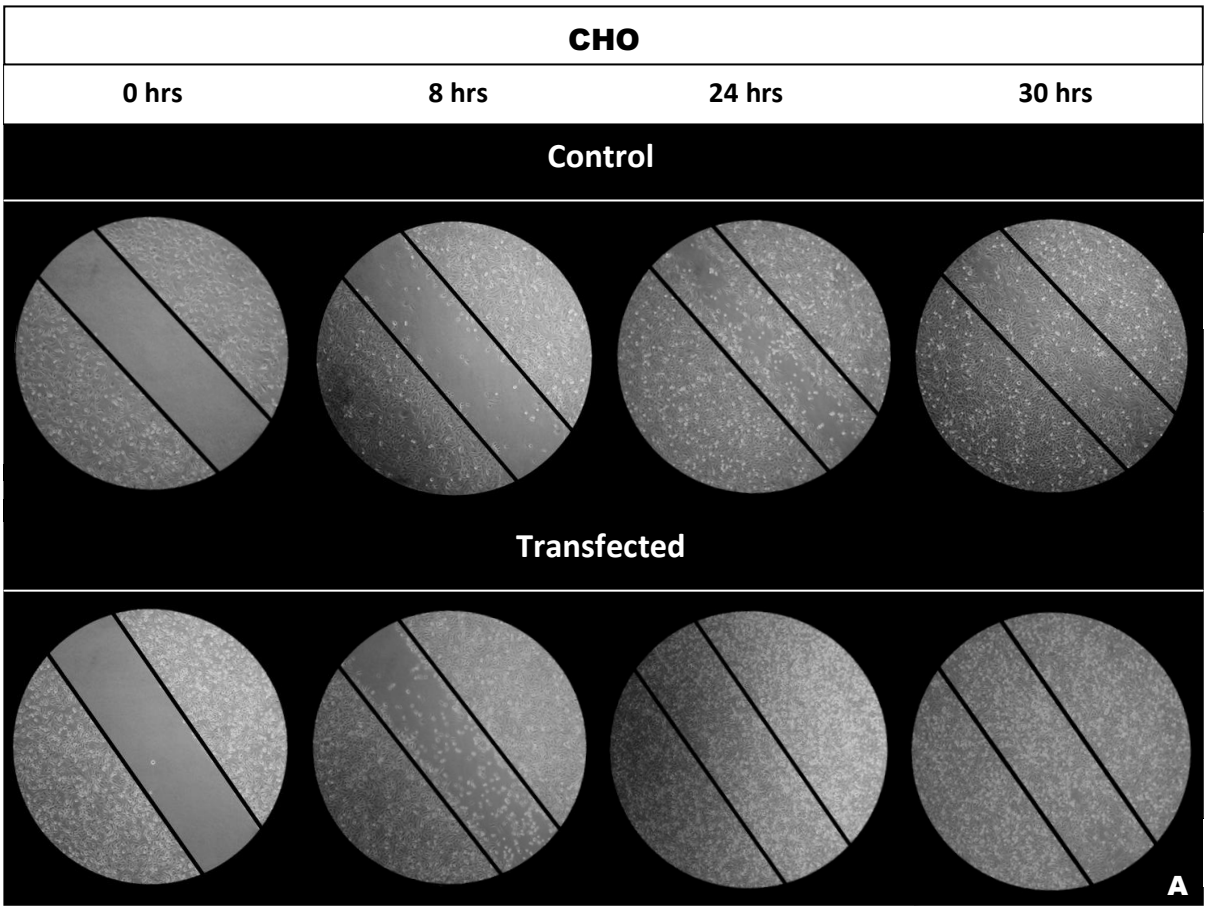

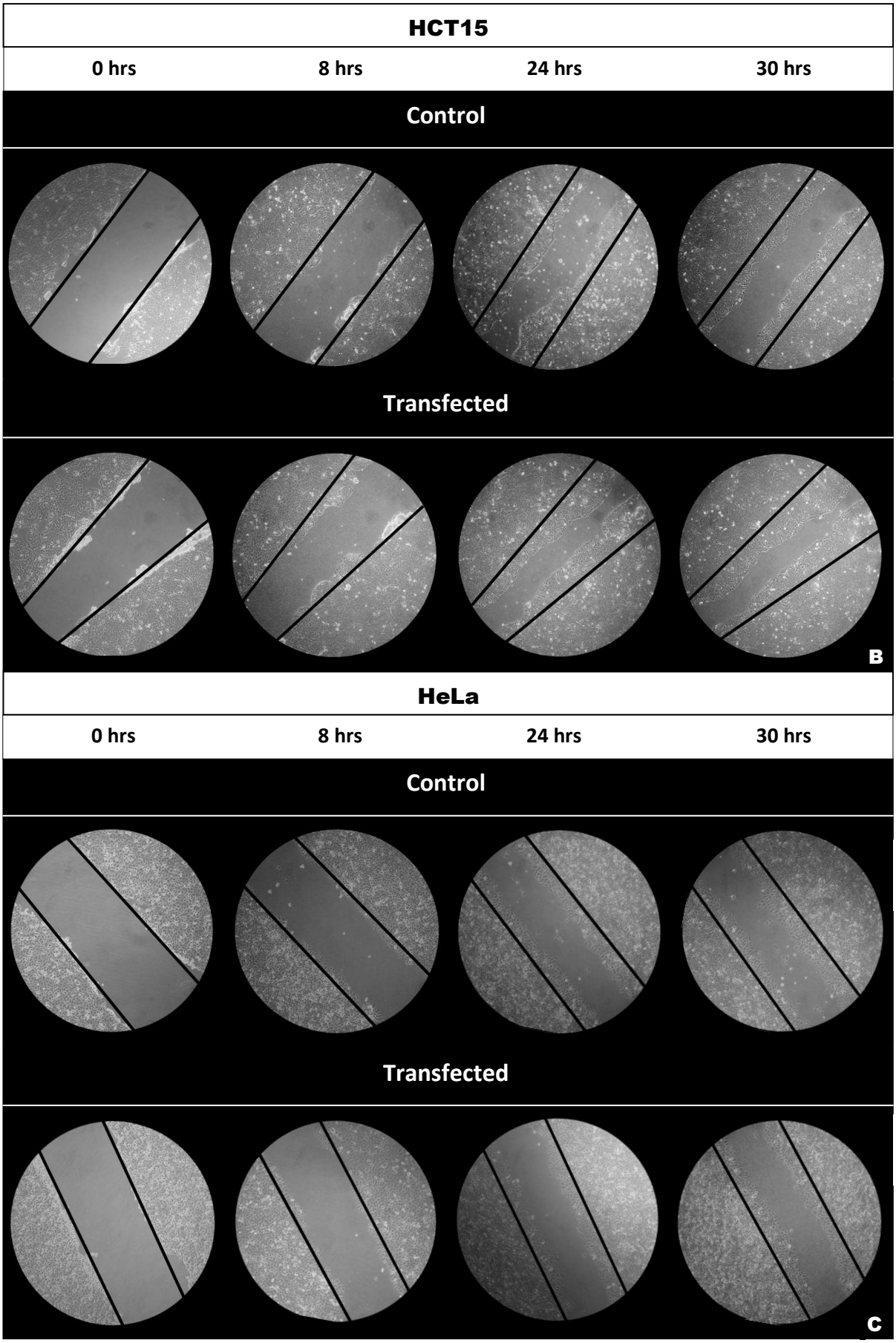

Figure 10 – Wound healing assay. Comparison between control and transfected cells for CHO (A), HCT15 (B) and HeLa (C), at 0, 8, 24 and 30 hours. Phase microscopy (original magnification: 200x).

During the assay, it was observed, in CHO and HCT15 cell lines, a higher cell migration rate in pcDNA3-fl*FN* transfected groups compared to control groups. In HeLa, no differences were observed between the two groups.

4.1.6 Angiogenesis assays: tube formation assay, real-time PCR for *VEGF-121*, *VEGF-165* and *VEGF-189*, *KDR*, *FLT-1*, *Angiopoietin-1* and *Angiopoietin-2*

Tube formation assay and quantification of the expression of *VEGF* isoforms (*VEGF-121*, *VEGF-165* and *VEGF-189*) and its receptors *KDR* and *FLT-1*, *Angiopoietin-1* and *Angiopoietin-2* were carried out to study the potential involvement of FN in angiogenesis.

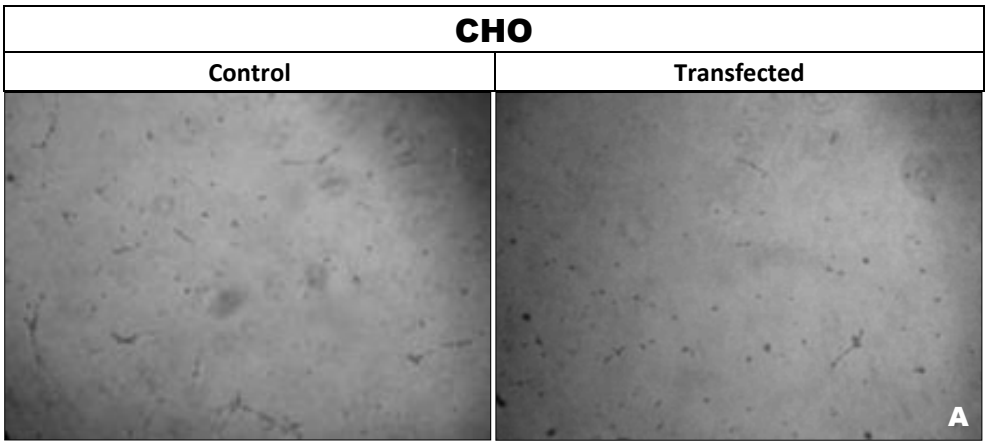

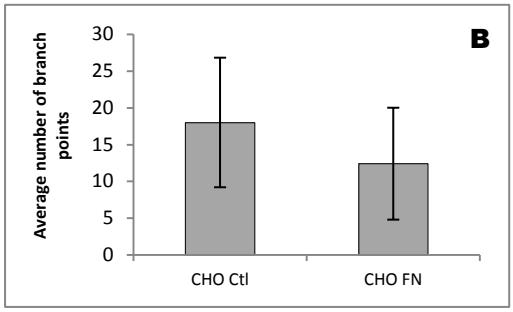

Figure 11 – Tube formation assay with conditioned medium from CHO cell line. (A) Representative images of Matrigel™-induced HUVEC tube formation in monoculture maintained in conditioned medium from control and transfected CHO. Phase microscopy (original magnification: 40x) (B) Average number of branch points in 5 high power fields. Error bars represent standard deviation.

Tube formation assay with conditioned medium from CHO revealed a lower number of branch points formed by HUVEC in transfected cells (figure 11).

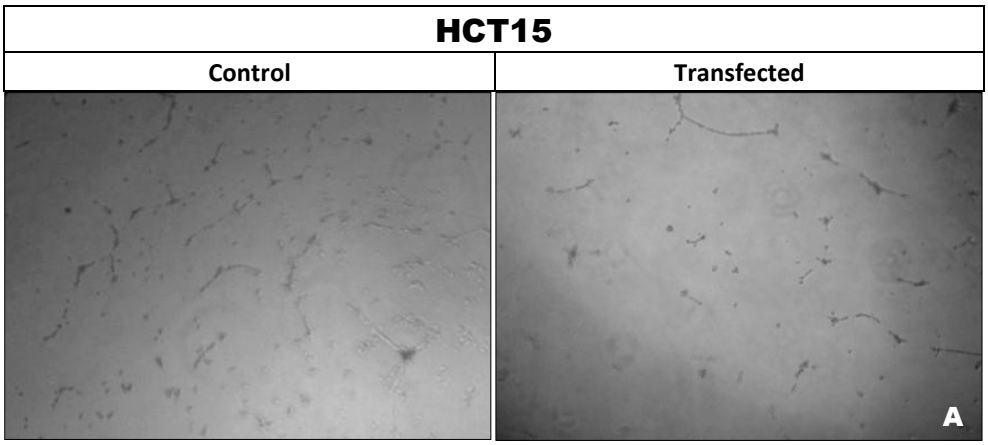

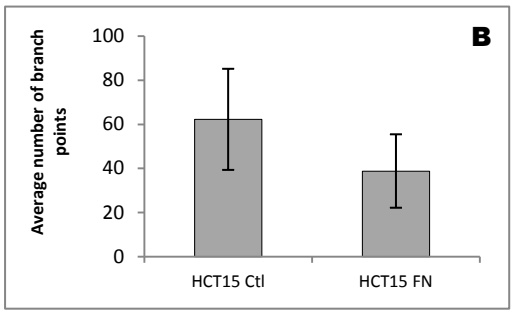

Figure 12 – Tube formation assay with conditioned medium from HCT15 cell line. (A) Representative images of Matrigel™-induced HUVEC tube formation in monoculture maintained in conditioned medium from control and transfected HCT15. Phase microscopy (original magnification: 40x) (B) Average number of branch points in 5 high power fields. Error bars represent standard deviation.

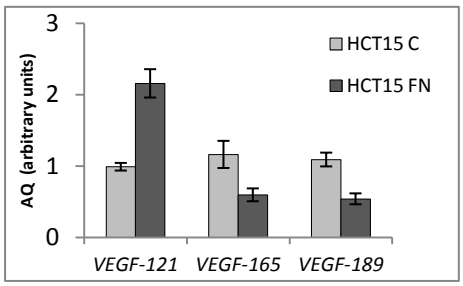

Figure 13 – Real-time-PCR for *VEGF* isoforms expression in HCT15. Absolute quantification of *VEGF-121*, *VEGF-165* and *VEGF-189* mRNA levels in control and transfected HCT15. Error bars represent standard deviation.

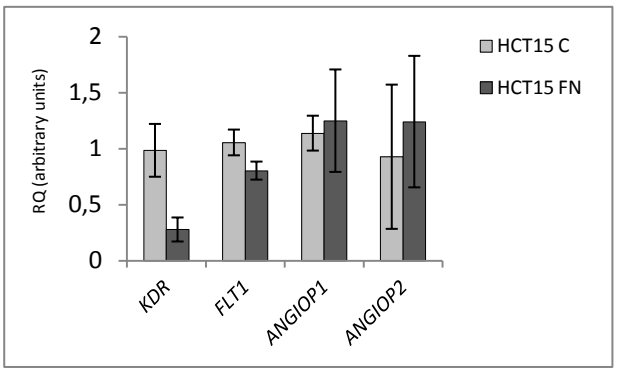

Figure 14 – Real-time-PCR for *KDR*, *FLT-1*, *Angiopoietin-1 (ANGIOP1)* and *Angiopoetin-2 (ANGIOP2)* in HCT15. Relative quantification for mRNA levels in control and transfected HCT15. Error bars represent standard deviation.

For HCT15, as in CHO, a lower number of branch points was verified in the tube formation assay with conditioned medium from transfecetd cells (figure 12). In relation to the expression levels of *VEGF* isoforms (figure 13), absolute quantification showed, in control cells, similar levels of *VEGF-121*, *VEGF-165* and *VEGF-189*. Transfected cells, on the other hand, differed from control group, exhibiting an increased *VEGF-121* expression and lower levels of the other isoforms.

For the same cell line, relative quantification (figure 14) revealed a decrease in VEGF receptors *KDR* and *FLT-1* expression, more evident in *KDR*, in transfected cells, and higher expression levels of *angiopoietin-2*.

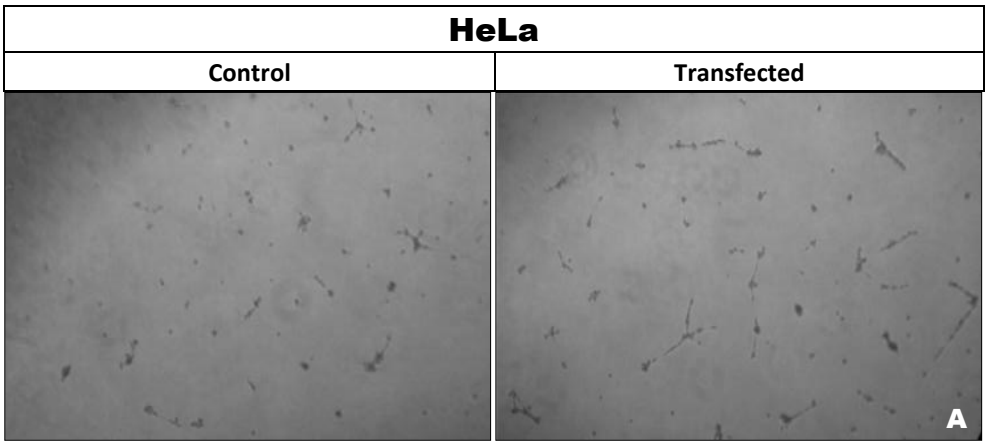

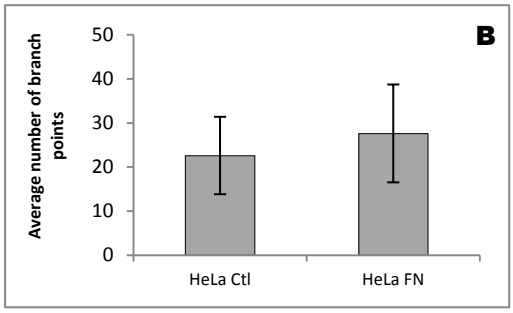

Figure 15 – Tube formation assay with conditioned medium from HeLa cell line. (A) Representative images of Matrigel™-induced HUVEC tube formation in monoculture maintained in conditioned medium from control and transfected HeLa. Phase microscopy (original magnification: 40x) (B) Average number of branch points in 5 high power fields. Error bars represent standard deviation.

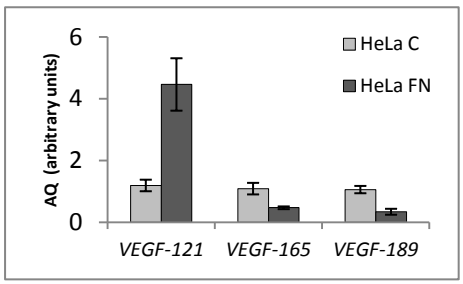

Figure 16 – Real-time-PCR for *VEGF* isoforms expression in HeLa. Absolute quantification of *VEGF-121*, *VEGF-165* and *VEGF-189* mRNA levels in control and transfected HeLa. Error bars represent standard deviation.

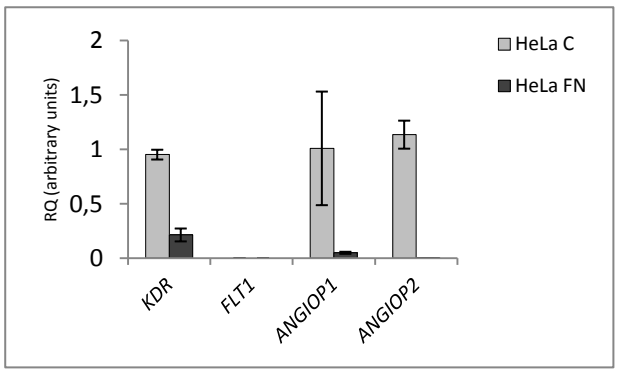

Figure 17 – Real-time-PCR for *KDR*, *FLT-1*, *Angiopoietin-1 (ANGIOP1)* and *Angiopoietin-2 (ANGIOP2)* in HeLa. Relative quantification of mRNA levels in control and transfected HeLa. Error bars represent standard deviation.

For HeLa, tube formation assay (figure 15) resulted in a tenuous difference in the number of branch points formed, showing a small increase when conditioned medium from transfected cells was used. Absolute quantification of *VEGF* isoforms (figure 16) showed, as in HCT15,

similar expression levels of *VEGF* isoforms in control cells, and, in transfected cells, in comparison to that group, an increased expression of *VEGF-121* and lower expression levels of the other isoforms.

By relative quantification (figure 17), a decreased expression of *KDR* and *angiopoietin-1* and *2* were detected in transfected cells.

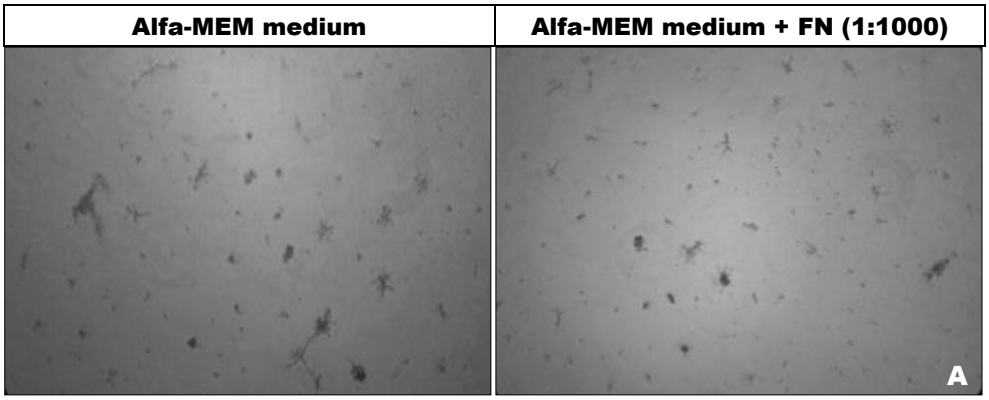

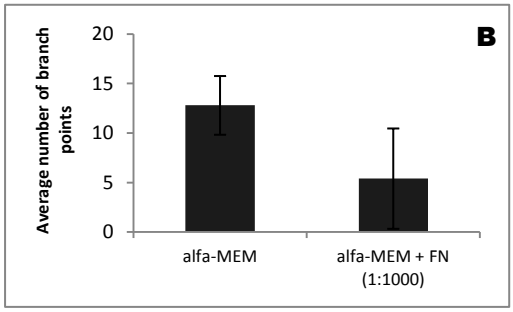

Figure 18 – Tube formation assay control experiment with supplemented Alfa-MEM medium and Alfa-MEM medium + FN (1:1000). (A) Representative images of Matrigel™-induced HUVEC tube formation in monoculture maintained in supplemented Alfa-MEM medium and Alfa-MEM medium + FN (1:1000). Phase microscopy (original magnification: 40x) (B) Average number of branch points in 5 high power fields. Error bars represent standard deviation.

Control experiment for tube formation assay using alfa-MEM medium resulted in a decrease of the number of branch points formed when FN was added to the medium (figure 18).

4.1.7 Quantification of *SCF* and *SDF*-1 expression by real-time PCR

Expression of *SCF* (*stem cell factor*, c-*Kit-ligand*) and *SDF-1* (*stromal cell-derived factor-1*) was addressed by real-time PCR. Relative quantification showed a decrease in the expression of both cytokines, at mRNA levels, in transfected cells, for both HCT15 and HeLa cell lines (figures 19 and 20).

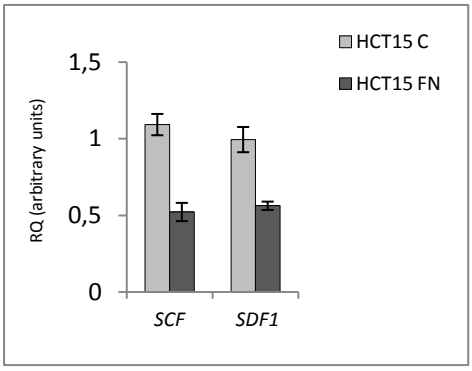

Figure 19 – Real-time-PCR for *SCF* and *SDF-1* in HCT15. Relative quantification of mRNA levels in control and transfected cells. Error bars represent standard deviation.

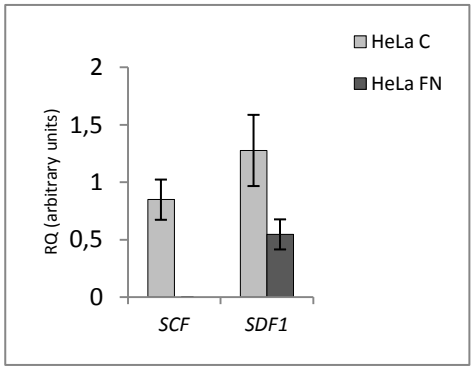

Figure 20 – Real-time-PCR for *SCF* and *SDF-1* in HeLa. Relative quantification of mRNA levels in control and transfected cells. Error bars represent standard deviation.

4.2 *IN VIVO* ASSAYS

4.2.1 Flow cytometric analysis of endothelial and hematopoietic progenitor cells

Analysis of endothelial and hematopoietic progenitor cells showed, for the animals inoculated with HCT15, an increase of endothelial progenitor cells (EPCs) (Sca+,Flk+ cells) since the inoculation (figure 21), both for the animals inoculated with control and transfected cells. That increase was more pronounced in the latter group. The same trend was found for hematopoietic progenitor cells (HPCs) (cKit+ cells) until the last time point (56 days), when the percentage of cKit+ cells was higher in the control group (figure 22).

In the animals inoculated with HeLa, it was not observed any trend in any of the groups, for EPCs (figure 23). For HPCs (figure 24), there was a decrease in the number of cKit+ cells, during the experiment, for the animals inoculated with control HeLa, and an increase for the animals inoculated with transfected HeLa.

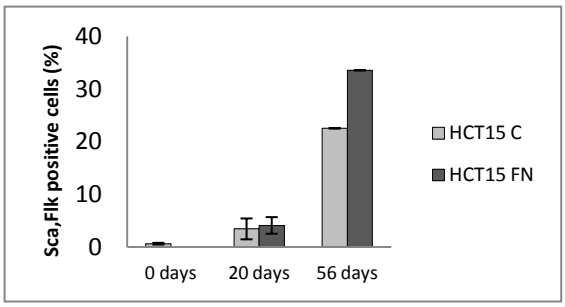

Figure 21 – Flow cytometric analysis of endothelial progenitor cells (Sca+,Flk+ cells) for mice inoculated with HCT15. Comparison of percentage of Sca+,Flk+ cells between control (C) and transfected subgroups (FN), at 0, 20 and 56 days. Error bars represent standard deviation.

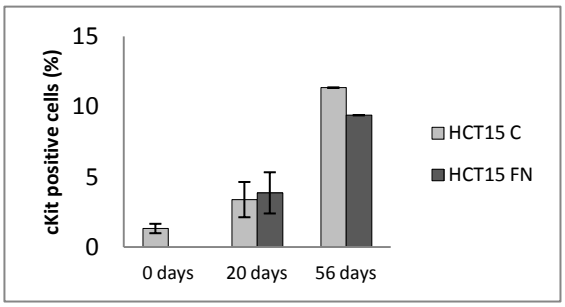

Figure 22 – Flow cytometric analysis of hematopoietic progenitor cells (cKit+) for mice inoculated with HCT15. Comparison of percentage of cKit+ cells between control (C) and transfected (FN) subgroups, at 0, 20 and 56 days. Error bars represent standard deviation.

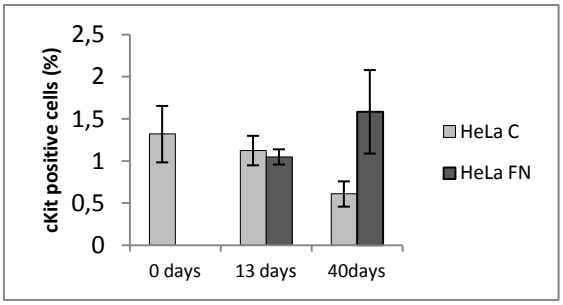

Figure 23 – Flow cytometric analysis of endothelial progenitor cells (Sca+,Flk+ cells) for mice inoculated with HeLa. Comparison of percentage of Sca+,Flk+ cells between control (C) and transfected (FN) subgroups, at 0, 13 and 40 days. Error bars represent standard deviation.

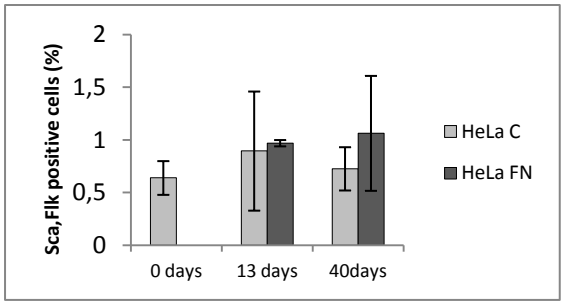

Figure 24 – Flow cytometric analysis of hematopoietic progenitor cells (cKit+) for mice inoculated with HeLa. Comparison of percentage of cKit+ cells between control (C) and transfected (FN) subgroups, at 0, 13 and 40 days. Error bars represent standard deviation.

4.2.2 Evaluation of FN expression in the serum of animal models by western blotting

A western blotting was carried out to quantify FN and its proteolytic fragments in the serum of the xenograft orthotopic BALB/c-SCID (figure 25).

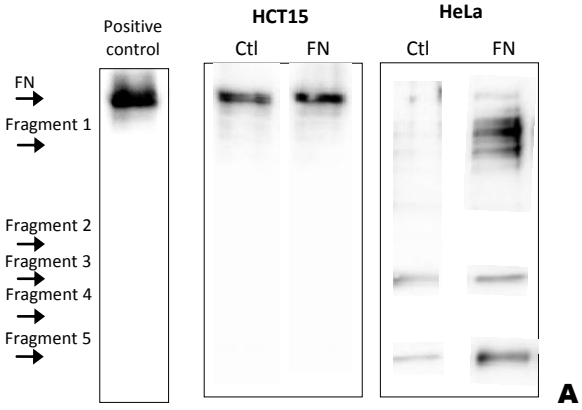

	HCT15		HeLa	
	Ctl	FN	Ctl	FN
FN	1	1.10	1	1.09
Fragment 3	—		1	1.38
Fragment 5	—		1	5.09

B

Figure 25 – Western blotting of FN immunoprecipitated from the serum of xenograft orthotopic BALB/c-SCID. (A) Reresentative western blotting analysis of FN from the serum of mice inoculated with control (Ctl) and transfected (FN) cells (HCT15 and HeLa). For each group, FN was immunoprecipitated with polyclonal anti-human FN. Membranes were detected with the same antibody. The positive control used is FN from human serum of a healthy individual, immunoprecipitated with polyclonal anti-FN1−C-Terminal and detected with the same antibody. Fragments denomination was arbitrary. (B) Western blotting quantification. Bands are compared between the two groups.

For both animal groups, FN levels were almost equivalent between mice inoculated with control and transfected cells. Fragments were detected only for the animals inoculated with

HeLa, in which higher levels were observed, especially for fragment 5, in the subgroup inoculated with transfected cells.

4.2.3 Histological analysis

Macroscopic observation showed that both groups of orthotopic mice developed tumor in the point of inoculation. A larger tumor mass was observed in the mice inoculated with the transfected cells, for both cell lines (figures 26 and 27).

Histological analysis consisted of tumor cells detection, by CK-19 and CK-7 staining for HCT15 and HeLa cells, respectively, E-cadherin and mast cells detection.

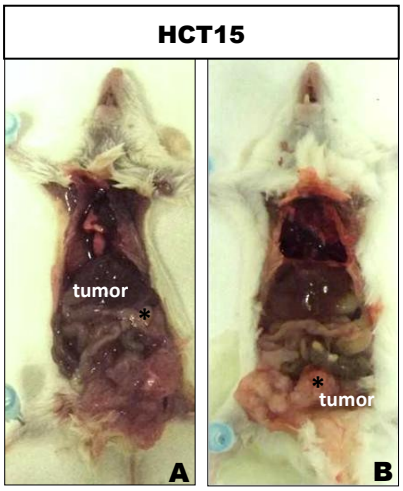

Figure 26 – Macroscopic observation of xenograft orthotopic BALB/c-SCID inoculated with HCT15. (A) Representative image of the animals inoculated with control HCT15. (B) Representative image of the animals inoculated with transfected HCT15.

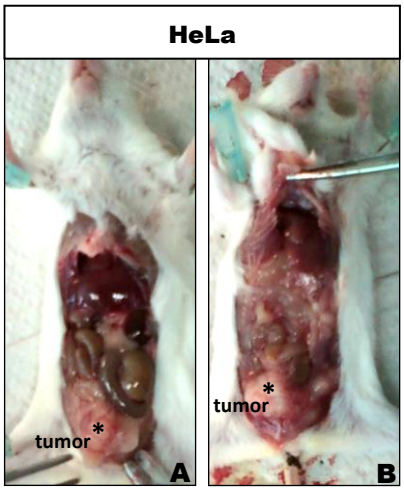

Figure 27 – Macroscopic observation of xenograft orthotopic BALB/c-SCID inoculated with HeLa. (A) Representative image of the animals inoculated with control HeLa. (B) Representative image of the animals inoculated with transfected HeLa.

4.2.1.1 Tumor cells detection in xenograft tumors

For mice inoculated with HCT15, histological analysis of the collected organs showed the presence of metastases in the liver of both subgroups (figure 29A). Lung metastases were also found but only for the control mice (figure 29B). Tumor analysis revealed a more invasive activity of cancer cells in control mice (figure 29C).

HCT15:

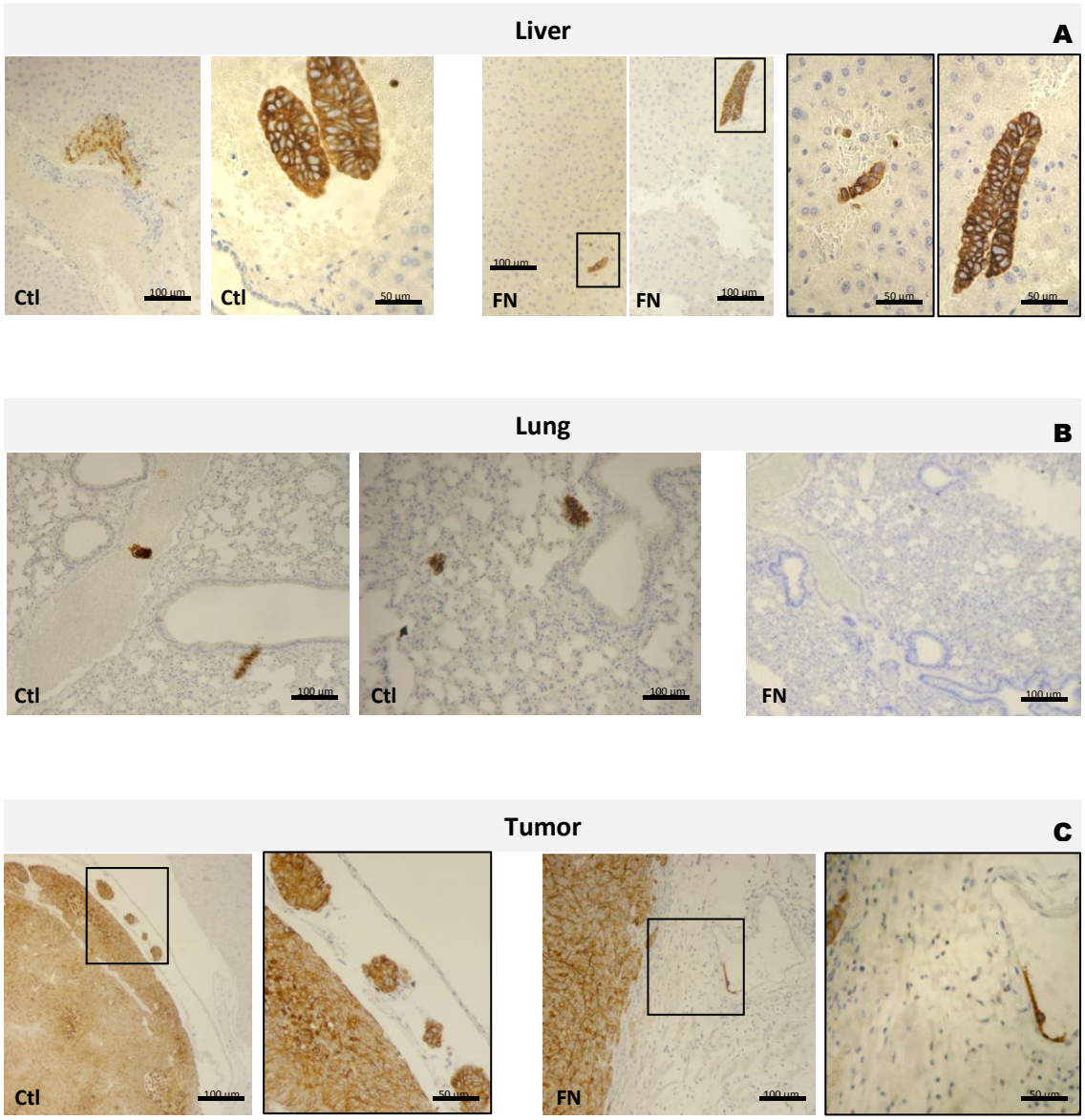

Figure 28 – Immunoreactivity for cytokeratin-19 (CK-19) in xenograft orthotopic BALB/c-SCID inoculated with control (Ctl) and transfected (FN) HCT15. Representative images of liver (A), lung (B) and tumor (C). Light microscopy (original magnifications: 40x and 100x). CK-19 stained in brown and nuclei in blue.

HeLa:

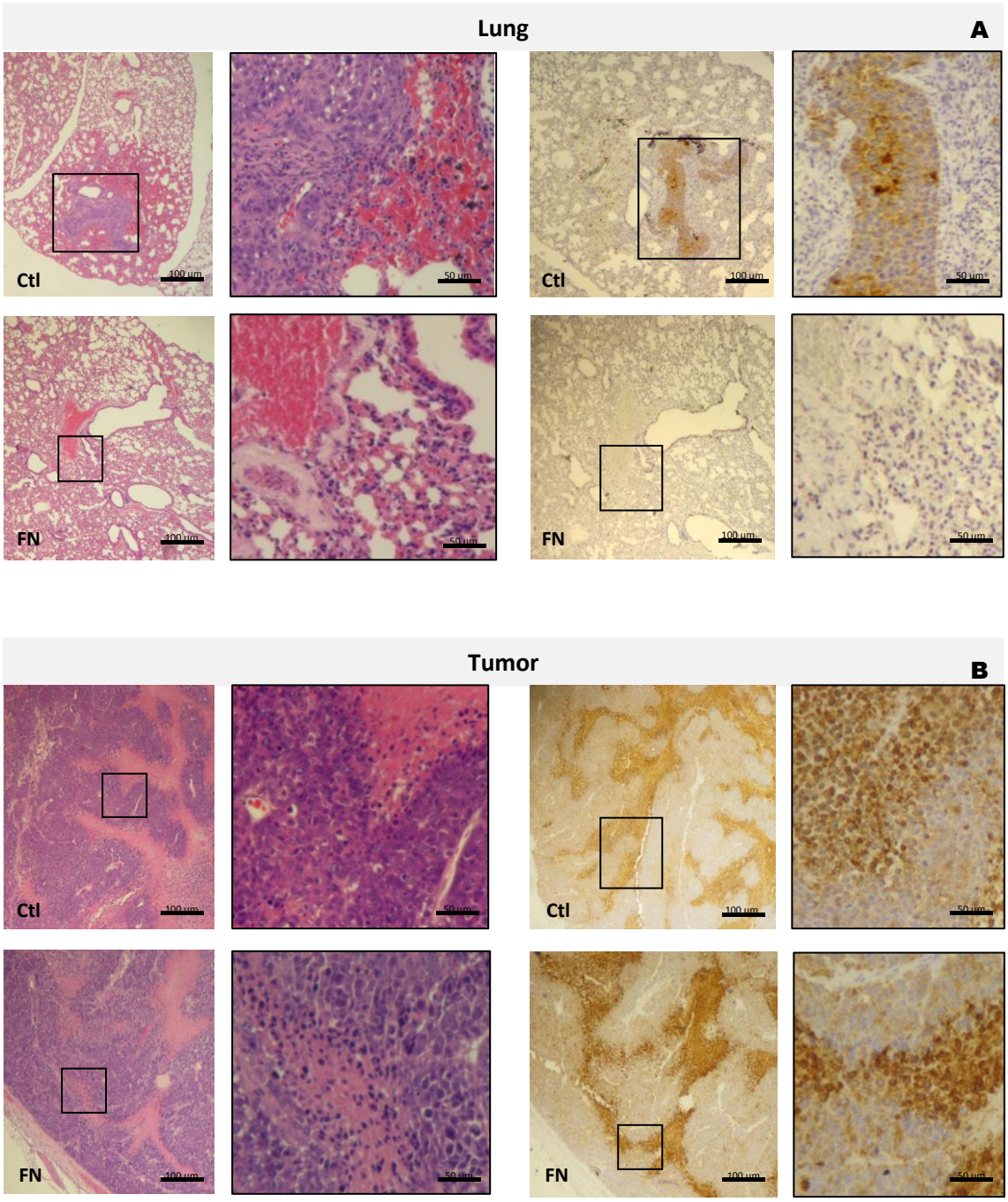

Figure 29 – Immunoreactivity for cytokeratin-7 (CK-7) and H&E (Hematoxylin and Eosin) in xenograft orthotopic BALB/c-SCID inoculated with control and transfected HeLa. Representative images of lung (A) and primary tumor (B). Light microscopy (original magnifications: 40x and 100x). CK-7 stained in brown and nuclei in blue.

For mice inoculated with HeLa, lung metastases were found in the control mice (figure 29A). Histological analysis of primary tumors showed no differences between mice inoculated with control and transfected HeLa (figure 29B).

4.2.3.2 Detection of E-chaderin in xenograft tumors

E-cadherin staining, performed on xenograft tumors, revealed no differences between mice inoculated with control and transfected HCT15 (figure 30A) and HeLa (figure 30B). In HeLa, only the normal tissue stains for E-cadherin.

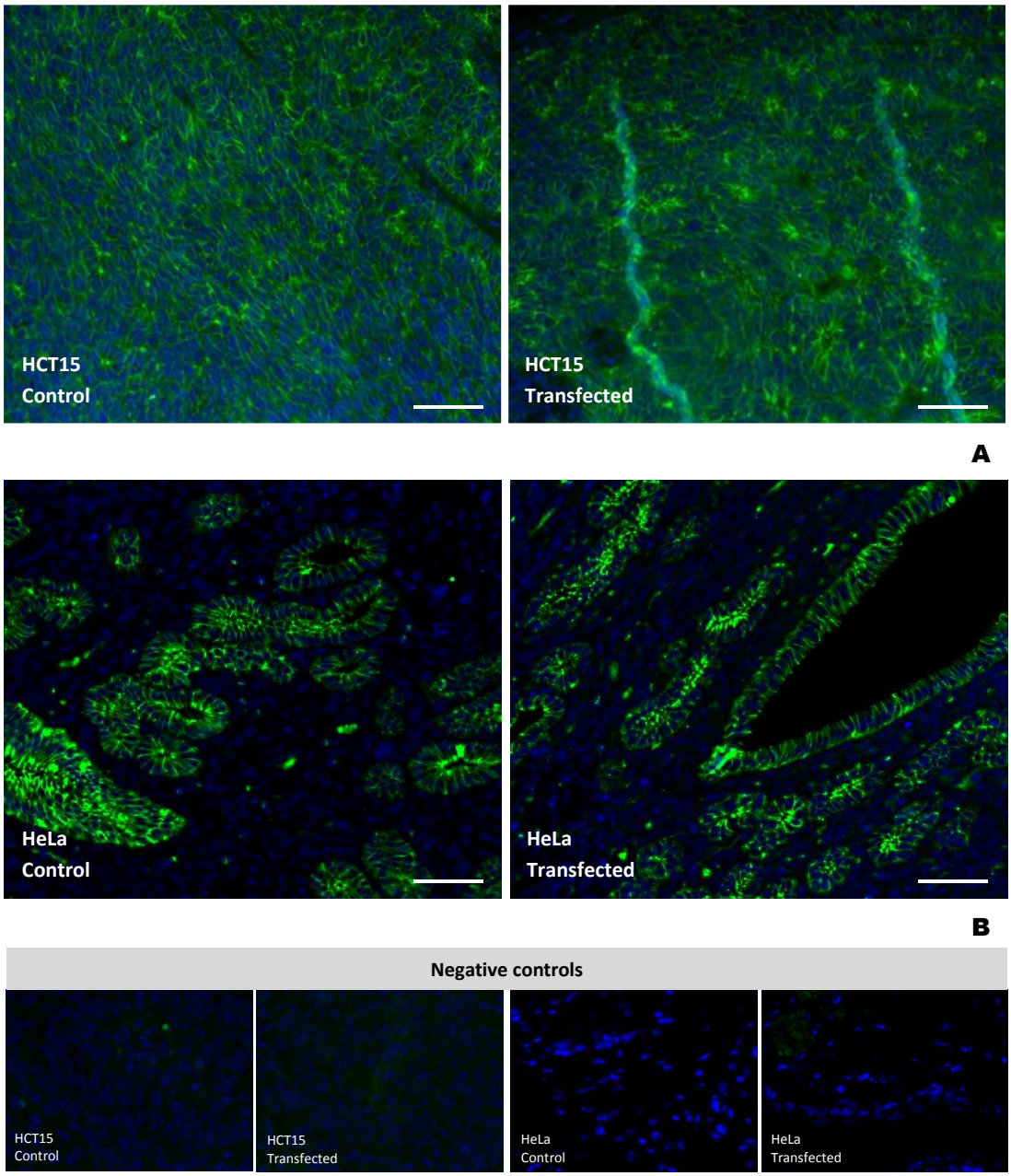

Figure 30 – Immunofluorescence for E-cadherin in the primary tumor of xenograft orthotopic BALB/c-SCID. Representative images for HCT15 (A) and HeLa (B) groups. Fluorescence microscopy (original magnification: 200x). Nuclei were stained with DAPI (blue). Scale bar: 100 µm.

4.2.3.3 Detection of mast cells in xenograft tumors

Mast cells detection revealed, for HCT15, a higher mast cells infiltration in tumor (figure 31A). For HeLa, no mast cells were detected (figure 31B).

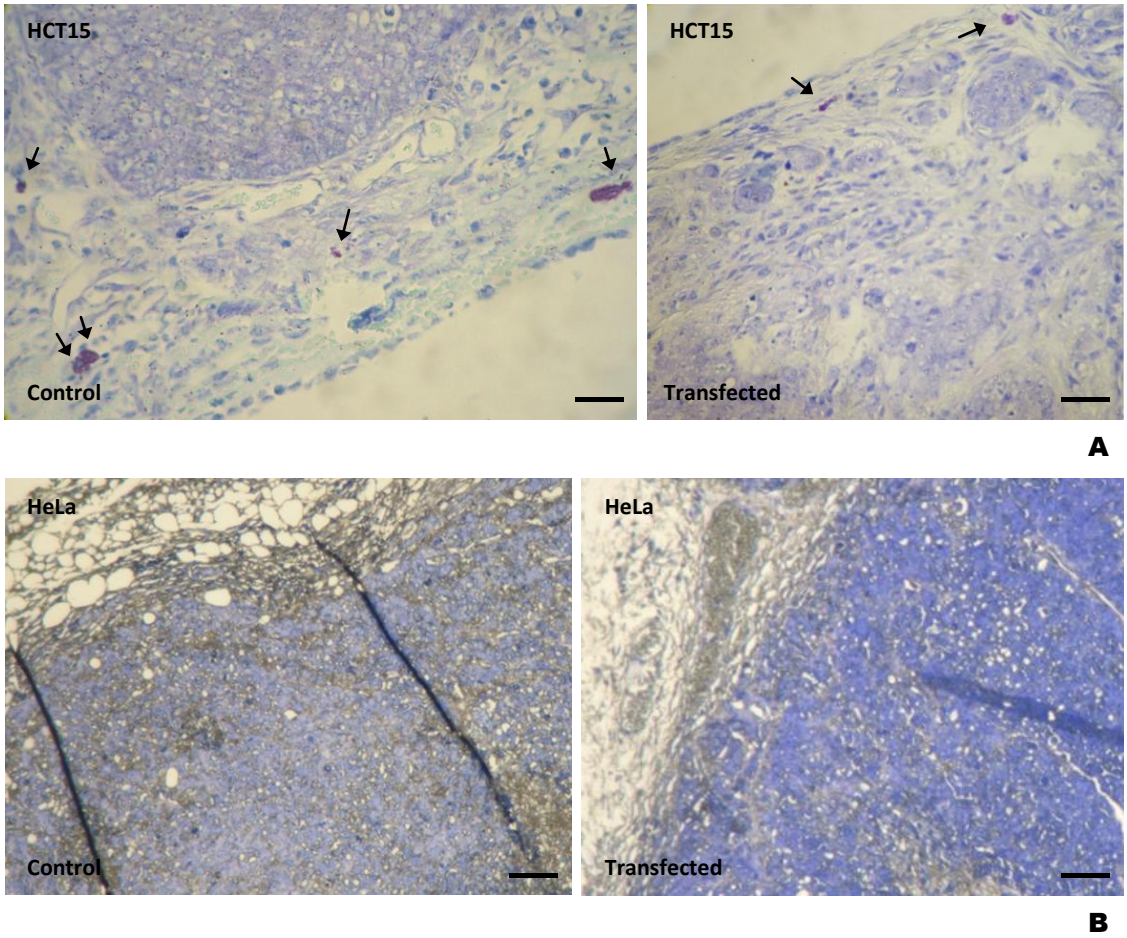

Figure 31 – Toluidine blue staining for mast cells in the primary tumor of xenograft orthotopic BALB/c-SCID. Representative images for HCT15 (A) and HeLa (B) groups. Light microscopy (original magnification: 100x). Mast cells are stained in violet (arrows). Scale bar: 50 µm.

5. Discussion

ECM represents a critical intervenient of oncogenic transformation. Cancer steps are significantly dependent on the permissive nature of the microenvironment and ECM proteolysis assumes great importance in this context (Chambers & Matrisian, 1997; Polette *et al*, 2004; Werb, 1997). FN is one of the most abundant components of ECM and several studies have related FN levels to tumor progression in cancer patients, observing an increase of both FN and FN fragments levels (Katayama *et al*, 1993; Kenny *et al*, 2008; Kenny & Lengyel, 2009; Labat-Robert, 2002; Labat-Robert *et al*, 1980; Warawdekar *et al*, 2006).

Based on this data, it was elected as global objective of this thesis to study the role of FN in tumor development and progression. For that purpose, as already described, for tumor cell lines HCT15 and HeLa, two groups were created, differing on the FN amounts produced, by transfection of a plasmid containing the *FN* gene (pcDNA3-fl*FN*). CHO cell line, used as a positive control, was subjected to the same *in vitro* experiment.

In a first approach, the *FN* mRNA levels quantified for each group (figure 2) confirmed the expected result after transfection: it was observed an obvious difference between the control and the transfected cells, especially in HCT15 and CHO cell lines. The elevated *FN* mRNA expression in transfected CHO – and since this cell line was used as a positive control due to its lack of a control mechanism of transcription – proved the success of the transfection. These results allowed the progression of the experiment.

To verify if the difference observed in mRNA was reflected in FN protein levels, western blotting and immunofluorescence analysis were carried out. Both techniques confirmed the expected difference between groups within each cell line, showing higher protein levels in transfected cells in comparison to control groups. In western blotting and real-time PCR, that difference was smaller in HeLa than in HCT15 and CHO, which was consistent with real-time PCR.

The results from western blotting (figures 3, 4 and 5) showed, for HCT15 and HeLa, the presence of FN fragments that were not observed in the positive control, an immunoprecipitated blood sample from a healthy individual. This fact corroborates the results from several studies, in which an increase of proteolytic fragmentation of FN was observed in cancer patients (Katayama *et al*, 1993; Kenny *et al*, 2008; Kenny & Lengyel, 2009; Labat-Robert, 2002; Labat-Robert *et al*, 1980; Warawdekar *et al*, 2006).

For CHO, FN fragments were also observed. Although CHO are not cancer cells, this is an altered cell line with great MMPs secreting activity, which could explain the pattern obtained.

The differences among conditions for the same cell line could be explained by the specificities of each antibody. Immunoprecipitation with polyclonal anti-FN1−C-Terminal revealed the smallest differences between groups. In fact, this is technically considered the less specific antibody once it is polyclonal and reacts with three species. Hence, a particular focus must be attributed to the results obtained from the other immunoprecipitations.

For CHO and HCT15, higher levels of FN fragments were obtained in transfected groups, which were expected due to the higher amounts of FN expressed.

For HeLa, the opposite was observed, but in a very discrete manner. In fact, for this cell line, the difference between groups regarding to FN amount was not very evident.

Immunofluorescence results (figures 6, 7 and 8) were consistent with the prior findings for FN expression. The results obtained for FN detection in CHO were consistent with the expectation for each antibody and additionally confirmed the success of the transfection.

For every cell line, the increase of FN in transfected cells was accompanied by an increase of integrins expression, which was reasonable once these are the FN receptors. The fact that this variation reached different integrins among cell lines may be explained by the different cell contexts.

Tenascin-C is an ECM molecule related to cell adhesion and detachment that interacts with FN (Chung *et al*, 1995), and is implicated in tumorigenesis (Orend & Chiquet-Ehrismann, 2006). Immunofluorescence showed tenascin-C expression in the cell lines tested, mainly in HCT15 and, even in a greater extent, HeLa. In fact, studies have implicated this glycoprotein as being highly expressed in the microenvironment of many solid tumors (Orend & Chiquet-Ehrismann, 2006), including colorectal carcinoma (Emoto *et al*, 2001; Sis *et al*, 2004) and uterine cervix cancer (Buyukbayram & Arslan, 2002). In CHO, it was observed an increased tenascinC expression in transfected cells, although with a very slight significance. For tumor cell lines HCT15 and HeLa, however, no difference was verified between groups.

MMPs activity was analyzed by zymography (figure 9). For every group, MMP-9 and MMP-2 enzymatic activities were detected. Besides the evidence that MMPs activity is strongly associated with tumorigenesis (Kessenbrock *et al*, 2010), MMP-9 and MMP-2 are thought to be the most important MMPs in metastasis (Coussens *et al*, 2002; Klein *et al*, 2004; Malemud, 2006; Serpa *et al*, 2010; Stetler-Stevenson, 1999).

For MMP-9, in transfected groups from both CHO and HCT15, results showed an increased enzymatic activity, although with more significance in HCT15. For MMP-2, that pattern is maintained in HCT15; in CHO, it was observed a decreased activity in transfected cells in comparison to control group. These increases in MMPs activity may be directly related to higher amounts of FN in media supernatants of transfected cells, which is cleaved by MMPs,

and/or FN may induce signaling pathways that culminate in an increased MMPs activity. MMPs upregulation, particularly MMP-9 and MMP-2, in fact, has been described for several neoplastic contexts (Duffy *et al*, 2000; Kenny & Lengyel, 2009; Klein *et al*, 2004), and some studies have related FN to MMPs upregulation as an inducer of multiple signaling pathways (Das *et al*, 2008; Han *et al*, 2006; Mitra *et al*, 2006; Sen *et al*, 2010).

For HeLa, results demonstrated a lower activity of both MMPs in transfected group, although the difference obtained has been very small. In fact, and considering the assays mentioned above, the difference in FN between control and transfected HeLa was not very accentuated, which can explain the results observed.

The results observed for MMPs activity are also consistent with the pattern obtained for FN fragments in western blotting.

In the study of cell migration, addressed by wound healing assay (figure 10), no differences were detected between HeLa groups, whereas in CHO and HCT15 a more accelerated directional cell migration was detected. The pattern observed is, once again, consistent with the prior results.

ECM proteolysis is one of the most important events required for cells migration (Hugo *et al*, 2007; Voulgari & Pintzas, 2009). MMPs play an important role in this context by cleaving several macromolecules of the ECM, facilitating tumor cells migration (Hay, 1995; Hugo *et al*, 2007; Voulgari & Pintzas, 2009). The results observed in wound healing assay may, therefore, be a consequence of those obtained from zymography.

The role of FN in tumor angiogenesis was addressed by tube formation assay and quantification of the expression of *VEGF-121*, *VEGF-165* and *VEGF-189*, VEGF receptors *KDR* and *FLT1*, and angiogenesis promoting growth factors *Angiopoietin-1* and *Angiopoietin-2*.

VEGF is one of the main inducers of endothelial cell proliferation, differentiation and permeability of blood vessels, regulating, therefore, angiogenesis and vasculogenesis (Witsch *et al*, 2010; Zwick *et al*, 2001). Alternative splicing of *VEGF* mRNA generates four different isoforms, VEGF-121, VEGF-165, VEGF-189 or VEGF-206. VEGF-121 is freely diffusible, whereas VEGF-189 is found tightly bound to ECM. VEGF-165 exhibits intermediate properties (Lee *et al*, 2005; Park *et al*, 1993).

Several studies have provided evidence for the role of VEGF signaling in tumor vascularization and metastasis (Padro *et al*, 2002; Trojan *et al*, 2004; Zwick *et al*, 2001).

Tube formation assay showed for CHO (figure 11) and HCT15 (figure 12) a decrease in the number of branch points formed by HUVEC. These observations, for HCT15, were accompanied by an increase of *VEGF-121* expression and a decrease for *VEGF-165* and *VEGF-189* (figure 13). In fact, VEGF-121 is not recognized as a bioactive isoform; the contrary is

observed for VEGF-165 and, even with greater evidence, VEGF-189 (Park *et al*, 1993). This evidence together with the lower expression levels of VEGF receptors (figure 14) can explain the previous observation in HUVEC.

For HeLa, the opposite was observed in tube formation assay (figure 15), but with a small significance. However, the same differences in VEGF isoforms expression (figure 16) were observed between control and transfected cells, as well as in *KDR* and angiopoietins (figure 17).

The control experiment showed, as in HCT15 and CHO, a decrease in the number of branch points formed when medium contained FN (figure 18).

These findings seem to correlate FN levels with a reduced angiogenic activity, contradicting some studies in which the opposite was suggested (Nicosia *et al*, 1993; Viji *et al*, 2008). A similar association was, however, verified *in vivo*, in breast cancer patients, for which an inverse relation between stromal FN and angiogenesis was observed (Takei *et al*, 1998). Other studies have introduced some fragments derived from FN as inhibitors of angiogenesis (Saiki *et al*, 1990; Yi & Ruoslahti, 2001).

Overall, the prior results appear to correlate FN levels with more aggressiveness in the neoplastic context, *in vitro*, suggesting a particular involvement in the migration of cancer cells.

In vivo, results obtained from western blotting (figure 25) differed from the ones observed for western blotting *in vitro* for cells media supernatants. Those results should, however, be considered with prudence, once the analysis was performed on the animals serum. In addition, due to limited volume of serum, only one antibody was used, which could have implied the loss of information.

In vivo, macroscopically, larger tumors were observed for mice inoculated with transfected cells, for both cell lines (figures 26 and 27). This observation, and considering the further results, relates tumor size to the progression of disease, associating smaller tumors to a more advanced tumorigenic process. In fact, the acquirement of an invasive ability is not directly dependent on the number of cells composing the tumor, but on its heterogeneity that favors the interaction with the local microenvironment, allowing, ultimately, the dissemination of the disease (Scheel *et al*, 2007; Voulgari & Pintzas, 2009)

Histological analysis of the xenograft tumors and the organs collected revealed, for the mice inoculated with HCT15 cells (figure 28), the presence of metastases in the liver of both subgroups, and in the lungs of control mice. Besides, for the latter animals, cancer cells in the

xenograft tumors appeared more invasive than in tumors of mice inoculated with transfected cells.

For mice inoculated with HeLa, control subgroup also differed from the subgroup inoculated with transfected cells, showing lung metastases that were not observed in the latter subgroup (figure 29).

E-cadherin is a cell-cell adhesion protein. Loss of E-cadherin function or expression has been implicated in cancer progression and metastasis, being one of the core elements of EMT (Hugo *et al*, 2007; Klymkowsky, 2005; Voulgari & Pintzas, 2009). E-chaderin detection on primary tumors showed no differences within subgroups for both cell lines (figure 30). This result appears not to attribute a relevant role of E-cadherin in the previous differences described within subgroups, for both cell lines.

BM-derived endothelial progenitor cells (EPCs) assume an important role in tumorigenesis by providing an alternative source of endothelial cells that contribute to neovessel formation, namely through paracrine secretion of proangiogenic growth factors as well as by direct luminal incorporation into sprouting nascent vessels (Lyden *et al*, 2001; Witsch *et al*, 2010). In fact, for mice inoculated with HCT15, after tumors formation induction it was observed a gradual increase of EPCs for both subgroups (figure 21). That increase was though more accentuated in mice inoculated with transfected cells. Indeed, as mentioned above, tumors from the latter subgroup were larger than in control. For HeLa, however, and despite the same difference regarding tumor mass size has been observed, no significant differences in EPCs were detected during the experiment (figure 23).

BM-derived mast cells have been implicated in tumor growth and invasion and associated with poor prognosis (Gao & Mittal, 2009; Strouch *et al*, 2010), being an abundant source of angiogenic factors and MMP-9 (Theoharides & Conti, 2004). Toluidin blue staining in xenograft tumors showed, for mice inoculated with HCT15, an enhanced mast cells infiltration in control subgroup (figure 31). This observation is, thus, consistent with the observations from tumor cells detection.

SCF is a cytokine that binds to cKit receptor (CD117) in mast cells, promoting their survival, proliferation and migration (Broudy, 1997). SDF-1 is a chemokine associated to tumor growth and angiogenesis, metastasis and recruitment of BM-derived cells (Kryczek *et al*, 2007). By quantifying, *in vitro*, the expression of these cytokines, lower levels were observed in transfected cells, for both cell lines (figures 19 and 20). Such results also support the previous observations. In addition, for mice inoculated with HCT15, lower levels of cKit+ cells were measured in the subgroup inoculated with transfected cells (figure 22), which is also according to the prior findings. For mice inoculated with HeLa, however, the same relation between SCF

and cKit was not observed (figure 24). In fact, cKit is also expressed in other cell types besides mast cells, including hematopoetic stem cells (Ronnstrand, 2004).

Results *in vivo* show, therefore, the occurrence of a more advanced tumorigenic process in the mice inoculated with control cells. However, *in vitro*, for HCT15, the results pointed to a greater aggressiveness of transfected cells, in the neoplastic context, based on the increased MMPs 9 and 2 activities that, in turn, were suggested to be related to the higher migration rate in wound healing assay also observed. In fact, despite representing a requirement for invasion, tumor cells with higher migration rates are not necessarily more invasive, since invasion is the result of the combination of several factors. One the other hand, *in vitro* conditions are very different form *in vivo* context, which includes a set of variables that are not present *in vitro*. A tumor exists within a tissue that is constituted by several cell types interacting continuously, and, by themselves, they can limit or enhance tumor progression; these conditions cannot be introduced in a culture dish. This evidence also allows the introduction of a new data: one of the more expressive findings *in vitro*, for HCT15, was the increased levels of fragment 5 in transfected cells, compared to control group. Indeed, several studies have demonstrated protective roles of fragments derived from FN (Humphries *et al*, 1986; Humphries *et al*, 1988; Kato *et al*, 2002; Saiki, 1997; Yi & Ruoslahti, 2001). Given these observations and the results obtained, this fragment arises as a possible explanation for the outcome of the experiment, for HCT15.

Nevertheless, it is important to refer the occurrence of technical fragilities concerning the number of animals used that revealed insufficient for such an experiment *in vivo*, so any final conclusion should be taken after validation of the *in vivo* model.

For HeLa, *in vitro* results revealed, collectively, very discrete differences between control and transfected cells. Adding to this outcome the same technical barriers verified for HCT15, the validation of the *in vivo* model also emerges as a priority.

5.1 Future perspectives

Considering the results obtained and the technical fragilities observed, the validation of the *in vivo* model represents the main concern. Nonetheless, it would be important to clarify the role of fragment 5 as an eventual therapeutic agent. For that, the sequencing of the fragment seems an important future task for further research that could include the reproduction of the present experiments.

6. Conclusions

The central aim of this thesis was the study of the role of FN in tumor development and progression. For that purpose several experiments were accomplished *in vitro*, on a first approach, and, subsequently, *in vivo*.

In vitro, after validation of the success of cells transfection by real-time PCR, western blotting and immunofluorescence, our findings suggested an association between increased FN levels and higher FN proteolysis. Besides, higher FN levels were also associated with increased MMPs 9 and 2 proteolytic activities, suggesting a direct involvement of FN, once this ECM glycoprotein is cleaved by MMPs, and/or its indirect participation by inducing specific signaling pathways that culminate in an increased expression or activation of MMPs.

The prior results also appeared to be related to the observed higher directional migration rates for cell groups exhibiting increased FN amounts.

In vitro findings, which suggested a correlation between FN levels and a more aggressive behavior by cancer cells, particularly towards migration, were not, however, confirmed *in vivo*, where a less advanced tumorigenic process was observed in mice inoculated with transfected cells. Indeed, a higher migration rate, although essential for tumor progression, does not necessarily imply a greater invasive activity, the main responsible for cancer dissemination. On the other hand, *in vitro* conditions do not include many variables existing *in vivo*.

These outcomes also prompted us to consider another data observed *in vitro* for HCT15, in which expressive elevated levels of fragment 5 were observed in the medium supernatant from transfected cells. Considering some literature that points out the protective roles of some fragments derived from FN, this finding may represent a possible explanation for the outcomes obtained.

As future work, nonetheless, we suggest the validation of the *in* vivo models to confirm the results, once some technical fragilities concerning the number of animals used were faced. The sequencing of fragment 5 could still be relevant for further investigation.

7. References

Akiyama SK (1996) Integrins in cell adhesion and signaling. *Hum Cell* **9:** 181-6

Akiyama SK, Olden K, Yamada KM (1995) Fibronectin and integrins in invasion and metastasis. *Cancer Metastasis Rev* **14:** 173-89

Akiyama SK, Yamada SS, Chen WT, Yamada KM (1989) Analysis of fibronectin receptor function with monoclonal antibodies: roles in cell adhesion, migration, matrix assembly, and cytoskeletal organization. *J Cell Biol* **109:** 863-75

Alberts B, Johnson A, Lewis J, Raff M, Roberts K, Walter P (2002) *Molecular Biology of the Cell*, 4th edn. New York: Garland Science

Allinen M, Beroukhim R, Cai L, Brennan C, Lahti-Domenici J, Huang H, Porter D, Hu M, Chin L, Richardson A, Schnitt S, Sellers WR, Polyak K (2004) Molecular characterization of the tumor microenvironment in breast cancer. *Cancer Cell* **6:** 17-32

Assoian RK, Marcantonio EE (1996) The extracellular matrix as a cell cycle control element in atherosclerosis and restenosis. *J Clin Invest* **98:** 2436-9

Auguste P, Gursel DB, Lemiere S, Reimers D, Cuevas P, Carceller F, Di Santo JP, Bikfalvi A (2001) Inhibition of fibroblast growth factor/fibroblast growth factor receptor activity in glioma cells impedes tumor growth by both angiogenesis-dependent and -independent mechanisms. *Cancer Res* **61:** 1717-26

Bissell MJ, Radisky D (2001) Putting tumours in context. *Nat Rev Cancer* **1:** 46-54

Bramhall SR, Hallissey MT, Whiting J, Scholefield J, Tierney G, Stuart RC, Hawkins RE, McCulloch P, Maughan T, Brown PD, Baillet M, Fielding JW (2002) Marimastat as maintenance therapy for patients with advanced gastric cancer: a randomised trial. *Br J Cancer* **86:** 1864-70

Bramhall SR, Rosemurgy A, Brown PD, Bowry C, Buckels JA (2001) Marimastat as first-line therapy for patients with unresectable pancreatic cancer: a randomized trial. *J Clin Oncol* **19:** 3447-55

Broudy VC (1997) Stem cell factor and hematopoiesis. *Blood* **90:** 1345-64

Bryan TM, Englezou A, Gupta J, Bacchetti S, Reddel RR (1995) Telomere elongation in immortal human cells without detectable telomerase activity. *EMBO J* **14:** 4240-8

Bugge TH, Kombrinck KW, Flick MJ, Daugherty CC, Danton MJ, Degen JL (1996) Loss of fibrinogen rescues mice from the pleiotropic effects of plasminogen deficiency. *Cell* **87:** 709-19

Buyukbayram H, Arslan A (2002) Value of tenascin-C content and association with clinicopathological parameters in uterine cervical lesions. *Int J Cancer* **100:** 719-22

Cao Y (2001) Endogenous angiogenesis inhibitors and their therapeutic implications. *Int J Biochem Cell Biol* **33:** 357-69

Cappellen D, De Oliveira C, Ricol D, de Medina S, Bourdin J, Sastre-Garau X, Chopin D, Thiery JP, Radvanyi F (1999) Frequent activating mutations of FGFR3 in human bladder and cervix carcinomas. *Nat Genet* **23:** 18-20

Chambers AF, Matrisian LM (1997) Changing views of the role of matrix metalloproteinases in metastasis. *J Natl Cancer Inst* **89:** 1260-70

Chantrain CF, Shimada H, Jodele S, Groshen S, Ye W, Shalinsky DR, Werb Z, Coussens LM, DeClerck YA (2004) Stromal matrix metalloproteinase-9 regulates the vascular architecture in neuroblastoma by promoting pericyte recruitment. *Cancer Res* **64:** 1675-86

Chesi M, Nardini E, Brents LA, Schrock E, Ried T, Kuehl WM, Bergsagel PL (1997) Frequent translocation t(4;14)(p16.3;q32.3) in multiple myeloma is associated with increased expression and activating mutations of fibroblast growth factor receptor 3. *Nat Genet* **16:** 260-4

Chung CY, Zardi L, Erickson HP (1995) Binding of tenascin-C to soluble fibronectin and matrix fibrils. *J Biol Chem* **270:** 29012-7

Colorado PC, Torre A, Kamphaus G, Maeshima Y, Hopfer H, Takahashi K, Volk R, Zamborsky ED, Herman S, Sarkar PK, Ericksen MB, Dhanabal M, Simons M, Post M, Kufe DW, Weichselbaum RR, Sukhatme VP, Kalluri R (2000) Anti-angiogenic cues from vascular basement membrane collagen. *Cancer Res* **60:** 2520-6

Coussens LM, Fingleton B, Matrisian LM (2002) Matrix metalloproteinase inhibitors and cancer: trials and tribulations. *Science* **295:** 2387-92

Das S, Banerji A, Frei E, Chatterjee A (2008) Rapid expression and activation of MMP-2 and MMP-9 upon exposure of human breast cancer cells (MCF-7) to fibronectin in serum free medium. *Life Sci* **82:** 467-76

Davies B, Brown PD, East N, Crimmin MJ, Balkwill FR (1993) A synthetic matrix metalloproteinase inhibitor decreases tumor burden and prolongs survival of mice bearing human ovarian carcinoma xenografts. *Cancer Res* **53:** 2087-91

DeBerardinis RJ, Lum JJ, Hatzivassiliou G, Thompson CB (2008) The biology of cancer: metabolic reprogramming fuels cell growth and proliferation. *Cell Metab* **7:** 11-20

Desoize B (2004) Stromal reaction and tumour growth. *Crit Rev Oncol Hematol* **49:** 173-6

Di Fiore PP, Pierce JH, Kraus MH, Segatto O, King CR, Aaronson SA (1987) erbB-2 is a potent oncogene when overexpressed in NIH/3T3 cells. *Science* **237:** 178-82

Duffy MJ, Maguire TM, Hill A, McDermott E, O'Higgins N (2000) Metalloproteinases: role in breast carcinogenesis, invasion and metastasis. *Breast Cancer Res* **2:** 252-7

Emoto K, Yamada Y, Sawada H, Fujimoto H, Ueno M, Takayama T, Kamada K, Naito A, Hirao S, Nakajima Y (2001) Annexin II overexpression correlates with stromal tenascin-C overexpression: a prognostic marker in colorectal carcinoma. *Cancer* **92:** 1419-26

Evan GI, Vousden KH (2001) Proliferation, cell cycle and apoptosis in cancer. *Nature* **411:** 342-8

Folkman J (1992) The role of angiogenesis in tumor growth. *Semin Cancer Biol* **3:** 65-71

Furcht LT, McCarthy JB, Palm SL, Basara ML, Enenstein J (1984) Peptide fragments of laminin and fibronectin promote migration (haptotaxis and chemotaxis) of metastatic cells. *Ciba Found Symp* **108:** 130-45

Gao D, Mittal V (2009) The role of bone-marrow-derived cells in tumor growth, metastasis initiation and progression. *Trends Mol Med* **15:** 333-43

Giavazzi R, Taraboletti G (2001) Preclinical development of metalloproteasis inhibitors in cancer therapy. *Crit Rev Oncol Hematol* **37:** 53-60

Giri D, Ropiquet F, Ittmann M (1999) Alterations in expression of basic fibroblast growth factor (FGF) 2 and its receptor FGFR-1 in human prostate cancer. *Clin Cancer Res* **5:** 1063-71

Han S, Ritzenthaler JD, Sitaraman SV, Roman J (2006) Fibronectin increases matrix metalloproteinase 9 expression through activation of c-Fos via extracellular-regulated kinase and phosphatidylinositol 3-kinase pathways in human lung carcinoma cells. *J Biol Chem* **281:** 29614-24

Hanahan D, Folkman J (1996) Patterns and emerging mechanisms of the angiogenic switch during tumorigenesis. *Cell* **86:** 353-64

Hanahan D, Weinberg RA (2000) The hallmarks of cancer. *Cell* **100:** 57-70

Hanahan D, Weinberg RA (2011) Hallmarks of cancer: the next generation. *Cell* **144:** 646-74

Harris CC (1996) p53 tumor suppressor gene: from the basic research laboratory to the clinic--an abridged historical perspective. *Carcinogenesis* **17:** 1187-98

Hay ED (1995) An overview of epithelio-mesenchymal transformation. *Acta Anat (Basel)* **154:** 8-20

Hayflick L (1997) Mortality and immortality at the cellular level. A review. *Biochemistry (Mosc)* **62:** 1180-90

Homandberg GA (2001) Cartilage damage by matrix degradation products: fibronectin fragments. *Clin Orthop Relat Res***:** S100-7

Huang HS, Nagane M, Klingbeil CK, Lin H, Nishikawa R, Ji XD, Huang CM, Gill GN, Wiley HS, Cavenee WK (1997) The enhanced tumorigenic activity of a mutant epidermal growth factor receptor common in human cancers is mediated by threshold levels of constitutive tyrosine phosphorylation and unattenuated signaling. *J Biol Chem* **272:** 2927-35

Hugo H, Ackland ML, Blick T, Lawrence MG, Clements JA, Williams ED, Thompson EW (2007) Epithelial--mesenchymal and mesenchymal--epithelial transitions in carcinoma progression. *J Cell Physiol* **213:** 374-83

Humphries MJ, Olden K, Yamada KM (1986) A synthetic peptide from fibronectin inhibits experimental metastasis of murine melanoma cells. *Science* **233:** 467-70

Humphries MJ, Yamada KM, Olden K (1988) Investigation of the biological effects of anti-cell adhesive synthetic peptides that inhibit experimental metastasis of B16-F10 murine melanoma cells. *J Clin Invest* **81:** 782-90

Hynes RO (1976) Cell surface proteins and malignant transformation. *Biochim Biophys Acta* **458:** 73-107

Hynes RO, Yamada KM (1982) Fibronectins: multifunctional modular glycoproteins. *J Cell Biol* **95:** 369-77

Kaplan RN, Riba RD, Zacharoulis S, Bramley AH, Vincent L, Costa C, MacDonald DD, Jin DK, Shido K, Kerns SA, Zhu Z, Hicklin D, Wu Y, Port JL, Altorki N, Port ER, Ruggero D, Shmelkov SV, Jensen KK, Rafii S, Lyden D (2005) VEGFR1-positive haematopoietic bone marrow progenitors initiate the pre-metastatic niche. *Nature* **438:** 820-7

Kaspar M, Zardi L, Neri D (2006) Fibronectin as target for tumor therapy. *Int J Cancer* **118:** 1331-9

Katayama M, Kamihagi K, Nakagawa K, Akiyama T, Sano Y, Ouchi R, Nagata S, Hino F, Kato I (1993) Increased fragmentation of urinary fibronectin in cancer patients detected by immunoenzymometric assay using domain-specific monoclonal antibodies. *Clin Chim Acta* **217:** 115-28

Kato R, Ishikawa T, Kamiya S, Oguma F, Ueki M, Goto S, Nakamura H, Katayama T, Fukai F (2002) A new type of antimetastatic peptide derived from fibronectin. *Clin Cancer Res* **8:** 2455-62

Kawaguchi T (2005) Cancer metastasis: characterization and identification of the behavior of metastatic tumor cells and the cell adhesion molecules, including carbohydrates. *Curr Drug Targets Cardiovasc Haematol Disord* **5:** 39-64

Kenny HA, Kaur S, Coussens LM, Lengyel E (2008) The initial steps of ovarian cancer cell metastasis are mediated by MMP-2 cleavage of vitronectin and fibronectin. *J Clin Invest* **118:** 1367-79

Kenny HA, Lengyel E (2009) MMP-2 functions as an early response protein in ovarian cancer metastasis. *Cell Cycle* **8:** 683-8

Kessenbrock K, Plaks V, Werb Z (2010) Matrix metalloproteinases: regulators of the tumor microenvironment. *Cell* **141:** 52-67

Klein G, Vellenga E, Fraaije MW, Kamps WA, de Bont ES (2004) The possible role of matrix metalloproteinase (MMP)-2 and MMP-9 in cancer, e.g. acute leukemia. *Crit Rev Oncol Hematol* **50:** 87-100

Klymkowsky MW (2005) Beta-catenin and its regulatory network. *Hum Pathol* **36:** 225-7

Kolibaba KS, Druker BJ (1997) Protein tyrosine kinases and cancer. *Biochim Biophys Acta* **1333:** F217-48

Kopp HG, Avecilla ST, Hooper AT, Rafii S (2005) The bone marrow vascular niche: home of HSC differentiation and mobilization. *Physiology (Bethesda)* **20:** 349-56

Kopp HG, Ramos CA, Rafii S (2006) Contribution of endothelial progenitors and proangiogenic hematopoietic cells to vascularization of tumor and ischemic tissue. *Curr Opin Hematol* **13:** 175-81

Kornblihtt AR, Pesce CG, Alonso CR, Cramer P, Srebrow A, Werbajh S, Muro AF (1996) The fibronectin gene as a model for splicing and transcription studies. *FASEB J* **10:** 248-57

Kornmann M, Ishiwata T, Beger HG, Korc M (1997) Fibroblast growth factor-5 stimulates mitogenic signaling and is overexpressed in human pancreatic cancer: evidence for autocrine and paracrine actions. *Oncogene* **15:** 1417-24

Kryczek I, Wei S, Keller E, Liu R, Zou W (2007) Stroma-derived factor (SDF-1/CXCL12) and human tumor pathogenesis. *Am J Physiol Cell Physiol* **292:** C987-95

Labat-Robert J (2002) Fibronectin in malignancy. *Semin Cancer Biol* **12:** 187-95

Labat-Robert J, Birembaut P, Adnet JJ, Mercantini F, Robert L (1980) Loss of fibronectin in human breast cancer. *Cell Biol Int Rep* **4:** 609-16

Lakka SS, Gondi CS, Yanamandra N, Dinh DH, Olivero WC, Gujrati M, Rao JS (2003) Synergistic down-regulation of urokinase plasminogen activator receptor and matrix metalloproteinase-9 in SNB19 glioblastoma cells efficiently inhibits glioma cell invasion, angiogenesis, and tumor growth. *Cancer Res* **63:** 2454-61

Lee S, Jilani SM, Nikolova GV, Carpizo D, Iruela-Arispe ML (2005) Processing of VEGF-A by matrix metalloproteinases regulates bioavailability and vascular patterning in tumors. *J Cell Biol* **169:** 681-91

Leikina E, Mertts MV, Kuznetsova N, Leikin S (2002) Type I collagen is thermally unstable at body temperature. *Proc Natl Acad Sci U S A* **99:** 1314-8

Levine AJ (1997) p53, the cellular gatekeeper for growth and division. *Cell* **88:** 323-31

Lopez-Armada MJ, Gonzalez E, Gomez-Guerrero C, Egido J (1997) The 80-kD fibronectin fragment increases the production of fibronectin and tumour necrosis factor-alpha (TNF-alpha) in cultured mesangial cells. *Clin Exp Immunol* **107:** 398-403

Lukashev ME, Werb Z (1998) ECM signalling: orchestrating cell behaviour and misbehaviour. *Trends Cell Biol* **8:** 437-41

Lyden D, Hattori K, Dias S, Costa C, Blaikie P, Butros L, Chadburn A, Heissig B, Marks W, Witte L, Wu Y, Hicklin D, Zhu Z, Hackett NR, Crystal RG, Moore MA, Hajjar KA, Manova K, Benezra R, Rafii S (2001) Impaired recruitment of bone-marrow-derived endothelial and hematopoietic precursor cells blocks tumor angiogenesis and growth. *Nat Med* **7:** 1194-201

Malemud CJ (2006) Matrix metalloproteinases (MMPs) in health and disease: an overview. *Front Biosci* **11:** 1696-701

Martin DC, Ruther U, Sanchez-Sweatman OH, Orr FW, Khokha R (1996) Inhibition of SV40 T antigen-induced hepatocellular carcinoma in TIMP-1 transgenic mice. *Oncogene* **13:** 569-76

Martin MD, Matrisian LM (2007) The other side of MMPs: protective roles in tumor progression. *Cancer Metastasis Rev* **26:** 717-24

Mitra A, Chakrabarti J, Banerji A, Das S, Chatterjee A (2006) Culture of human cervical cancer cells, SiHa, in the presence of fibronectin activates MMP-2. *J Cancer Res Clin Oncol* **132:** 505-13

Mosher DF, Fogerty FJ, Chernousov MA, Barry EL (1991) Assembly of fibronectin into extracellular matrix. *Ann N Y Acad Sci* **614:** 167-80

Mosher DF, Sottile J, Wu C, McDonald JA (1992) Assembly of extracellular matrix. *Curr Opin Cell Biol* **4:** 810-8

Nagaraj S, Gupta K, Pisarev V, Kinarsky L, Sherman S, Kang L, Herber DL, Schneck J, Gabrilovich DI (2007) Altered recognition of antigen is a mechanism of CD8+ T cell tolerance in cancer. *Nat Med* **13:** 828-35

Nguyen M, Arkell J, Jackson CJ (2001) Human endothelial gelatinases and angiogenesis. *Int J Biochem Cell Biol* **33:** 960-70

Nicosia RF, Bonanno E, Smith M (1993) Fibronectin promotes the elongation of microvessels during angiogenesis in vitro. *J Cell Physiol* **154:** 654-61

Olden K, Yamada KM (1977) Mechanism of the decrease in the major cell surface protein of chick embryo fibroblasts after transformation. *Cell* **11:** 957-69

Orend G, Chiquet-Ehrismann R (2006) Tenascin-C induced signaling in cancer. *Cancer Lett* **244:** 143-63

Padro T, Bieker R, Ruiz S, Steins M, Retzlaff S, Burger H, Buchner T, Kessler T, Herrera F, Kienast J, Muller-Tidow C, Serve H, Berdel WE, Mesters RM (2002) Overexpression of vascular endothelial growth factor (VEGF) and its cellular receptor KDR (VEGFR-2) in the bone marrow of patients with acute myeloid leukemia. *Leukemia* **16:** 1302-10

Page-McCaw A, Ewald AJ, Werb Z (2007) Matrix metalloproteinases and the regulation of tissue remodelling. *Nat Rev Mol Cell Biol* **8:** 221-33

Pankov R, Yamada KM (2002) Fibronectin at a glance. *J Cell Sci* **115:** 3861-3

Park JE, Keller GA, Ferrara N (1993) The vascular endothelial growth factor (VEGF) isoforms: differential deposition into the subepithelial extracellular matrix and bioactivity of extracellular matrix-bound VEGF. *Mol Biol Cell* **4:** 1317-26

Park MT, Lee SJ (2003) Cell cycle and cancer. *J Biochem Mol Biol* **36:** 60-5

Patel RS, Odermatt E, Schwarzbauer JE, Hynes RO (1987) Organization of the fibronectin gene provides evidence for exon shuffling during evolution. *EMBO J* **6:** 2565-72

Perona R (2006) Cell signalling: growth factors and tyrosine kinase receptors. *Clin Transl Oncol* **8:** 77-82

Polette M, Nawrocki-Raby B, Gilles C, Clavel C, Birembaut P (2004) Tumour invasion and matrix metalloproteinases. *Crit Rev Oncol Hematol* **49:** 179-86

Potts JR, Campbell ID (1996) Structure and function of fibronectin modules. *Matrix Biol* **15:** 313-20

Pupa SM, Menard S, Forti S, Tagliabue E (2002) New insights into the role of extracellular matrix during tumor onset and progression. *J Cell Physiol* **192:** 259-67

Renan MJ (1993) How many mutations are required for tumorigenesis? Implications from human cancer data. *Mol Carcinog* **7:** 139-46

Ronnov-Jessen L, Petersen OW, Bissell MJ (1996) Cellular changes involved in conversion of normal to malignant breast: importance of the stromal reaction. *Physiol Rev* **76:** 69-125

Ronnstrand L (2004) Signal transduction via the stem cell factor receptor/c-Kit. *Cell Mol Life Sci* **61:** 2535-48

Saiki I (1997) Cell adhesion molecules and cancer metastasis. *Jpn J Pharmacol* **75:** 215-42

Saiki I, Murata J, Makabe T, Nishi N, Tokura S, Azuma I (1990) Inhibition of tumor angiogenesis by a synthetic cell-adhesive polypeptide containing the Arg-Gly-Asp (RGD) sequence of fibronectin, poly(RGD). *Jpn J Cancer Res* **81:** 668-75

Santos SC, Dias S (2004) Internal and external autocrine VEGF/KDR loops regulate survival of subsets of acute leukemia through distinct signaling pathways. *Blood* **103:** 3883-9

Scheel C, Onder T, Karnoub A, Weinberg RA (2007) Adaptation versus selection: the origins of metastatic behavior. *Cancer Res* **67:** 11476-9; discussion 11479-80

Sen T, Dutta A, Maity G, Chatterjee A (2010) Fibronectin induces matrix metalloproteinase-9 (MMP-9) in human laryngeal carcinoma cells by involving multiple signaling pathways. *Biochimie* **92:** 1422-34

Seppa HE, Yamada KM, Seppa ST, Silver MH, Kleinman HK, Schiffmann E (1981) The cell binding fragment of fibronectin is chemotactic for fibroblasts. *Cell Biol Int Rep* **5:** 813-9

Serpa J, Caiado F, Carvalho T, Torre C, Goncalves LG, Casalou C, Lamosa P, Rodrigues M, Zhu Z, Lam EW, Dias S (2010) Butyrate-rich colonic microenvironment is a relevant selection factor for metabolically adapted tumor cells. *J Biol Chem* **285:** 39211-23

Shingu K, Fujimori M, Ito K, Hama Y, Kasuga Y, Kobayashi S, Itoh N, Amano J (1998) Expression of fibroblast growth factor-2 and fibroblast growth factor receptor-1 in thyroid diseases: difference between neoplasms and hyperplastic lesions. *Endocr J* **45:** 35-43

Singh RK, Gutman M, Bucana CD, Sanchez R, Llansa N, Fidler IJ (1995) Interferons alpha and beta down-regulate the expression of basic fibroblast growth factor in human carcinomas. *Proc Natl Acad Sci U S A* **92:** 4562-6

Sis B, Sagol O, Kupelioglu A, Sokmen S, Terzi C, Fuzun M, Ozer E, Bishop P (2004) Prognostic significance of matrix metalloproteinase-2, cathepsin D, and tenascin-C expression in colorectal carcinoma. *Pathol Res Pract* **200:** 379-87

Song S, Ewald AJ, Stallcup W, Werb Z, Bergers G (2005) PDGFRbeta+ perivascular progenitor cells in tumours regulate pericyte differentiation and vascular survival. *Nat Cell Biol* **7:** 870-9

Sporn MB (1996) The war on cancer. *Lancet* **347:** 1377-81

Sporn MB, Todaro GJ (1980) Autocrine secretion and malignant transformation of cells. *N Engl J Med* **303:** 878-80

Stetler-Stevenson WG (1999) Matrix metalloproteinases in angiogenesis: a moving target for therapeutic intervention. *J Clin Invest* **103:** 1237-41

Strouch MJ, Cheon EC, Salabat MR, Krantz SB, Gounaris E, Melstrom LG, Dangi-Garimella S, Wang E, Munshi HG, Khazaie K, Bentrem DJ (2010) Crosstalk between mast cells and pancreatic cancer cells contributes to pancreatic tumor progression. *Clin Cancer Res* **16:** 2257-65

Takei H, Iino Y, Horiguchi J, Maemura M, Koibuchi Y, Nagaoka H, Yokoe T, Oyama T, Morishita Y (1998) Angiogenesis and stromal fibronectin expression in invasive breast carcinoma. *Int J Oncol* **12:** 517-23

Tamkun JW, Hynes RO (1983) Plasma fibronectin is synthesized and secreted by hepatocytes. *J Biol Chem* **258:** 4641-7

Tammela T, Enholm B, Alitalo K, Paavonen K (2005) The biology of vascular endothelial growth factors. *Cardiovasc Res* **65:** 550-63

Theoharides TC, Conti P (2004) Mast cells: the Jekyll and Hyde of tumor growth. *Trends Immunol* **25:** 235-41

Tlsty TD (2001) Stromal cells can contribute oncogenic signals. *Semin Cancer Biol* **11:** 97-104

Tlsty TD, Coussens LM (2006) Tumor stroma and regulation of cancer development. *Annu Rev Pathol* **1:** 119-50

Torisu H, Ono M, Kiryu H, Furue M, Ohmoto Y, Nakayama J, Nishioka Y, Sone S, Kuwano M (2000) Macrophage infiltration correlates with tumor stage and angiogenesis in human malignant melanoma: possible involvement of TNFalpha and IL-1alpha. *Int J Cancer* **85:** 182-8

Trojan L, Thomas D, Knoll T, Grobholz R, Alken P, Michel MS (2004) Expression of pro-angiogenic growth factors VEGF, EGF and bFGF and their topographical relation to neovascularisation in prostate cancer. *Urol Res* **32:** 97-103

Vander Heiden MG, Cantley LC, Thompson CB (2009) Understanding the Warburg effect: the metabolic requirements of cell proliferation. *Science* **324:** 1029-33

Vihinen P, Kahari VM (2002) Matrix metalloproteinases in cancer: prognostic markers and therapeutic targets. *Int J Cancer* **99:** 157-66

Viji RI, Kumar VB, Kiran MS, Sudhakaran PR (2008) Modulation of cyclooxygenase in endothelial cells by fibronectin: relevance to angiogenesis. *J Cell Biochem* **105:** 158-66

Voulgari A, Pintzas A (2009) Epithelial-mesenchymal transition in cancer metastasis: mechanisms, markers and strategies to overcome drug resistance in the clinic. *Biochim Biophys Acta* **1796:** 75-90

Waalkes S, Atschekzei F, Kramer MW, Hennenlotter J, Vetter G, Becker JU, Stenzl A, Merseburger AS, Schrader AJ, Kuczyk MA, Serth J (2010) Fibronectin 1 mRNA expression correlates with advanced disease in renal cancer. *BMC Cancer* **10:** 503

Wang Y, Becker D (1997) Antisense targeting of basic fibroblast growth factor and fibroblast growth factor receptor-1 in human melanomas blocks intratumoral angiogenesis and tumor growth. *Nat Med* **3:** 887-93

Warawdekar UM, Zingde SM, Iyer KS, Jagannath P, Mehta AR, Mehta NG (2006) Elevated levels and fragmented nature of cellular fibronectin in the plasma of gastrointestinal and head and neck cancer patients. *Clin Chim Acta* **372:** 83-93

Werb Z (1997) ECM and cell surface proteolysis: regulating cellular ecology. *Cell* **91:** 439-42

Wernert N (1997) The multiple roles of tumour stroma. *Virchows Arch* **430:** 433-43

Wilson CL, Heppner KJ, Labosky PA, Hogan BL, Matrisian LM (1997) Intestinal tumorigenesis is suppressed in mice lacking the metalloproteinase matrilysin. *Proc Natl Acad Sci U S A* **94:** 1402-7

Witsch E, Sela M, Yarden Y (2010) Roles for growth factors in cancer progression. *Physiology (Bethesda)* **25:** 85-101

Wu Y, Hooper AT, Zhong Z, Witte L, Bohlen P, Rafii S, Hicklin DJ (2006) The vascular endothelial growth factor receptor (VEGFR-1) supports growth and survival of human breast carcinoma. *Int J Cancer* **119:** 1519-29

Yang L, Huang J, Ren X, Gorska AE, Chytil A, Aakre M, Carbone DP, Matrisian LM, Richmond A, Lin PC, Moses HL (2008) Abrogation of TGF beta signaling in mammary carcinomas recruits Gr-1+CD11b+ myeloid cells that promote metastasis. *Cancer Cell* **13:** 23-35

Yi M, Ruoslahti E (2001) A fibronectin fragment inhibits tumor growth, angiogenesis, and metastasis. *Proc Natl Acad Sci U S A* **98:** 620-4

Zwick E, Bange J, Ullrich A (2001) Receptor tyrosine kinase signalling as a target for cancer intervention strategies. *Endocr Relat Cancer* **8:** 161-73

Appendices

Appendix A

Solutions prepared for the experimental work:

EDTA decalcifying solution
For 1L: 100 g EDTA (ethylenediaminetetraacetic acid disodium dihydrate); 100 ml formaldehyde; destilled water up to 1 L. pH 7

PBS Tween 20
For 1L: 1 ml Tween 20; PBS 1X up to 1 L.

TBS 10X
For 1L: 8 g sodium chloride; 0.63 g Tris; 4.4 ml hydrochloric acid (1M); destilled water up to 1 L. pH 7.4-7.6

Toluidine blue solution	
Toluidine blue stock solution For 100 ml: 1 g toluidine blue; 100 ml 70% (v/v) ethanol. pH 7.4-7.6	**Toluidine blue working dilution** For 50 ml: 5 ml toluidine blue stock solution; 45 ml 1% (w/v) sodium chloride (pH 2.3).

Zymography solutions	
Running gel (10% polyacrilamide gel with gelatin) For 10 ml: 3.33 ml 30% (w/v) acrylamide 2.5 ml 1.5 M Tris, pH 8.8 3 ml destilled water 1 ml 1.2% (w/v) gelatin 50 µl 20% (/w/v) SDS (sodium dodecyl sulfate) 33.3 µl 10% (w/v) APS (ammonium persulfate)	**Stacking gel** For 3 ml: 500 µl 30% acrylamide 380 µl 1.0 M Tris, pH 6.8 2.1 ml destilled water 30 µl 10% (w/v) SDS (sodium dodecyl sulfate) 30 µl 10% (w/v) APS (ammonium persulfate) 3 µl TEMED (Tetramethylethylenediamine)

6.7 µl TEMED (Tetramethylethylenediamine)	
Low salt collagenase buffer 10 X For 1L: 60.6 g Tris base 117 g sodium chloride 5.5 g calcium chloride Destilled water up to 1 L pH 7.6	**Collagenase buffer 1X** For 1L: 100 ml stock solution 900 ml destilled water 670 µl 30% (w/v) Brij
Destain solution For 1L: 100 ml glacial acetic acid 300 ml methanol 600 ml destilled water	
Coomassie brilliant blue stock solution For 500 ml: 250 ml methanol 0.25 g Coommassie brilliant blue 200 ml destilled water 50 ml acetic acid	**Coomassie working dilution** For 500 ml: 150 ml coomassie brilliant blue stock solution 350 ml destain solution

LB medium **Loading buffer (Bromophenol blue)** **PBS 10X** **Polyacrilamide gel (10%)** **Transfer buffer**	**(Sambrook & Russel, 2001)**

Reference:

Sambrook J, Russel DW (2001) *Molecular cloning: a laboratory manual*, 3rd edn. New York: Cold Spring Harbor Laboratory Press.

Appendix B

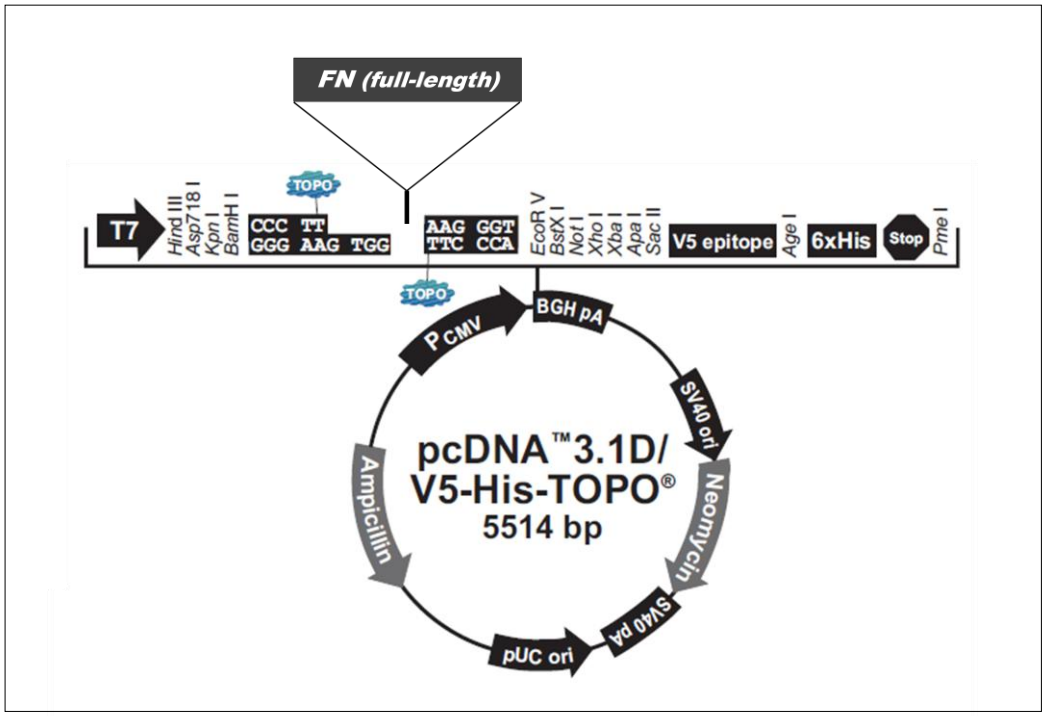

Figure 32 – Map of pcDNA3-fl*FN*. Adapted from "pcDNA™3.1 Directional TOPO® Expression Kit" handbook.